2022

Characterization of the Phenotype and Functional Properties of Myeloid Subpopulations in Chronic Inflammatory Conditions

Krystla Leandra Ong
University Of Alabama At Birmingham

CHARACTERIZATION OF THE PHENOTYPE AND FUNCTIONAL PROPERTIES OF MYELOID SUBPOPULATIONS IN CHRONIC INFLAMMATORY CONDITIONS

by

KRYSTLE LEANDRA ONG

LALITA SHEVDE-SAMANT, COMMITTEE CHAIR
ELIZABETH BROWN
NATHANIEL ERDMANN
ZDENEK HEL
SOORYANARAYANA VARAMBALLY

A DISSERTATION

Submitted to the graduate faculty of The University of Alabama at Birmingham,
in partial fulfillment of the requirements for the degree of
Doctor of Philosophy

BIRMINGHAM, ALABAMA

2022

CHARACTERIZATION OF THE PHENOTYPE AND FUNCTIONAL PROPERTIES OF MYELOID SUBPOPULATIONS IN CHRONIC INFLAMMATORY CONDITIONS

KRYSTLE LEANDRA ONG

BIOMEDICAL SCIENCES

ABSTRACT

Myeloid cells represent a subset of leukocytes traditionally recognized as first responders to acute inflammatory stimuli. In recent years, there has been a growing appreciation of the role of myeloid cells as critical regulators of the immune system in disease pathogenesis and progression. Chronic inflammatory diseases including viral infections, autoimmune diseases, and malignancies are frequently associated with altered myelopoiesis characterized by a profound shift in the myeloid cell phenotype and function. The work presented in this dissertation provides an insight into dysregulated myelopoiesis and myeloid heterogeneity in multiple myeloma (MM), human immunodeficiency virus-1 (HIV-1), and coronavirus disease-19 (COVID-19). We identify a distinct myeloid phenotype in a subset of MM patients that is characterized by significant differences in the properties of granulocytic and monocytic subpopulations indicative of altered myelopoiesis. Characteristic features of the phenotype, termed MM2, are associated with myeloma-defining events and advanced stage disease. We identify and characterize an immature neutrophil (imN) subpopulation defined as $CD16^{-}CD10^{-}$ $CXCR2^{lo}CD64^{+}CD66b^{+}$ with distinct phenotype and function. imNs are readily identifiable in whole blood in HIV-1, COVID-19, and MM and demonstrate signs of proliferative activity. Furthermore, we examine the interactions between neutrophils and

platelets as a mechanism for promoting the low-density neutrophil phenotype. Overall, these findings provide a framework for future investigations focusing on altered myeloid phenotype and function in chronic inflammatory diseases and novel approaches for therapeutic intervention.

Keywords: Altered myelopoiesis, myeloid heterogeneity, immune suppression, low-density neutrophils, multiple myeloma, leukocyte-platelet interactions

DEDICATION

First and foremost, I dedicate this dissertation to my grandparents. Without your sacrifices and commitment to our family's education, this work would not be possible. I also dedicate this work to my loving partner, Connor, and all of our family members for your unconditional love and support

ACKNOWLEDGEMENTS

To my mentor, Dr. Zdenek Hel, for your support and mentorship throughout my Ph.D. studies and help with transitioning to the next step in my career.

To my committee members, Dr. Lalita-Shevde-Samant, Dr. Elizabeth Brown, Dr. Nathaniel Erdmann, and Dr. Sooryananana Varambally, for helping me develop into the scientist and person I aspire to be and always supporting me in my career goals.

To all past and present members of the Hel lab - thank you for creating a friendly and professional work environment and helping with designing and executing experiments. A special thank you to Marcus Darrell Davis, who has been my lab partner in crime and mischief for the past six years.

Finally, thank you to all of my friends and family for their endless support and love. This accomplishment would not have been possible without you. To my partner, Connor Wingrove, for his constant support and motivation. To my best friend, Sarah Askew, for her close friendship and support for the past nine years. Lastly, thank you to my wonderful parents, Kati and Daniel Ong, whose sacrifices, unconditional love, and support made it possible for me to achieve this goal.

TABLE OF CONTENTS

Page

LIST OF TABLES

LIST OF FIGURES

IMMATURE NEUTROPHIL SUBPOPULATIONS IN ACUTE AND CHRONIC INFECTION AND CANCER

NEUTROPHIL-PLATELET INTERACTIONS PARTIALLY CONTRIBUTE TO THE INDUCTION OF THE LOW-DENSITY NEUTROPHIL PHENOTYPE

LIST OF ABBREVIATIONS

aHSCT	autologous hematopoetic stem cell transplant
APRIL	TNF ligand superfamily 13
BAFF	B-cell activating factor
BME	bone marrow microenvironment
BMPC	bone marrow plasma cell
CCL	chemokine ligand
CCL11	C-C motif chemokine 11
CCR3	chemokine receptor 3
CD142	tissue factor
CD62L	L-selectin
CFSE	Carboxyfluorescein succinimidyl ester
Cl Mo	classical monocytes
CMoP	common monocyte progenitor
COVID-19	Coronavirus-19
CVD	cardiovascular diseases
CVID	common variable immunodeficiency syndrome
CX3CR1	C-X3-C chemokine receptor 1
CXCL10	C-X-C motif chemokine ligand 10
CXCL8	IL-8
CXCR2	CXC chemokine receptor 2

CXCR4	CXC chemokine receptor 4
DAMP	danger-associated molecular pattern
DCF	dichloro fluorescein
DS	during salmon staging system
Eos	eosinophils
FCγRI	CD64
FCγRIII	CD16
FLC	free light chain
fMLF	N-Formylmethionine-leucyl-phenylalanine
FMO	fluorescence minus one
G-CSF	granulocyte colony-stimulating factor
GM-CSF	granulocyte-macrophage colony-stimulating factor
G-MDSC	granulocytic myeloid-derived suppressor cell
GMP	granulocyte-monocyte progintor
H2-DCFDA	2',7'-dichlorodihydrofluorescein
HD	healthy donors
HIV-1	human immunodeficiency virus-1
IFNγ	interferon-γ
Ig	immunoglobulin
IL-12	interleukin-12
IL-1B	interleukin-1B
IL21R	interleukin 21 receptor

IL-6	interleukin-6
IL-8	interleukin-8
IMAGE	Integrated Molecular And Genetic Epidemiology
imLDN	immature low-density neutrophil
imN	immature neutrophil
LDN	low-density neutrophil
LFA-1	lymphocyte function-associated antigen
LOX-1	lectin-type oxidized LDL receptor 1
LTB4	leukotriene B4
Mac-1	CD11b
MGUS	monoclonal gammopathy of undetermined significance
MHCs	major histocompatibility complexes
mLDN	mature low-density neutrophil
MM	multiple myeloma
M-MDSC	monocytic myeloid-derived suppressor cell
mN	mature neutrophil
MPC	monocyte-platelet complex
MPO	myeloperoxidase
MTG	MitoTracker™ Green
NADPH	nicotinamide adenine dinucleotide phosphate
NET	neutrophil extracellular trap
NGAL	gelatinase-associated lipocalin

NLR	neutrophil: lymphocyte ratio
NPC	neutrophil-platelet complex
PAMP	pathogen-associated molecular pattern
PAR1	protease-activated receptor 1
PBMC	peripheral blood mononuclear cell
PD-L1	programmed-death ligand 1
PMA	Phorbol myristate acetate
PMN	Polymorphonuclear cell
PMN-MDSC	polymorphonuclear myeloid-derived suppressor cell
PRR	pattern recognition receptor
PSGL-1	P-selectin glycoprotein ligand-1
Pt Mo	patrolling monocytes
R-ISS	revised and updated international staging system
ROS	reactive oxygen species
SARS-CoV-2	severe acute respiratory syndrome coronavirus 2
SLE	systemic lupus erthymatosus
SMM	smoldering myeloma
TAN	tumor-associated neutrophil
TCR	T-cell receptor
TLR	toll-like receptor
TLR4	toll-like signaling receptor 4
TME	tumor microenvironment

TMRE	tetramethylrhodamine ethyl ester
TNF-B	tumor necrosis factor-B
TNF-RI	tumor necrosis factor receptor 1
TNF-α	tumor necrosis factor-α
TRAIL	TNF-related apoptosis-inducing ligand
TRAP-6	thrombin receptor activator peptide 6
T-reg	T-regulatory cell
WBN	whole blood neutrophil
ΔΨm	mitochondrial membrane potential

INTRODUCTION

NEUTROPHILS IN THE INNATE IMMUNE SYSTEM

Neutrophils, first discovered by Paul Ehrlich in 1880 [1], are polymorphonuclear leukocytes recognized as essential effector cells of the innate immune system [2, 3]. Produced by the bone marrow, neutrophils comprise 50-70% of all nucleated cells with an estimated daily production of up to 2 x 10^{11} cells [4]. Neutrophils undergo several maturation stages characterized by changes the in nuclear morphology and sequential formation of granules [5, 6]. The early myeloblast and promyelocyte stages display banded and non-segmented nuclei, respectively [5]. The start of granule formation marks the transition from the myeloblast to promyelocyte stage, during which primary (azurophil) granules are formed [5, 6]. Azurophilic enzymes, including myeloperoxidase (MPO) and elastase [5-7], exert microbicidal properties and contribute to the digestion of microorganisms [6, 8, 9]. Specific (secondary) granule enzymes, including lactoferrin that exerts antibacterial properties [10, 11] and gelatinase granule enzymes that are critical for neutrophil migration [12, 13], are filled at the myelocyte and metamyelocyte stages, respectively [6]. From the metamyelocyte stage, the nucleus continues to form distinct lobes until the neutrophil becomes a fully mature polymorphonuclear cell [5].

Neutrophils are critical to the innate immune response. They are traditionally recognized as the first leukocytes recruited to the sites of inflammation [2, 3] with the ability to migrate to secondary lymphoid organs, including the lymph nodes [14-16]. CXC motif chemokine receptors 2 (CXCR2) and 4 (CXCR4) antagonistically mediate the release

of neutrophils from the bone marrow [17, 18] and inflammatory mediators, including interleukin-8 (IL-8) and leukotriene B4 (LTB4), facilitate the activation and initiation of the leukocyte recruitment cascade, including diapedesis toward the site of inflammation [19-21]. Neutrophils cooperate with other immune cell types to effectively mediate the inflammatory response and eliminate pathogens.

Increasing evidence demonstrates that neutrophil cross-talk with innate and adaptive immune cells results in a potent immune response. For example, macrophage interactions with apoptotic or activated neutrophils in a model of *Mycobacterium tuberculosis* infection demonstrated enhanced microbicidal activity and upregulation of pro-inflammatory cytokines, including tumor necrosis factor- α (TNF-α) and interleukin-6 (IL-6) [22, 23]. Further, supernatant from mouse neutrophil culture, previously exposed to *Toxoplasma gondii*, was shown to induce the maturation of bone marrow-derived dendritic cells and production of cytokines TNF and interleukin-12 (IL-12) [24]. Human neutrophils have been demonstrated to induce the maturation of monocyte-derived dendritic cells mediated through Mac-1 and DC-SIGN expressed by neutrophils and dendritic cells, respectively through direct cell-cell contact [25, 26]. Regarding adaptive immune cells, neutrophils were demonstrated to secrete and regulate cytokines that are critical for the maturation and differentiation of B cells, including B cell-activating factor (BAFF) and TNF ligand superfamily 13 (APRIL) [27, 28], and have been shown to facilitate the activation of naïve $CD4^+$ T cells in the lung during infection with *Mycobacterium tuberculosis* [29].

THE FUNCTIONS OF NEUTROPHILS IN ACUTE AND CHRONIC INFLAMMATORY CONDITIONS

The role of neutrophils during acute infection

During acute inflammatory conditions, signals, including danger-associated molecular patterns (DAMPs) released by damaged or dying cells and toll-like receptors (TLRs) expressed on sentinel cells, induce the rapid recruitment of neutrophils to the site of inflammation [2, 30, 31]. Neutrophils and other myeloid cells attempt to contain the infection, consequently reducing the risk of systemic inflammation [2, 32]. However, in cases where myeloid cells are overwhelmed, the demand for granulocytes dramatically increases. A switch from steady-state granulopoiesis to emergency granulopoiesis, characterized by rapid *de novo* generation and release of immature and mature neutrophils into peripheral blood, occurs to replenish dying cells [32].

Once at the site of infection, neutrophils employ multiple mechanisms to eliminate invading pathogens. Pro-inflammatory cytokines, including granulocyte colony-stimulating factor (G-CSF), interleukin-1β (IL-1β), and TNF-α, play critical roles in the activation of nicotinamide adenine dinucleotide phosphate (NADPH) oxidase [33-36]. NADPH oxidase produces reactive oxygen species (ROS); mainly superoxide anion and hydrogen peroxide [37]. Phagocytosis, the ingestion of microbes or foreign material, involves hydrolytic enzymes including lysozyme, lipases, and proteases. These antimicrobial proteins are secreted into the phagosome to break down pathogens and further promote ROS release, enhanced by exposure to cytokines tumor necrosis factor-β (TNF-β) or interferon-γ (IFN-γ) [2, 38, 39].

NETosis, discovered by Volker Brinkmann in 2004, is a novel mechanism by which neutrophils release neutrophil extracellular traps (NETs) [40]. NETs are large web-like structures of decondensed chromatin containing microbicidal proteins to kill large pathogens [40, 41]. Accumulating evidence suggests NETs prevent the dissemination of pathogens by their direct elimination utilizing proteases and antimicrobial proteins [41-43]. NETs have been demonstrated to reduce the activation threshold of T cells, enhancing T cell response to antigens providing a bridge between the innate and adaptive immune systems [44].

The role of neutrophils during chronic inflammatory diseases

Though neutrophils play a critical role in the initial host defense, compelling evidence has provided a deeper appreciation for neutrophils as a dynamic cell population with diverse functions in chronic inflammatory settings. Pathologically-activated neutrophils recruited by inflammatory mediators, IL-1β, IL-12, GM-CSF, TGF-β, and TNF-α [45-49], express elevated levels of programmed-death ligand 1 (PD-L1) and exert immunosuppressive functions including interference with T-cell signaling and function through release of arginase-1, peroxynitrite, and hydrogen peroxide.

Primed neutrophils can contribute to a chronic inflammatory disease state through several mechanisms, including the synthesis and secretion of cytokines and chemokines. Activated neutrophils continually produce TNF-α, IL-1β, IL-12, and TGF-β, which serve as inflammatory mediators to sustain the activation of neutrophils and other immune cells [45-48]. In addition, stimuli including TNF-α and granulocyte-macrophage colony-stimulating factor (GM-CSF) promote the production and release of IL-8 [50], critical to

neutrophil functions including respiratory burst, degranulation, and chemotaxis [51, 52]. Further, chemotactic factors released by cancer cells have been shown to activate and recruit alternatively differentiated neutrophils, thus promoting their tumor-protective effects. Chemokine receptor agonists CXCR1 and CXCR2 have been suggested to serve as critical mediators of cancer-associated NETosis [53, 54].

Emerging evidence strongly suggests that excessive and deregulated NET formation promotes the development of multiple chronic inflammatory diseases, including arterial thrombosis [55, 56], cardiovascular diseases (CVD) [57-59], and cancer [60-63]. NETs provide a scaffold for platelets and red blood cells and promote the release of procoagulant factors including tissue factor and platelet factor XII, resulting in thrombus formation [55, 64]. NETs have been implicated in the development of cancer-associated thrombosis in multiple cancer models, including mammary and lung carcinomas [60]. Strong associations between NET formation and the frequency of neutrophils in the TME have been described [65, 66]. NETs have been imaged in the tumor microenvironment (TME) [67, 68]. Cedervall et al. demonstrated the ability of NETs to trap circulating tumor cells that subsequently survive and proliferate thus promoting metastasis [69].

Neutrophil phenotype and function are inevitably influenced by several factors, including the extracellular environment and cytokine milieu. Studies have demonstrated that the reprogramming of myeloid differentiation in the bone marrow due to the cytokine environment results in a profound shift of neutrophil phenotype and function in disease [70, 71]. Specific research into distinct neutrophil subpopulations and their functions have contributed to our understanding of the diverse roles neutrophils play in chronic inflammatory diseases.

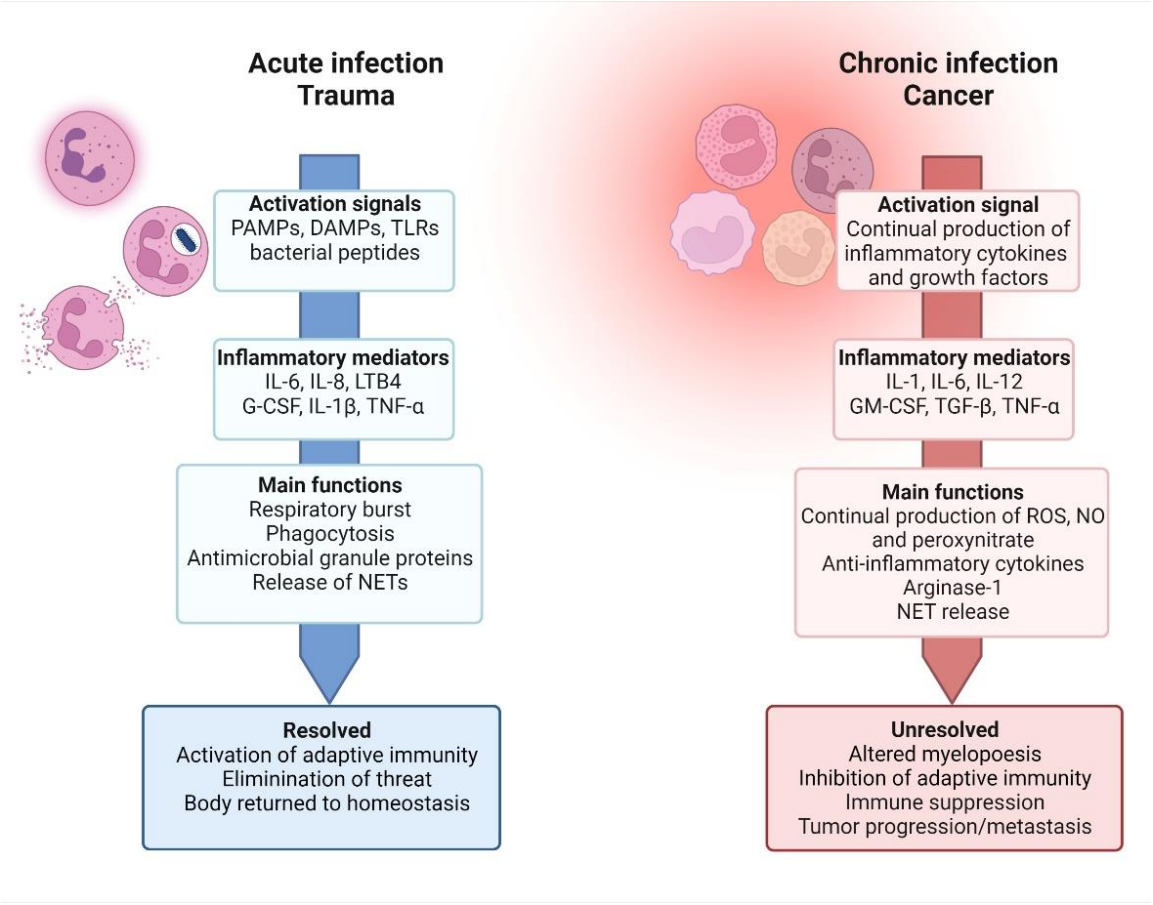

Figure 1. Neutrophil functions in acute and chronic inflammatory diseases. Left panel: acute infection or acute trauma-associated activation signals, including pathogen-associated molecular patterns (PAMPs), danger-associated molecular patterns (DAMPs), toll-like receptors (TLRs) ligands, and bacterial peptides, mobilize neutrophils from the bone marrow mediated by interleukin-8 (IL-8) and granulocyte-colony stimulating factor (G-CSF). Classic neutrophil functions activate the adaptive immune system and eliminate the threat. Right panel: chronic infection or cancer-associated activation signals, including the consistent production of inflammatory cytokines, continually activate neutrophils and promote alternative and immunosuppressive functions, including consistent production of reactive oxygen species (ROS), nitric oxide (NO), and release of neutrophil extracellular traps (NETs), contributing to the inhibition of adaptive immunity and immune suppression. Created with BioRender.com

NEUTROPHIL HETEROGENEITY AND FUNCTIONS OF DISTINCT SUBPOPULATIONS

The knowledge regarding the phenotypic, functional, and transcriptional diversity of neutrophils has substantially increased due to the identification of novel neutrophil subpopulations in acute and chronic inflammatory conditions [70, 72-75]. The discovery of neutrophil subpopulations with specific roles and functions in disease has changed our understanding of neutrophil plasticity and their potential clinical implications [76, 77]. These observations strongly suggest that neutrophil progenitors, immature, and mature neutrophil subpopulations have critical and distinct roles in inflammatory diseases.

Neutrophil progenitor subpopulations

A proliferating subpopulation of neutrophil progenitors, preNeus, was first identified by Evrard et al. in 2018 [76]. PreNeus were observed to be expanded in the bone marrow and spleen during conditions of immune stress induced by sepsis or tumor-related factors [76]. Subsequent studies performed by Kwok et al. and Dinh et al. in 2020 independently described additional early neutrophil progenitors, including proNeu1, proNeu2, and eNeps [77, 78]. Kwok et al. described subpopulations proNeu1 and proNeu2 that represent early committed neutrophil progenitor and intermediate neutrophil progeny, respectively, and mapped the neutrophil development process using combinatorial methods based on single-cell sequencing technologies [77]. They proposed that proNeu1 was the first committed neutrophil progenitor that arose from the granulocyte-monocyte progenitor (GMP) which then matured into proNeu2, preNeu, and finally progressed to the immature neutrophil stage corresponding to myeloblasts [77]. They further observe that the proNeu1

subpopulation was expanded in the early phases of a sepsis model; however, both proNeu1 and proNeu2 could give rise to mature neutrophils [77].

Dinh et al. proposed that early neutrophil progenitors (eNeps), which co-express CD71 and CD117, serve as precursors to preNeus [78]. In addition, the study identified five separate neutrophil subpopulations in the bone marrow that integrate into the neutrophil maturation pathway [76, 78]. Though Zhang et al. provide a detailed summary regarding the knowledge of identified neutrophil subpopulations, it remains unclear whether the immature subpopulations and progenitors develop into functionally distinct neutrophils [79]. These data strongly suggest a critical role for neutrophil progenitor subpopulations in disease and provide the foundation for potential therapeutic interventions. The infusion of proNeus in the bone marrow after stem cell transplantation was proposed as a potential approach to rapidly repopulate neutrophils and strengthen the immune system [77].

In addition to neutrophil progenitor subpopulations, a $Ly6G^{lo}CXCR2^{-}CD101^{neg}$ immature neutrophil subpopulation in mice was observed to be positively correlated with tumor burden in an orthotopic pancreatic tumor model suggestive of immunosuppressive activity [76]. Further, $CD71^{+}$ immature neutrophils were reported to be expanded in the circulating blood and TME in melanoma patients [78].

Low-density neutrophils

Hacbarth and Kajdacsy-Balla first discovered a subpopulation of neutrophils in patients with systemic lupus erythematosus (SLE) that exhibited lower density and co-localized with monocytes and lymphocytes in the peripheral blood mononuclear cell (PBMC) layer after density gradient centrifugation [75]. Patients with SLE had a

significantly higher frequency of low-density neutrophils (LDNs) compared to healthy donors [75]. LDNs have since been described to be expanded in other conditions, including autoimmune diseases, human immunodeficiency virus-1 (HIV-1), CVD, common variable immunodeficiency syndrome (CVID), and cancer [70, 73, 80, 81].

LDNs exert immunosuppressive functions including interference with T-cell function and differentiation and ROS production [82, 83]. LDN frequency was positively correlated with decreased expression of the zeta chain of the T-cell receptor (TCR) primarily used in T-cell signaling [83]. LDNs are shown to be resistant to ROS through Nrf2 [84]. Recent studies have demonstrated that LDNs can release hydrogen peroxide upon bacterial stimulation or in cancerous conditions inhibiting T-cell function [83, 85]. Further, LDN-derived ROS has been demonstrated to modify the TCR, resulting in the interference with T-cell binding to major histocompatibility complexes (MHCs) and induction of antigen-specific tolerance [86]. Our laboratory had previously reported that the frequency of LDNs are significantly increased in HIV-1-infected patients and the expression of PD-L1 on LDNs increases upon co-incubation of LDNs with HIV-1 virions [80]. Additionally, we observed reduced expression of the zeta chain of the TCR correlated with high PD-L1 expression on neutrophils.

Previously studied as one subpopulation, the phenotypic, transcriptional, and functional heterogeneity of LDNs has become increasingly appreciated. Sagiv et al. reported that LDNs consist of immature (imLDN) and mature (mLDN) subpopulations, indicated by differences in nuclear morphology and size in peripheral blood of lung and breast cancer patients [70]. In addition, CD10 expression, associated with mature neutrophils [87], was reported to be absent on imLDNs in SLE and cancer patients [74,

88]. Detailed transcriptional analyses reveal that $CD10^-$ imLDNs exert enhanced transcriptional activity demonstrating an upregulation of genes associated with cell cycle progression and decreased expression of genes related to chemotaxis [74]. In addition, $CD10^-$ imLDNs displayed increased expression of transcription factors GF11 and CEBPE which were previously reported to be expressed by neutrophil progenitors [74, 76]. $CD10^+$ mLDNs demonstrated upregulated expression of genes associated with Type-I IFN signaling and phagocytosis relative to $CD10^-$ imLDNs [74].

A deeper investigation is needed to elucidate the distinct functions of imLDN and mLDN subpopulations; however, multiple studies have indicated that LDN subpopulations have distinct functional capabilities [74, 88, 89]. Mistry et al. showed that imLDNs released significantly higher amounts of MPO relative to mLDNs, but were impaired in their ability to form NETs spontaneously [74]. mLDNs demonstrated increased chemotaxis and phagocytosis relative to imLDNs [74]. In malignant conditions, imLDNs were shown to promote the survival and proliferation of T-cells, whereas mLDNs inhibited T-cell proliferation mediated by the release of arginase [88]. Further, Hsu et al. demonstrated that imLDNs contain enhanced global bioenergetic capacity utilizing glutamate and proline catabolism in the absence of glucose and facilitate liver metastasis formation [89].

THE ROLES OF MONOCYTES IN THE IMMUNE SYSTEM

Monocytes are mononuclear phagocytes derived from common monocyte progenitors (CMoPs) in the bone marrow [90]. They comprise an estimated five to ten percent of peripheral leukocytes in humans and are traditionally recognized as circulating precursors to monocyte-derived cells, including macrophages and monocyte-derived dendritic cells, following tissue extravasation [91-93]. However, the phenotypic and

functional heterogeneity of monocytes has become more appreciated in recent years [94-96]. Passlick et al. first identified two monocyte subsets in humans: classical ($CD14^{+}CD16^{-}$) and non-classical (patrolling) ($CD14^{low}CD16^{+}$) with an additional transitional phase identified as intermediate monocytes ($CD14^{+}CD16^{+}$) [94].

Classical monocytes constitute the majority of the monocyte pool in humans and following the release from the bone marrow, extravasate into tissues and differentiate into monocyte-derived cells or convert to non-classical monocytes in circulation under homeostatic conditions [91, 93, 97]. During inflammatory conditions, classical monocytes recruit other monocytes and dendritic cell precursors mediated by CCR2 chemokine signaling and antimicrobial factors [98, 99]. In addition, classical monocytes perform phagocytosis, participate in tissue repair and antigen presentation [99], and are suggested to play a key role in the induction of specific T-cell subsets, including cytotoxic and helper T-cells [100, 101]. Four distinct classical monocyte subsets have been recently discovered through high dimensional mass cytometry in coronary artery disease (CAD) warranting further investigation into their functional heterogeneity [102].

Non-classical or patrolling monocytes are estimated to have a lifespan of seven days in humans and are known to patrol the vasculature, including arterioles and venules, for cellular debris utilizing lymphocyte function-associated antigen (LFA-1) and C-X3-C motif chemokine receptor 1 (CX3CR1) [97, 103]. Patrolling monocytes recruit neutrophils to dispose of damaged endothelial cells through toll-like receptor 7 (TLR7) signaling and are suggested to promote tissue repair through the tightly regulated release of inflammatory cytokines [104]. Patrolling monocyte subsets have been described in chronic inflammatory diseases, including HIV-1, Crohn's disease, and CAD [102, 105]. Mass cytometry reveals

at least three distinct patrolling monocyte subsets [102]. A SLAN/M-DC8^{+} patrolling monocytic subset, with a distinct transcriptional profile, was demonstrated to produce substantial amounts of TNF-α and suggested to be a central player in the hyper-activation of the immune system in HIV infection [102, 105]. Independently, expansion of the SLAN/M-DC8^{+} monocytic subset was reported to be positively correlated with CAD severity [102]. More information is needed to understand the role of this subset in other diseases.

THE ROLE OF MYELOID SUBPOPULATIONS IN CANCER

A new paradigm is emerging regarding the role of myeloid cell subsets in tumorigenesis and metastasis. Multiple studies demonstrate that sustained inflammation due to properties of the TME and cytokine milieu promote altered myelopoiesis and the release of physiologically distinct myeloid cell subsets [71, 106]. Specifically, the characterization of distinct myeloid-derived suppressor cell (MDSC) [107], monocyte [108], and neutrophil phenotypes [70], has contributed significantly to the current knowledge of tumorigenic properties.

Myeloid-derived suppressor cells

MDSCs are immunosuppressive cells that are expanded in multiple cancer types, are implicated in promoting tumor progression, and are associated with poor clinical outcomes [109-111]. MDSCs are further subdivided into two subpopulations: monocytic (M-MDSC) and polymorphonuclear or granulocytic (PMN-MDSC/G-MDSC), characterized in humans as CD33^{+}CD15^{-}HLA-DR^{low}CD11b^{+}CD14^{+} and CD33^{int}CD15^{+}CD66b^{+}CD11b^{+}CD14^{-}, respectively. M-MDSCs display a similar phenotype to monocytes while PMN-MDSCs resemble neutrophil phenotype and

morphology [106, 112]. While M-MDSCs are distinct from monocytes and macrophages, PMN-MDSCs are considered mostly synonymous with LDNs [113]. Lectin-type oxidized LDL receptor 1 (Lox-1) expression was recently proposed as a marker to identify PMN-MDSCs in cancer [114] but has not yet been verified in other diseases.

M-MDSCs and PMN-MDSCs utilize different mechanisms to perform their immunosuppressive functions [109]. M-MDSCs produce nitric oxide to suppress effector T-cell responses [106, 115]. PMN-MDSCs produce ROS to generate peroxynitrite interfering with T-cell signaling, migration, and function, and release arginase-1 (arg-1), in both antigen specific and non-specific manner [86, 109, 116]. In addition, PMN-MDSCs directly promote the differentiation of naïve $CD4^+$ T-cells or Th17 cells into T-regulatory (T-regs) cells via production of soluble factors including TGF-β [117, 118]. While M-MDSCs are reported to have increased immunosuppressive activity relative to PMN-MDSCs, PMN-MDSCs are found at significantly higher frequencies in most cancers, suggesting that both populations have potent roles in systemic immune suppression [106, 109].

Monocytes and macrophages

Investigations regarding the phenotypic and functional changes in cancer-induced monopoiesis have primarily focused on the characterization of tumor-associated macrophages (TAMs) [108]. The M1 and M2 phenotypes are characterized by protumoral and anti-tumoral functions, respectively [108]; however the current knowledge regarding the role of circulating monocytes in cancer settings remain limited. Several studies have reported the downregulation of costimulatory molecules including CD86, and of MHC class II cell surface receptor HLA-DR on circulatory monocytes [119-121]. Decreased

HLA-DR expression has been associated with poor survival in melanoma and remission in pediatric lymphoproliferative malignancies [119, 121].

In cancerous conditions classical monocytes have demonstrated altered responses when exposed to inflammatory stimuli, including lower STAT1 phosphorylation and impaired secretion of TNFα [122, 123]. Classical monocytes are hypothesized to give rise to TAMs due to the positive correlations observed between monocyte and macrophage frequencies in malignancy, but this has not been determined experimentally [124, 125]. Multiple studies demonstrate a significant downregulation of HIF1α on classical monocytes, suggesting that the classical monocyte response in cancer-induced hypoxic environments may be impaired [123, 126].

Interest in patrolling monocytes has increasingly grown with the identification of distinct subpopulations in cancerous conditions including $Tie2^{+}$ monocytes [127]. Tie2-expressing monocytes comprise an estimated twenty percent of circulating monocytes and have been demonstrated to play an important role in angiogenesis and secrete pro-angiogenic factors, including VEGF and COX2 [127, 128]. Similar to classical monocytes, patrolling monocytes are suspected to give rise to TAMs and tumor-promoting cells [129, 130]. A study in MM suggests that patrolling monocytes act as precursors to osteoclasts, which promote the proliferation of myeloma cells through direct cell-to-cell contact [129, 131].

The expansion of circulating monocyte subsets, specifically intermediate monocytes, has been proposed as a biomarker for diagnosing breast cancer and oral squamous cell carcinoma [132, 133]. The lymphocyte to monocyte ratio (LMR) has been suggested as a prognostic factor in malignancies, including pancreatic, colorectal, and

ovarian cancer. The meta-analyses reveal that low LMR significantly predicts poor overall survival and disease-free survival, whereas high LMR is associated with better overall survival [134-136].

Neutrophils

Increased frequency of tumor-associated neutrophils (TANs) and high neutrophil-to-lymphocyte ratios (NLRs) have been previously correlated with poor clinical outcomes [137-140]. There is a growing interest in the characterization of TANs and their functions in the TME. TANs can exert both pro- and anti-tumoral functions within the TME [141, 142]. Pro-tumoral functions of TANs include the secretion of tumor-promoting and pro-angiogenic factors and enzymes including neutrophil elastase, oncostatin M, vascular endothelial growth factor, and MMP9 [143-146]. MMP9 participates in the remodeling of the extracellular matrix, promoting tumor cell dissemination and angiogenesis [142, 147]. However, neutrophils have been suggested to inhibit the proliferation of tumor cells through the production of TNF-related apoptosis-inducing ligand (TRAIL), which induces apoptosis when bound to its receptor [148]. In addition, transfection with G-CSF was associated with inhibition of tumor growth due to an influx of neutrophils at the tumor site in a colon adenocarcinoma model [149].

Recently, two distinct phenotypes of TANs have been described and provide more clarity regarding neutrophil polarity and contrasting functions. TGF-β predominantly regulates TAN polarization resulting in two distinct phenotypes: N1 and N2 [150, 151]. N1, characterized by high TNF-α and low arg-1 levels [151], exerts anti-tumoral effects through antibody-dependent cytotoxicity, increased NADPH oxidase activity, and activation of other immune cells, including T and B lymphocytes and dendritic cells [141,

150, 152-154]. Conversely, N2 TANs, characterized by the upregulation of chemokine ligands CCL4, CCL12, and IL-8 [151], have demonstrated pro-tumoral effects through the production of arginase, activation of T-regs, and recruitment of other immunosuppressive cells, including macrophages [150, 151, 155].

Reports regarding N1 TANs are limited to *ex vivo* experiments in which N1 polarization was induced by the manipulation of the concentration of cytokines in a controlled environment. Jablonska et al. demonstrated that endogenous IFN-β could polarize TANs to an N1 phenotype [156]. N1 and N2 dynamics were further investigated with the depletion of TANs at varying stages of tumor progression in a mouse model of Lewis lung carcinoma [157]. Investigators reported that TANs from early tumor stages demonstrated higher cytotoxicity and produced elevated NO and hydrogen peroxide; however, TANs from later stages of tumor progression acquired a pro-tumorigenic N2 phenotype [157]. Whether N1 TANs are only inducible through *ex vivo* manipulation or result from the biological reprogramming of the TME remains to be elucidated.

Table 1. Myeloid cell subpopulations in cancer.

Myeloid cell subpopulations in cancer						
Feature/ Characteristic	**Neutrophils**	**Monocytes**			**MDSCs**	
		classical	**intermediate**	**patrolling**	**granulocytic**	**monocytic**
Phenotypic markers (human)	$CD15^{+}$ $CD14^{lo}$ $CD11b^{+}$ $CD66b^{+}$ $CD54^{hi}$ $CD10^{hi}$	$CD14^{+}$ $CD16^{-}$ $CCR2^{+}$ $CX3CR1^{lo}$ $HLA\text{-}DR^{+}$	$CD14^{+}$ $CD16^{+}$ $CCR2^{lo}$ $HLA\text{-}DR^{+}$	$CD14^{low}$ $CD16^{+}$ $CCR2^{-}$ $CX3CR1^{+}$ $HLA\text{-}DR^{+}$	$CD33^{int}$ $CD15^{+}$ $CD66b^{+}$ $CD11b^{+}$ $CD14^{-}$ $LOX\text{-}1^{+}$ $CD84^{+}$	$CD33^{+}$ $CD15^{-}$ $HLA\text{-}DR^{lo}$ $CD11b^{+}$ $CD14^{+}$ $CD84^{+}$ $CXCR1^{+}$
Phenotypic markers (mouse)	$Ly6G^{+}$ $Ly6C^{lo}$ $CD11b^{+}$	$Ly6C^{hi}$ $CD43^{lo}$ $CX3CR1^{lo}$	$Ly6C^{int}$ $CD43^{hi}$ $CX3CR1^{hi}$	$Ly6C^{lo}$ $CD43^{hi}$ $CX3CR1^{hi}$	$Ly6G^{+}$ $Ly6G^{+}$ $Ly6C^{lo}$ $CD11b^{+}$ $CD84^{+}$	$Ly6G^{-}$ $Ly6C^{hi}$ $CD11b^{+}$ $CD84^{+}$
Developmental/ polarization factors	GM-CSF G-CSF SCF	GM-CSF SCF IL-3 IL-6	inflammatory factors	inflammatory factors	GM-CSF IL-1β IL-6 HIF1a VEGF	M-CSF HIF1a VEGF
Functions	Antitumoral: Antibody-dependent cytotoxicity, increased NADPH oxidase, activation of T and B lymphocytes Protumoral: Arginase production, activation of T-regulatory cells, recruitment of immune-suppressive cells	Phagocytosis induction of specific T-cell subsets	Undetermined	Recruitment of neutrophils, release of inflammatory cytokines, angiogenesis	Production of ROS generating peroxynitrite interfering with T-cell signaling, migration, and function	Production of nitric oxide and arginase to suppress effector T cells
Differentiation stage(s)	Neutrophils with mostly segmented nuclei	Differentiation to TAMs or conversion to patrolling monocytes	Differentiation to patrolling monocytes	Suspected to differentiate into TAMs	Neutrophils with banded and segmented nuclei	Differentiation into TAMs
Clinical associations	NLR used as prognostic marker in many cancers (colorectal, prostate)	Low LMR predicts poor overall survival	Frequency proposed as a biomarker for breast cancer and oral squamous cell carcinoma	Suspected to contribute to myeloma development in the bone marrow	Higher frequency associated with poor overall outcome in malignancy	Higher frequency associated with poor overall outcome in malignancy

References (human): [97, 114, 129, 130, 158-160]

References (mouse): [70, 130, 158]

MULTIPLE MYELOMA

Multiple myeloma is a hematological malignancy characterized by the accumulation of terminally differentiated plasma cells and development of end-organ damage, including renal insufficiency, hypercalcemia, anemia, and formation of lytic bone lesions [161, 162]. The prevalence of developing precursory diseases, including monoclonal gammopathy of undetermined significance (MGUS), disproportionately affects Black Americans and increases with older age with most patients experiencing a long pre-clinical phase prior to diagnosis with MM [163-166]. While MGUS has a low risk of progression to MM [167], the development of the intermediate precursor condition, smoldering multiple myeloma (SMM), has a significantly higher risk with a reported fifty-one percent of patients progressing to MM within five years [168]. Although notable advancements have been made in the prognosis and treatment of MM, it is an inevitably fatal disease currently accounting for an estimated twenty-two percent of deaths in the United States due to hematological malignancies [169].

This dissertation utilizes the current MM definition and diagnoses guidelines based on the 2014 International Myeloma Working Group [162]. These criteria state that the diagnosis of MM requires the presence of clonal bone marrow plasma cells (BMPCs) > 10 percent or biopsy-proven plasmacytoma (extramedullary or bony) and the presence of one or more MM-defining events. MM-defining events may include organ damage (hypercalcemia, renal insufficiency, anemia, presence of lytic bone lesions, or severe osteopenia), BMPCs > 60 percent, involved to uninvolved serum free light chain (FLC) ratio > 100, or greater than one focal bone lesion detected by magnetic resonance imaging (MRI). Although several demographic characteristics, including age, sex, race, family

history, and obesity, have been well documented as risk factors for MM, the association between chronic inflammation and tumorigenesis in MM remains largely unexplored [170-172].

Immune control by neutrophil subpopulations

Knowledge regarding innate immunological dysregulation in MM is limited. Multiple studies have demonstrated that NLR at diagnoses, and separately > 100 days after autologous stem cell transplantation, can predict outcome in MM patients [173-175]. Due to the infiltration of neoplastic cells in the bone marrow, neutrophils have been shown to have increased arg-1 expression and reduced lysozyme activity [176, 177]. Several studies have investigated the roles of myeloid cells in sustaining or promoting MM. PMN-MDSC frequency is increased in MM and was found to correlate with the frequency of T-regulatory cells [178, 179]. PMN-MDSCs have been shown to confer protection to MM cells from chemotherapy-induced cytotoxicity [180], inhibit T cells, and regulate the growth of MM cells in the BME [179]. In addition, arg-1 is observed to be upregulated in PMN-MDSC and associated with CD64 expression and STAT3 signaling [176, 181]. Decreased phagocytic capacity and ROS production have also been reported [181]. Recently, soluble factors in sera from MM patients were demonstrated to induce autophagy in neutrophils, which was suggested to upregulate survival signals within the plasma cell niche of the BME [182].

Crosstalk between myeloid subpopulations and cells in the TME

Experimental models suggest neutrophils, LDNs, and PMN-MDSCs play an important role in MM pathogenesis [183, 184]. Giallongo et al. showed that mesenchymal stem cells from MM promoted the generation of immunosuppressive PMN-MDSCs [183].

These PMN-MDSCs demonstrated bone resorption ability as indicated by the presence and number bone pits, and were able to digest significantly more bone matrix relative to MDSC generated from HD or MGUS patients [183]. In addition, MM cells were shown to promote the development of MDSCs that induced MM cell growth in a bidirectional manner [184]. Other myeloid cell subpopulations, including patrolling monocytes and macrophages, have been implicated in the progression of MM promoting osteoclast formation and angiogenesis [129, 185]. Eosinophils have been observed to accelerate MM progression in synergy with IL-17-producing cells induced by gut microbiota [186]. Although there is a clear relationship between myeloid cells and MM progression, further investigations are needed to elucidate the mechanisms and functions promoting MM disease. Several studies have identified critical molecules that promote chronic inflammation and immune suppression in MM, leading to new investigations into therapeutic approaches.

Novel immune targets

Although current front line therapies are evidenced to reduce immune suppression in the BME of MM, there has been a growing interest in new immunotherapeutic targets [187]. Recently, several studies have implicated IL-18 as a critical contributor to disease progression in MM. IL-18 is suggested to activate TAMs, promote the expansion of natural killer cells, and regulate the maturation of MDSCs in MM [188-190]. Nakamura et al. show that mice deficient in IL-18 exhibited protection against MM progression [188]. CD84, previously identified as a critical receptor in regulating the survival of chronic lymphocytic leukemia cells, was found to be associated with the upregulation of MDSC-promoting genes [191, 192]. CD84 expression was positively correlated with PD-L1 expression on MDSCs [192]. Although IL-18 and CD84 are suggested to be critical regulators of immune

suppression in MM, further investigations are needed to determine their therapeutic potential.

PLATELET-LEUKOCYTE INTERACTIONS AND COMPLEXES

Platelets are major contributors to the development of pathologic conditions such as thrombosis and inflammation and are activated through exposure to platelet agonists, including adenosine diphosphate (ADP) and pro-coagulant factors [193, 194]. Activated platelets are known to prime neutrophils and monocytes enhancing their adhesion to the vascular endothelium, response to chemokines, and production of cytokines [195-198]. Activated platelets form neutrophil-platelet complexes (NPCs) and monocyte-platelet complexes (MPCs) which increase their functionality in pro-inflammatory conditions [199-201].

Leukocyte-platelet complex formation is predominantly mediated by P-selectin (CD62P) expressed on platelets, and P-selectin glycoprotein ligand-1 (PSGL-1) expressed on monocytes and neutrophils [202-204]. These interactions are further stabilized through the binding of platelet glycoprotein Ibα to MAC-1 (CD11b/CD18) [205]. Activated platelets secrete sCD40, which binds CD40L on leukocytes promoting complex formation [206, 207]. Platelet-leukocyte complexes or aggregates are increased in many chronic diseases. Increased NPC and MPC frequencies have been reported during bacterial infection, sepsis, cardiovascular disease, COVID-19, and cancer with recent studies characterizing the interactions between platelets and specific monocytic subsets [208-213].

Monocyte-platelet interactions

MPCs are suggested to play an important role in disease pathogenesis with monocyte-platelet interactions exhibiting increased monocyte phagocytosis, ROS

production, and cytokine secretion mediated through platelet factor 4 (CXCL4) [214-217]. Preliminary data demonstrate that different platelet activators can promote downstream M1 or M2 polarization [216, 217]. Hemoglobin-activated platelets were demonstrated to promote the differentiation of classical monocytes to a pro-inflammatory M1-like phenotype, indicated by elevated levels of TNF-α and IL-1β [216]. Separately, platelets were observed to skew monocytes to an M1-like phenotype in the presence of lipopolysaccharide, which was shown to be dependent upon the GPIb-CD11b axis [217]. ADP-stimulated platelets have been suggested to promote the conversion of intermediate monocytes to patrolling monocytes that differentiate into M2-like macrophages [215].

Neutrophil-platelet interactions

NPCs are suggested to play an important role in the immune response during inflammatory diseases. Neutrophil-platelet interactions are observed to promote neutrophil activation and recruitment, phagocytosis, ROS production, and NETosis [199, 218, 219]. P-selectin-deficient platelets in a mouse model of acute lung injury failed to induce NETosis due to inadequate binding of neutrophils and platelets resulting in decreased NPC formation [220]. Consistent with this study, Zhang et al. reported co-cultured neutrophils and platelets with enhanced P-selectin expression resulted in elevated NET production [221].

The effect of the interactions between specific neutrophil subsets and platelets remains under-investigated. A study in psoriasis demonstrated a positive correlation between the frequency of LDN-platelet aggregates with the signs of early atherosclerotic non-calcified coronary burden [222]. The study suggests LDN-platelet aggregates may significantly contribute to the development of cardiovascular-related comorbidities [222].

Recently Lecot et al. showed that platelets form NPCs preferentially with LDNs which demonstrated distinct molecular signatures related to enhanced chemotaxis and migration in cancer patients [223].

Platelet engulfment by leukocytes

Interestingly, several case studies have reported the engulfment of platelets by leukocytes in different diseases and conditions [224-228]. In 2001 Criswell et al. demonstrated that majority of platelets appeared to be phagocytosed by neutrophils and monocytes in a rare case of EDTA-dependent pseudothrombocytopenia [226]. Neutrophil and monocyte phagocytosis has been reported in cases of malignant hypertension, bacteria-induced thrombocytopenia, acute myocardial infarction, and end stage renal disease [225, 227-229].

Maugeri et al. were the first to propose a mechanism to this phenomenon [225]. They demonstrated that neutrophils rapidly phagocytose platelets activated by thrombin receptor activator peptide-6 (TRAP-6). The phagocytic clearance of platelets is dependent on platelet-leukocyte adhesion mediated by the P-selectin/PSGL-1 axis and activation of β2-integrin Mac-1 [225]. The authors propose that blocking of the P-selectin/PSGL-1 axis results in decreased neutrophil degranulation contributing to the regulation of vascular inflammation [225]. However, the implications of neutrophil-platelet interactions on the low-density phenotype remain to be elucidated.

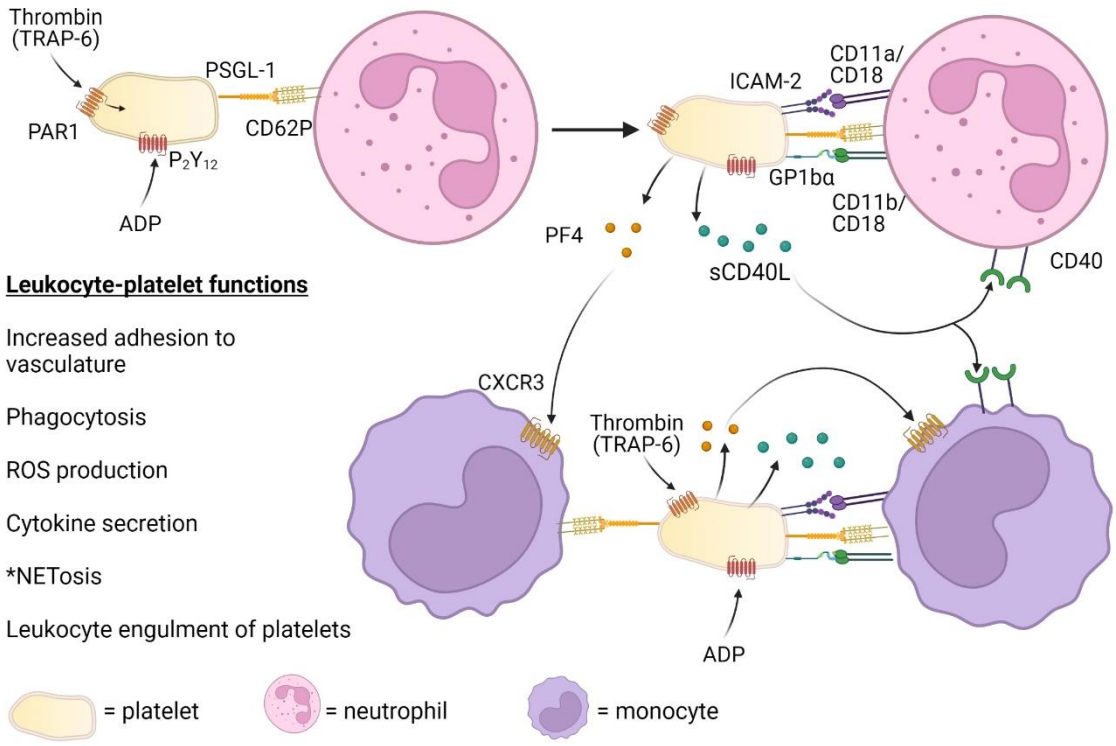

Figure 2. Implications of platelet-leukocyte interactions on myeloid function.
Activated platelets bind to neutrophils or monocytes through the P-selectin (CD62P)/ PSGL-1 axis and MAC-1/ICAM-2 complex. Activated platelets release sCD40L and PF4 promoting further platelet-leukocyte interactions and downstream functions, including increased adhesion to the endothelium, cytokine secretion, and release of neutrophil extracellular traps (NETosis). Neutrophils or monocytes have the ability to engulf platelets. Created with BioRender.com.

SCOPE OF DISSERTATION

A novel paradigm regarding the shift in myeloid cell phenotype and function during acute and chronic inflammatory conditions is emerging. Contributing to the field's current knowledge, this dissertation focuses on the identification and characterization of myeloid subpopulations and leukocyte-platelet interactions in acute and chronic inflammatory states including HIV-1, COVID-19, and MM. We (1) provide a detailed report of the specific phenotypic and functional characterization of mature and immature neutrophil subpopulations expanded in inflammatory diseases; (2) identify an altered myeloid phenotype in MM that is associated with myeloid dysregulation and advanced stage disease; and (3) explore the underlying mechanisms of the low-density neutrophil phenotype focusing on the interactions between platelets and neutrophils. Altogether, this work contributes to our understanding of the changing dynamics of myeloid cells in specific inflammatory environments and their relationship to other immune cells. These findings may significantly impact our understanding of the role of neutrophils and myeloid cells in chronic diseases and contribute to the design of novel therapeutic approaches.

TWO DISTINCT MYELOID CELL PHENOTYPES INDICATE ALTERED MYELOPOIESIS IN PATIENTS WITH MULTIPLE MYELOMA

by

KRYSTLE L. ONG, MARCUS D. DAVIS, KALYN K. PURNELL, HANNAH CUTSHALL, HARISH C. PAL, ASHLEY N. CONNELLY, CHRISTIAN X. FAY, VALERIYA KUZNETSOVA, ELIZABETH E. BROWN, ZDENEK HEL

Submitted to *Frontiers in Immunology*

Format adapted for dissertation

Abstract

Hematologic malignancies, including multiple myeloma (MM), promote systemic immune dysregulation resulting in an alteration and increased plasticity of myeloid cell subsets. To determine the heterogeneity of the myeloid cell compartment in the peripheral blood of patients with MM, we performed a detailed investigation of the phenotype and function of myeloid subpopulations. We report that a subset of MM patients, referred to as MM2, exhibits a specific myeloid cell phenotype indicative of altered myelopoiesis characterized by significant changes in the properties of circulating granulocytic, monocytic, and eosinophilic populations. Compared to healthy controls or MM1 patients, neutrophils from MM2 patients exhibit a less differentiated phenotype characterized by high surface levels of CD64 (FcγRI), low levels of CD10 and CXC chemokine receptor 2 (CXCR2), increased capacity for the production of mitochondrial reactive oxygen species, and an expansion of immature CD15+CD16- neutrophil subset. Classical and patrolling monocytes from MM2 patients express elevated levels of CD64 and markers of activation. MM2 eosinophils display lower levels of C-C Chemokine receptor 3 (CCR3), Toll-like receptor 4 (TLR4, CD284), and tissue factor (TF, CD142). The MM2 phenotype is independent of age, race, sex, and treatment type. Characteristic features of the MM2 phenotype are associated with myeloma-defining events including elevated involved/uninvolved immunoglobulin free light chain (FLC) ratio at diagnosis. Detailed

characterization of an altered myeloid phenotype can improve the monitoring and prognosis of multiple myeloma and provide instrumental tools for the identification of patients with an increased risk of progression to advanced-stage disease.

Introduction

Multiple myeloma (MM) is a malignancy of post-germinal center terminally differentiated plasma cells producing antibodies and complexes of immunoglobulin heavy and light chains (1). Diagnosis is based on several myeloma-defining events including an accumulation of monoclonal plasma cells in the bone marrow microenvironment (BME), the presence of end-organ damage, or, in the absence of end-organ damage, elevated involved to uninvolved immunoglobulin free light chain (FLC) ratio and presence of at least one bone lesion by magnetic resonance imaging (1, 2). The reprogramming of immune cells in MM promotes angiogenesis (3) and immunosuppression (4) contributing to disease progression to extramedullary sites. Chronic inflammatory diseases, including solid and hematological malignancies, are frequently associated with pathologic dysregulation of the myeloid cell compartment including altered neutrophil functions (5). During unresolved chronic inflammation, growth factors contribute to the reprogramming of the BME resulting in altered granulopoiesis and recruitment of transcriptionally and physiologically distinct myeloid cells (6, 7). Recent studies demonstrate the plasticity of innate immune cells, specifically neutrophils (6, 8), polymorphonuclear myeloid-derived suppressor cells (PMN-MDSCs) (7, 9-11), and monocyte subpopulations (12, 13) in chronic pathologic conditions.

Neutrophils represent the most abundant circulating leukocyte population equipped for the sensitive detection of bacterial and viral products during inflammatory responses

(14). Previously, we demonstrated that neutrophils from individuals infected with human immunodeficiency virus-1 exert inhibitory effects on T-cell function and proliferation characterized by programmed death-ligand 1 (PD-L1) expression and release of reactive oxygen species (ROS) (15). Further, interferon-γ stimulation of neutrophils plays a critical role in PD-L1 expression and suppression of lymphocyte proliferation in endotoxemia (16). Reports of immunosuppressive properties of neutrophils and PMN-MDSCs, including increased arginase-1 expression and differences in phagocytic and oxidative burst capacities, support the critical role of neutrophils in fostering the tumor microenvironment promoting myelomagenesis (4, 11, 17). Neutrophils and PMN-MDSCs are expanded in the BME and peripheral blood of patients with MM (9, 18-22), protect MM cells from chemotherapy-induced toxicity resulting in reduced chemoselectivity (23) and inhibit T-cell immune response (24). The neutrophil to lymphocyte ratio is increased in some MM patients and has been utilized to predict outcomes in newly diagnosed patients, patients that have previously undergone autologous hematopoietic stem cell transplant (aHSCT), and transplant ineligible patients in MM. (25-27).

Monocytes, circulating macrophage precursors, are subdivided into classical and non-classical or patrolling monocyte subsets with distinct phenotypes and functions (28). In the BME, increased frequency of patrolling monocytes was observed in patients with MM relative to patients with pre-MM conditions, including monoclonal gammopathy of undetermined significance and smoldering multiple myeloma (13). Patrolling monocytes promote an increase in osteoclast formation by upregulating the expression of IL-21 receptor, supporting a pivotal role of monocytes in MM disease progression (13).

Macrophages from patients with MM use vasculogenic mimicry to contribute to neovessel construction following exposure to angiogenic cytokines (29).

Our knowledge regarding the heterogeneity of granulocytic and monocytic subpopulations, the innate immune phenotype, and how this phenotype affects the presentation of MM patients remains limited. In this study, we investigated the heterogeneity of the phenotypic profiles of neutrophilic, monocytic, and eosinophilic subpopulations in patients with MM and examined the relationship between distinct MM innate immune phenotypes and myeloma-defining events.

Materials and methods

Multiple myeloma study population and control selection

Eligible MM patients with histologically confirmed diagnoses enrolled in the Integrated Molecular And Genetic Epidemiology study (IMAGE) (30) were included. Eligible patients were included from the Integrative Molecular And Genetic Epidemiology study (30). Patients with a diagnosis of MM were identified based on the ICD-9 classifications (203) or International Classification of Disease for Oncology third revision code 9732/3 and confirmed based on revised and updated International Multiple Myeloma Working Group classification criteria for MM (1). Myeloma was defined by the cumulative presence of clonal bone marrow plasma cells > 10 percent or biopsy-proven bony or extramedullary plasmacytoma and presence of one or more MM defining events including organ damage (hypercalcemia, renal insufficiency, anemia, or lytic bone lesions or severe osteopenia, or pathologic fractures attributed to plasma cell proliferative disorder), clonal bone marrow plasma cells > 60 percent, serum involved to uninvolved FLC ratio > 100, or more than one focal bone lesion (> 5 mm) identified as previously reported (1). Each MM

case was reviewed by an expert panel to ensure consistent case definitions and to minimize phenotype misclassification. Patients with extramedullary or solitary plasmacytoma or other plasma cell proliferative disorders were excluded (n=2). An additional 2 MM patients were excluded based on treatment status. After eligibility screening, a total of 35 MM patients, all previously treated as specified in Table 1, were included in this investigation. Diagnostic and defining clinical features including clonal bone marrow plasma cells (%), serum monoclonal (M)-protein, involved to uninvolved FLC ratio > 100, immunoglobulin (Ig) isotype (IgG, IgA), clonality (kappa, lambda), end-organ damage [hypercalcemia (serum calcium, >11.5 mg/dl), renal insufficiency (serum creatinine, >177.0 μmol/L (>2 mg/dl) or estimated creatinine clearance <40 mL/min per 1.73 m2), anemia (normochromic, normocytic with hemoglobin >2 g/dl below the lower limit of normal or hemoglobin <10 g/dl)], bone involvement (radiologic evidence of lytic lesions, severe osteopenia or pathologic fractures1), and the revised and updated International Staging System (R-ISS) (1), and the Durie Salmon (DS) staging system (31) were determined by laboratory studies, medical history or physical examination as appropriate.

Controls were recruited through the 1917 Clinic at Dewberry at the University of Alabama at Birmingham. Eligible controls were 43 years of age and older without a history of monoclonal gammopathy of undetermined significance, smoldering multiple myeloma, MM, or other cancers. Participant characteristics are summarized in Table 1.

Sample collection

All methods were performed in accordance with the relevant guidelines and regulations. Peripheral blood was collected by certified phlebotomists in tubes containing acid citrate dextrose (ThermoFisher, Waltham, MA) from MM patients or controls

following informed consent. Data acquisition was performed by the IMAGE study team. Study protocols were approved by the Institutional Review Board of the University of Alabama at Birmingham (IRB protocols 141218001 and 071106009).

Materials

A/B human serum was purchased from ThermoFisher. All solutions and materials for cell counting and the cell counter were purchased by Nexcelom (Lawrence, MA). Antibodies for flow cytometry were purchased from BioLegend (San Diego, CA) unless indicated otherwise (Supplemental Table 1). Dimethyl sulfoxide (DMSO), Dulbecco's phosphate buffer solution (DPBS), and Ethylenediaminetetraacetic acid (EDTA) were purchased from Corning (Corning, NY). Phorbol myristate acetate (PMA (Sigma Aldrich, St. Louis, MO) was dissolved in DMSO at a concentration of 1mg/ml. 2',7'-dichlorodihydrofluorescein (H2-DCFDA) (Sigma Aldrich) was dissolved in DMSO at a concentration of 1mM. All antibody stain panels were made in 10% A/B human serum in DPBS.

Whole blood staining

Twenty milliliters of ACD-treated blood was collected from MM patients or controls and processed within three hours of the collection as described previously (32). Briefly, fifty microliters of whole blood were stained for 30 minutes with 50 µl of pre-mixed antibodies for the base panel and whole blood staining (Appendix A: Supplemental Methods Table 1) at 4°C. Samples were washed with 4 ml 0.1M EDTA in DPBS and centrifuged at 200 x g for 5 minutes. Red blood cell lysis and fixation was performed in 1 ml of 1x 1-step Fix/lyse buffer (Invitrogen, Waltham, MA) at room temperature for 15 minutes. Samples were washed with 2% fetal bovine serum (FBS) (Atlanta Biologicals,

Atlanta GA) in DPBS, centrifuged for 5 minutes at 200 x g, and suspended in equal parts 2% FBS in DPBS and intracellular fixation buffer (IC fix) (Invitrogen). All samples were held at 4°C prior to analysis and acquired on the Attune NxT flow cytometer (ThermoFisher) within 24 hours of processing, and FlowJo V 10.7 (FlowJo LLC, Ashland, OR) was used for data analysis.

Processing and staining of peripheral blood mononuclear cells (PBMCs)

Four ml of whole blood was diluted with 4 ml of DPBS and layered onto 4 ml of discontinuous Ficoll-Paque PREMIUM density gradient (1.078g/ml) (GE Healthcare, Chicago, IL). The samples were centrifuged for 30 minutes at 400 x g. The PBMC layer was isolated into 10 ml of DPBS, centrifuged at 300 x g for 10 minutes, washed with 10 ml of DPBS, and centrifuged at 200 x g for 10 minutes. PBMCs were suspended in 10% A/B human serum in DPBS. Twenty µl of cell suspension was stained with 20 µl Viastain^{TM} Acridine Orange/ Propidium Iodide Staining Solution for 2 minutes at RT. 20 µl of stained cells were loaded on a hemocytometer and counted using the Cellometer K2 Fluorescent Viability Cell Counter. Aliquots of 1 x 10^6 PBMCs/50 µl were suspended in 10% A/B human serum and incubated at 4°C for 30 minutes. Samples were stained with 50 µl of pre-mixed antibodies for the base panel and PBMC staining (Supplementary Table 1) at 4°C for 30 minutes, washed with 2% FBS in DPBS, and suspended in equal parts 2% FBS in DPBS and IC fix. Sample acquisition and analysis were performed as described in "whole blood staining."

Gating strategy for phenotype characterization

Single cells were identified and doublets were removed using forward scatter height and area. For all phenotypic analyses, $CD3^+$ and $CD19^+$ events corresponding to T and B

lymphocytes, respectively, were removed. For monocyte analyses, CD14 and CD16 were utilized following the removal of $CD15^+$ and $CCR3^+$ events. Patrolling monocytes (Pt Mo) were identified as $CD16^{high}CD14^{low}$ and classical monocytes (Cl Mo) as $CD16^{low}CD14^{high}$ (Supplemental Figure 1). For neutrophil analyses, $CD193^+$ (CCR3) and $CD14^+$ events were removed. Mature neutrophils (mNs) were identified as $CD16^{high}$ and immature neutrophils (imNs) as $CD16^-$. For eosinophils, $CCR3^+$ and $CD15^+$ were analyzed following the removal of $CD14^+$ and $CD16^+$ events (Supplemental Figure 1). This gating strategy was used for whole blood and PBMC analyses.

Quantification of innate immune cells

Fifty microliters of fresh whole blood from healthy or MM patients were stained with 50 µl of a separate pre-mixed antibody absolute count panel for 30 minutes at 4°C (Supplemental Table 1). Red blood cell lysis and fixation were performed in 1 ml of 1x 1-step Fix/lyse buffer at RT for 15 minutes. 50 µl of CountBright™ Absolute Counting Beads (ThermoFisher) were added to samples using a pre-determined concentration given by the manufacturer. Samples were held at 4°C prior to acquisition and acquired on the Attune NxT flow cytometer (ThermoFisher) within 24 hours of processing and analyzed with FlowJo V 10.7 (FlowJo LLC). Bead counts were determined per the instructions by the manufacturer. Briefly, the bead adjustment factor was calculated by dividing the number of beads gated by the pre-determined concentration of beads per 50 µl. Leukocytes were gated with side scatter and forward scatter area and total neutrophils were gated using $CD15^+CD14^-$ gate with adjustment performed by multiplying cell counts by the bead adjustment factor.

For quantification of neutrophil or monocyte subsets in whole blood, the percentages of the subset gate from total neutrophils (imN and mN) or monocytes (Pt Mo and Cl Mo) were multiplied by the adjusted total neutrophil or monocyte count. A count threshold of 150 imN per sample was determined based on the calculated mean imN frequency of samples. The majority of healthy controls did not meet the event threshold for imNs and were excluded in the phenotypic analyses.

For quantification of neutrophils in the PBMC layer, the percentage of total LDNs was gated and multiplied by the percentage of total neutrophils in whole blood. LDN subsets were quantified by multiplying the percent of the subset of total neutrophils by the PBMC neutrophil count.

Adjustment of median fluorescent intensities (MFIs) for phenotypic analyses

The SPHERO^{TM} Ultra Rainbow Calibration Particle Kit (Spherotech Inc., Lake Forest, IL) was utilized to assess variation in laser fluorophore intensities with rainbow beads acquired at each time of sample acquisition. Histogram overlays including rainbow beads acquired at baseline and each subsequent sample after were generated of each fluorophore. The need for MFI adjustment was determined by the difference of emission peaks varying by a half log or greater. If adjustments were needed, histogram emission peaks 1-6 were gated for each fluorophore, as demonstrated in the company protocol, and the mean MFI was determined for each peak. The difference between peak MFIs was calculated by subtracting the current MFI from the baseline MFI. The percentage difference was determined by dividing the mean MFI difference by the MFI at baseline for each peak. Mean peak percent difference was determined by averaging percentages of peaks 3-6 for each fluorophore. MFIs of specific markers were then multiplied by the percentage

corresponding to the fluorophore the marker was conjugated to, resulting in the normalized MFI.

Assessment of intracellular expression of Ki67

Intracellular staining was performed using the Cytofix/Cytoperm™ Fixation/Permeabilization Kit (BD Biosciences). One hundred microliters of whole blood from MM patients were isotonically lysed as described in "isotonic lysis of cells." PBMCs were isolated, and 2.5 x 10^5 PBMC aliquots were suspended in 50 µl of 10% A/B human serum in DPBS for 30 minutes at 4°C. Fifty microliters of the extracellular Ki67 antibody panel were added for 30 minutes at 4°C (Supplementary Table 1). The fixation and permeabilization were performed according to the manufacturer's protocol. Samples were then stained with 5 µl of Ki67 antibody for 30 minutes at 4°C. Samples were washed with 2% FBS in DPBS and centrifuged for 5 minutes at 200 x g. This step was repeated. The final pellet was suspended in equal parts 2% FBS in DPBS and IC fix. Sample acquisition and analysis were performed as described in above with a final cytogram visualized by side scatter and Ki67 and quartile gate applied using a fluorescence minus one (FMO) for APC to set the negative gate and determine Ki67-positive cells.

LEGENDplex™ protocol for measuring plasma markers and cytokine levels in plasma

The LEGENDplex™ Human Essential Immune Response Panel 740929 13-plex kit and LEGENDplex™ customization kit, including CCL2, CCL11, CRP, CXCL10, D-dimer, G-CSF, IFNγ, IL-18, IL-1β, IL-6, CXCL9, and TNF-R1 were utilized (BioLegend). Plasma samples were stored at -80°C. For the assay, the samples were thawed, centrifuged for 10 minutes x 500 g, and filtered using the filter plate for LEGENDplex™ Assay (BD Biosciences). Samples were processed according to the manufacturer's instructions for the

filter plate assay. In brief, 25 µl aliquots were added to the 96-well plate with 25 µl assay buffer for samples, 25 µl of Matrix B for standards, and 12.5 µl of the pre-mixed immune bead solution at RT covered on a shaker for 2 hours in the dark. Unbound beads were removed with gentle vacuum pressure and then washed with 1X wash buffer. 12.5 µl of detection antibody was added to samples and incubated for 1 hour covered on a shaker at RT in the dark. 12.5 µl of SA-PE was added to samples and incubated for 1 hour covered and shaking at RT in the dark. Samples were washed with 1X wash buffer and manually transferred to FACs tubes with a final volume of 150 µl per sample. The template for data acquisition and instrument set up was performed as described in the manufacturer's protocol on the BD Symphony™ (BD Biosciences) the same day. Analyses were performed utilizing the online LEGENDplex™ Data Analysis Software (BioLegend).

Measurement of soluble plasma markers by ELISA

Plasma was collected after single discontinuous density gradient centrifugation as described in "the processing of peripheral blood mononuclear cells (PBMCs)" and stored at -80°C until use. Plasma levels of sCD14 and lipocalin-2 (NGAL) were measured using commercial ELISA kits Hycult HK320 and Hycult HK330 (Hycult Biotechnology, Uden, the Netherlands), and sCD163 using commercial ELISA kit Quantikine DC1630 (R&D Systems, Minneapolis, MN) according to the manufacturer's instructions. The final dilution ratio was 1:80 for sCD14 and NGAL and 1:10 for sCD163. Absorbance was measured with the ELx808™ Biotek absorbance microplate reader (Biotek, Winooski, WT), and concentrations were calculated using Gen5™ data analysis software (BioTek) based on a standard curve.

Isotonic lysis of cells

Two milliliters of isotonic lysis buffer (155 mM NH_4Cl, 10mM KHCO3, 0.1mM EDTA in water sterile filtered with a Steritop 0.22µm filter) (16) was added to 50-100 µl of whole blood and set on a rotator for 5 minutes or until the red blood cells were lysed. Two milliliters of 2% FBS in DPBS was added and samples were centrifuged for 5 minutes at 200 x g. The pellet was suspended in 500 µl of 2% FBS in DPBS for immediate acquisition for functional assays or 10% human A/B serum in DPBS for further processing for proliferation assessment.

Assessment of ROS and mitochondrial superoxide production

Fifty microliters of whole blood or isolated PBMCs (1 x 10^6 aliquots per 50 µl) were stained with the ROS antibody panel in pre-warmed tubes (Appendix A: Supplemental Methods Table 1). A final concentration of 20µM of H2-DCFDA was added, and samples were simultaneously stimulated with or without 10nM of PMA. Samples were incubated at 37°C for 30 minutes. Samples were lysed as described in "isotonic lysis of cells," acquired within 30 minutes after preparation, and analyzed via flow cytometry. The same protocol was performed for superoxide production, utilizing the MitoSOX antibody panel, and a final concentration of 2mM of MitoSOX™ Red (Invitrogen) was added to samples simultaneously with PMA stimulation (Supplemental Table 1).

Assessment of mitochondrial mass and mitochondrial activity

Fifty microliters of fresh whole blood or isolated PBMCs (1 x 10^6 cells per 50 µl sample) from MM patients or controls were stained with the MitoTracker Green antibody panel using pre-warmed tubes (Appendix A: Supplemental Methods Table 1). A final concentration of 1 µM of MitoTracker™ Green FM (MTG) (Invitrogen) was added to tubes

to determine mitochondrial mass. Simultaneously, a final concentration of 500nM tetramethylrhodamine ethyl ester (MitoStatus TMRE) (BD Biosciences) was added to determine mitochondrial membrane potential (ΔΨm). Samples were incubated at 37°C for 30 minutes and lysed as described in "isotonic lysis of cells." The samples were analyzed by flow cytometry within 30 minutes. ΔΨm was adjusted to the mitochondrial mass of a corresponding sample and presented as ΔΨm/MTG ratio.

Assessment of phagocytosis

Fifty microliters of fresh whole blood or isolated PBMCs (1×10^6 per 50 µl sample) from MM patients or HD was stained with a premade antibody mix base panel and the pHrodo antibody panel using pre-warmed tubes (Appendix A: Supplemental Methods Table 1). 10 µl of pHrodoTM Red E. coli BioParticles™ (ThermoFisher) was added to determine the phagocytic capacity of leukocytes as indicated by an increase in pHrodo™ red fluorescence indicating a decrease in pH. Samples were incubated at 37°C for 30 minutes. Samples were processed as described in "whole blood staining."

Statistical analysis

Tests for statistical significance of myeloid phenotype marker expressions ($p<0.05$) were conducted using the Mann-Whitney rank-sum test between MM cases and controls. Correlations between marker expression and clinical parameters were evaluated using the Spearman rank-order test. Tests for statistical significance of marker expressions stratified by disease stage were performed using the Kruskal-Wallis one-way ANOVA followed by Dunn's Multiple Comparison post hoc test. The myeloid phenotype of MM patients relative to clinical parameters was calculated using logistic regression adjusted for confounders

(race, sex, age, and treatment type). All calculations were performed with GraphPad Prism (GraphPad Software Inc., La Jolla, CA) or Stata v.16.0 (StataCorp, College Station, TX).

Results

A subset of MM patients demonstrates an altered neutrophil phenotype

To determine the heterogeneity of the myeloid cell compartment in peripheral blood of patients with MM, whole blood cells were characterized using pre-determined antibodies designed to assess myeloid cell differentiation and activation (Supplemental Table 1). Comprehensive analyses revealed two distinct phenotypes characterized by specific patterns of surface antigen expression on neutrophils, monocytes, and eosinophils. Neutrophil phenotype was assessed on two distinct neutrophil subsets, $CD15^{+}CD16^{-}$ and $CD15^{+}CD16^{+}$, consistent with immature (imN) and mature (mN) neutrophils (33, 34) (Figure 1A). As shown in Figure 1B-C, a subset of MM patients exhibited an increase in surface levels of CD64 (FcγRI) on mNs, indicative of a lower maturation status of circulating neutrophils (33, 35). MM patients were grouped into two distinct subsets, with MM1 defined as neutrophil $CD64^{low}$ and MM2 defined as $CD64^{high}$ ($p<0.0001$; Figure 1B-C).

Table 1. Control and multiple myeloma patient demographics and diagnostic clinical and laboratory characteristics of MM patients by MM1 and MM2 phenotypes

		Combined Population				
Clinical feature and laboratory characteristics	**Controls (N=19)**	**Total MM Cases (N=35)**	***P***	**MM1 Phenotype (n=22)**	**MM2 Phenotype (n=13)**	***P***
Demographic characteristics						
Male sex, N (%)	10 (52.6)	17 (48.6)	0.78	9 (40.9)	8 (61.5)	0.24
Black race, N (%)	11 (57.9)	12 (34.3)	0.09	7 (31.8)	5 (38.5)	0.69
Age, median (range)	54 (43-65)	66 (43-79)	**<0.0001**	64 (43-79)	68 (58-76)	0.12
Laboratory parameters, median (range)*						
Clonal bone marrow plasma cells (BMPC), %		50 (3-97)		60 (3-97)	40 (10-80)	0.35

Calcium, mg/dL	9.6 (7.6-15.5)	9.1 (7.6-14.9)	10.4 (9.5-15.5)	0.08
Albumin, mg/dL	3.5 (1.7-4.7)	3.6 (1.7-4.5)	3.5 (2.4-4.7)	0.90
Creatinine, mg/dL	1.0 (0.5-5.2)	0.9 (0.5-5.2)	1.4 (0.7-4.2)	0.15
Hemoglobin, g/dL	10.9 (6.5-14.9)	11.1 (7.6-14.9)	10.5 (6.5-14.2)	0.30
β2-microglobulin, mg/L	3.7 (1.1-23.9)	3.6 (1.4-21.0)	5.3 (1.1-23.9)	0.48
Lactate Dehydrogenase (LDH), XXX units	165 (110-355)	177 (130-355)	151 (110-332)	0.51
Monoclonal protein, total g (dL)	2.3 (0.3-5.8)	2.3 (0.3-4.0)	2.6 (0.3-5.8)	0.71
Paraprotein Assessment				
Myeloma type, N (%)				
IgG	17 (48.6)	10 (45.5)	7 (53.9)	
IgA	11 (31.4)	8 (36.4)	3 (23.1)	
Light chain restricted	7 (20.0)	4 (18.2)	3 (23.1)	0.71
FLC type, N (%)				
Kappa	20 (57.1)	10 (45.5)	10 (76.9)	
Lambda	15 (42.9)	12 (54.6)	3 (23.1)	0.07
Involved: uninvolved FLC ratio ≥ 100, N (%)	12 (41.4)	3 (16.7)	9 (81.8)	****0.001**
End organ damage, N (%)				
Hypercalcemia	6 (17.1)	1 (4.6)	5 (38.5)	****0.01**
Renal involvement	7 (20.0)	4 (18.2)	3 (23.1)	0.73
Anemia	19 (54.3)	12 (54.6)	7 (53.9)	0.97
Bone	20 (57.1)	12 (54.6)	8 (61.5)	0.69
International Staging System-Revised				
I	7 (21.2)	4 (19.1)	3 (25.0)	
II	18 (54.6)	13 (61.9)	5 (41.7)	
III	4 (24.2)	4 (19.1)	4 (33.3)	0.51
Treatment, N (%)				
Pharmacologic only	12 (34.3)	6 (27.3)	6 (46.2)	
Bone marrow transplant	13 (37.1)	7 (31.8)	6 (46.2)	
Maintenance therapy	8 (22.9)	7 (31.8)	1 (7.7)	
Pharmacologic and radiation	2 (5.7)	2 (9.1)	0 (0)	0.21

*Laboratory features determined from serum

***P*-values adjusted for sex, age, race, and treatment type: Involved : uninvolved FLC ratio $P_{adj} = 0.009$; hypercalcemia $P_{adj} = 0.23$.

The lower maturation status of neutrophils from MM2 patients was further supported by reduced levels of CXC chemokine receptor 2 (CXCR2), CD10, and CD15 compared to neutrophils from MM1 patients or healthy donors (Figure 1C). Neutrophils from MM2 patients displayed elevated levels of PD-L1 relative to MM1 ($p<0.001$) or controls ($p<0.01$) suggestive of enhanced immunosuppressive potential (10, 11, 15, 36) (Figure 1C). There was no indication of neutrophil activation as determined by an absence of changes in the surface levels of CD16 or lectin-type oxidized LDL receptor 1 (Lox-1) and an absence of surface shedding of CD31 or CD62L (33, 37-39) (Figure 1C and Supplemental Figure 2A). Similarly, no indication of neutrophil degranulation was observed on neutrophils from MM2 patients as determined by an absence of changes in the levels of degranulation markers myeloperoxidase (MPO), CD11b, CD63, or CD66b (40-43) (Figure 1C and Supplemental Figure 2A). The neutrophil: lymphocyte ratio did not significantly differ between controls, MM1, and MM2 patients (Supplemental Figure 2B). Overall, these data indicate the presence of a phenotypically distinct and alternatively differentiated mature neutrophil population in MM2 patients that does not exhibit typical signs of activation or degranulation.

Immature neutrophils are expanded in MM patients and demonstrate proliferative activity

Immature neutrophils (imNs) display $SSC^{high}CCR3^{-}CD15^{+}CD16^{-}CD10^{low}$ phenotype and a distinct transcriptional signature (33, 44, 45). imNs and neutrophil progenitors were reported to be expanded in chronic diseases and associated with immune suppression in various cancers, including melanoma and lung cancer (9, 46-48). MM2 patients exhibited a significant expansion of imNs relative to MM1 ($p<0.01$) or controls ($p<0.001$; Figure 1A). imNs from MM2 patients displayed higher intracellular expression

of a proliferation marker Ki67 relative to MM1 (p<0.02; Figure 1D-E). A significant positive correlation was observed between the frequency of imNs and the percentage of $Ki67^+$ imNs (Figure 1F; correlation coefficient R=0.62, p=0.04), and a trend for a positive correlation was observed between imN frequency and Ki67 expression (Figure 1G). imNs expressed higher levels of CD64 on MM2 relative to MM1 (p<0.05) with no significant difference in the expression of other markers tested (Figure 1H and Supplemental Figure 2D). with no significant difference in the expression of other markers tested (Figure 1H and Supplemental Figure 2C).

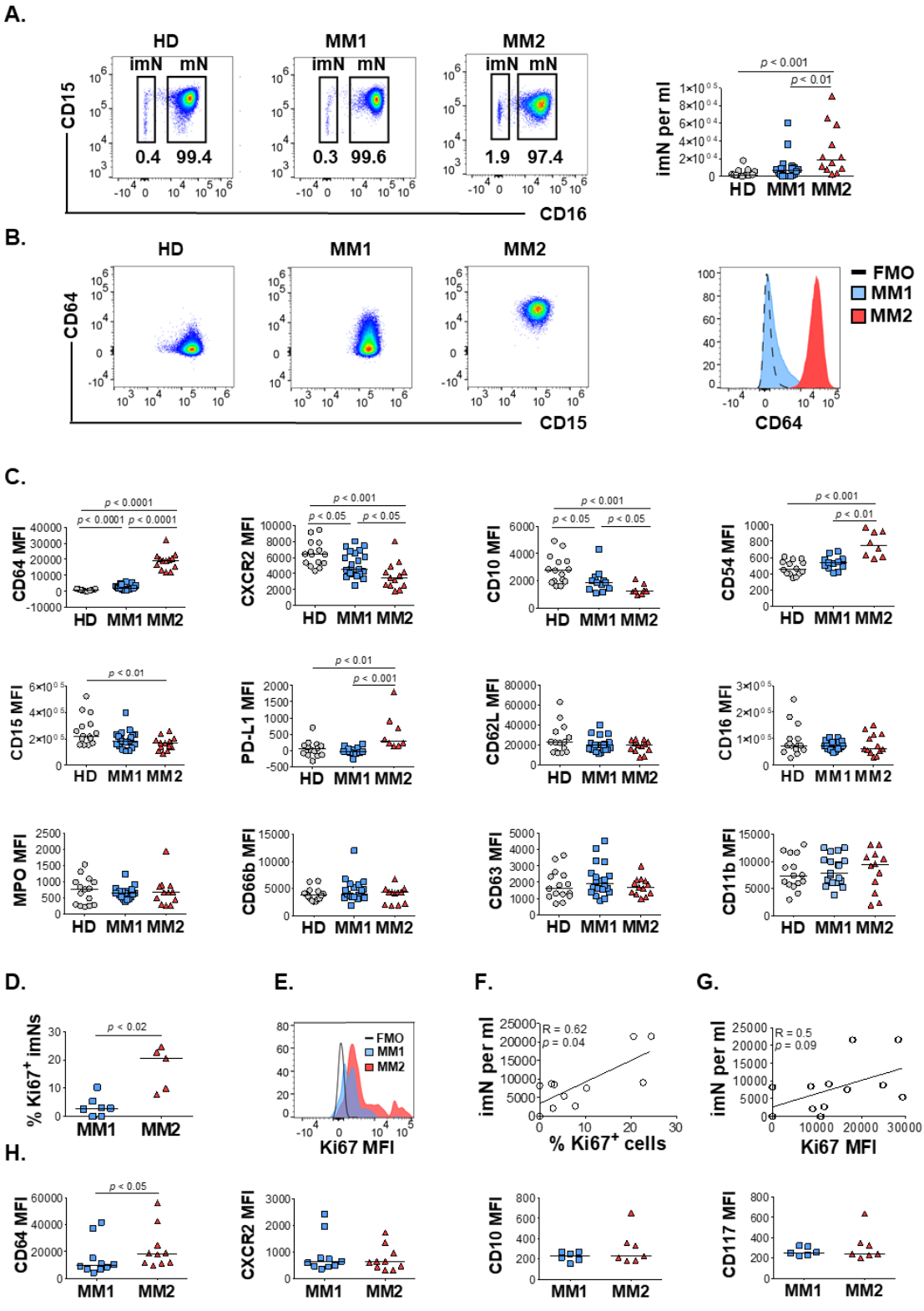
A.
HD
MM1
MM2
imN
mN
0.4
99.4
0.3
99.6
1.9
97.4
CD15
CD16
imN per ml
p < 0.001
p < 0.01
HD MM1 MM2
B.
CD64
CD15
FMO
MM1
MM2
C.
CD64 MFI
CXCR2 MFI
CD10 MFI
CD54 MFI
CD15 MFI
PD-L1 MFI
CD62L MFI
CD16 MFI
MPO MFI
CD66b MFI
CD63 MFI
CD11b MFI
D.
% Ki67+ imNs
p < 0.02
E.
Ki67 MFI
F.
imN per ml
R = 0.62
p = 0.04
% Ki67+ cells
G.
R = 0.5
p = 0.09
H.
CD64 MFI
CXCR2 MFI
CD10 MFI
CD117 MFI

Figure 1. A subset of MM patients exhibits an altered neutrophil phenotype. (A) Left panel: representative cytograms of $CD15^{+}CD16^{+}$ mNs and $CD15^{+}CD16^{-}$ imNs in whole blood of a healthy donor (HD), MM1, and MM2 patients. Right panel: the frequency of imN per ml of blood of HD, MM1, and MM2 patients. **(B)** Representative cytograms of mNs of HD, MM1, and MM2 patients and histogram overlay of CD64 expression. **(C)** Levels of expression of maturation and activation markers on mNs of HD, MM1, and MM2 patients. **(D)** Percentage of $Ki67^{+}$ imNs of total imNs. **(E)** Histogram overlay of Ki-67 intracellular expression on imNs and **(F)** a correlation between imN frequency and percentage of $Ki67^{+}$ imNs. **(G)** Correlation between imN frequency and MFI of $Ki67^{+}$ imNs. **(H)** Levels of expression of maturation and activation surface markers on imNs of HD, MM1, and MM2 patients. MFI, median fluorescent intensity; FMO, fluorescence minus one. Statistical analyses were performed using the Mann-Whitney rank-sum test **(A, C-D and H)** or Spearman correlation **(F-G)**. Spearman correlation coefficients R and *p* values are indicated; bars and lines represent median values and simple linear regression analysis, respectively.

Mature low-density neutrophils exhibit a distinct phenotype in MM2 patients

Low-density neutrophils (LDNs) or PMN-MDSCs represent a heterogeneous neutrophil subpopulation with distinct phenotype and function that is expanded in chronic inflammatory conditions (9, 15, 18, 36, 44, 49). LDNs co-localize with lymphocytes following cell separation by density gradient centrifugation. MM2 patients demonstrated increased frequencies of total LDNs ($p<0.05$) and immature LDNs (imLDNs) ($p<0.001$) relative to controls (Figure 2A, B).

Mature LDNs (mLDNs) from MM2 patients exhibited less differentiated neutrophil phenotype relative to MM1 patients as indicated by elevated CD117 ($p<0.01$) and CD64 ($p<0.0001$) (46, 47, 50) (Figure 2C). Consistent with the findings in whole blood, mLDNs from MM2 patients exhibited a significant decrease in CD15 expression relative to controls ($p<0.05$; Figure 2C). imLDNs from MM2 exhibited significantly higher expressions of CD64 ($p<0.01$) and CD62L ($p<0.05$) relative to MM1 (Figure 2D).

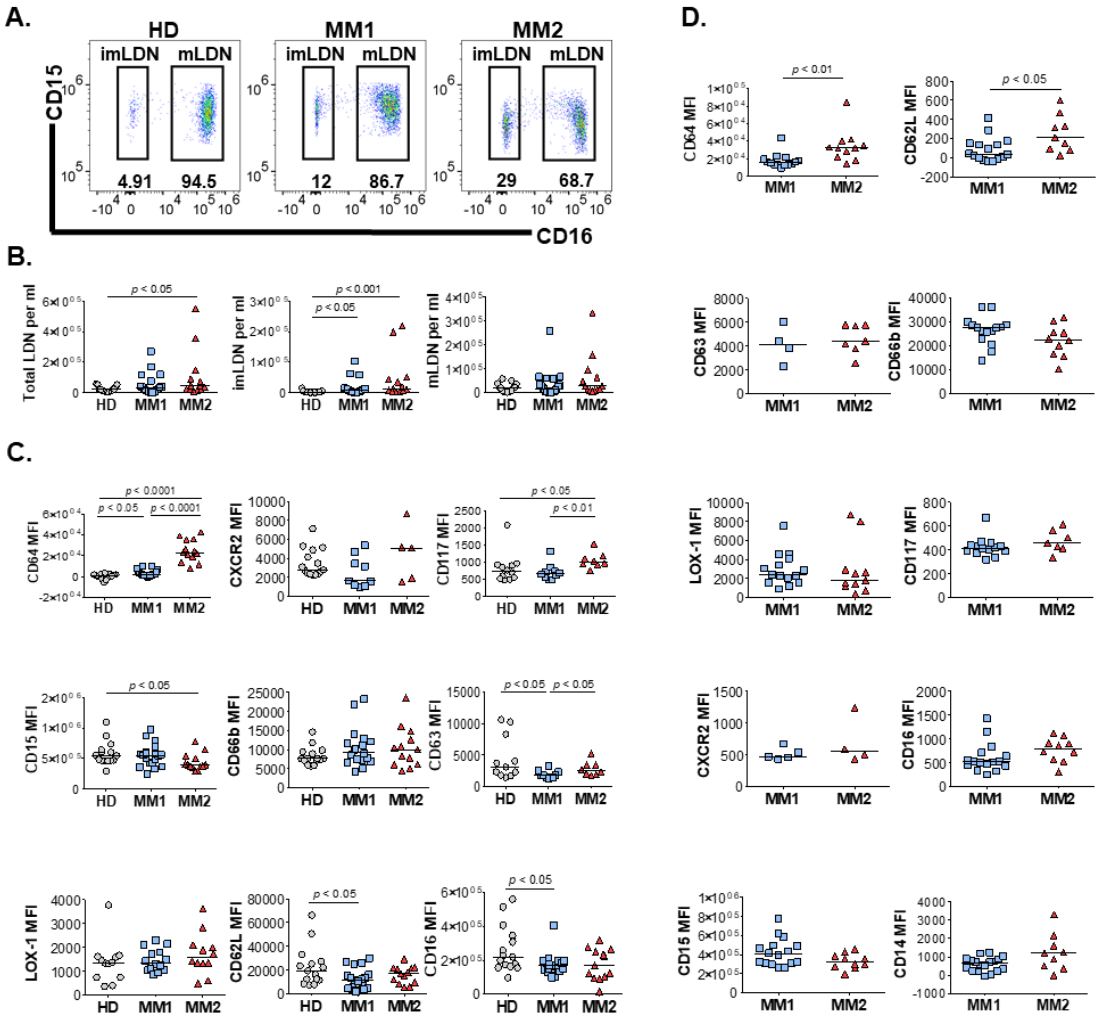

Figure 2. Distinct phenotypes on low-density neutrophils in MM1 and MM2 patients. **(A**) Representative cytograms of $CD15^{+}CD16^{+}$ mLDNs and $CD15^{+}CD16^{-}$ imLDNs. **(B)** Frequencies of total LDNs, imLDNs, and mLDNs in the blood of HD, MM1, and MM2 patients. **(C, D)** Surface marker expression of maturation, degranulation, and activation markers on mLDNs **(C)** or imLDNs **(D)** of HD, MM1, and MM2 patients. MFI, median fluorescent intensity; statistical analyses were performed using the Mann-Whitney rank-sum test with *p* values indicated. Bars represent median values.

MM2 patients demonstrate altered monocytic and eosinophilic phenotypes

To address monocytic heterogeneity in MM, the phenotypes of classical ($CD16^{low}CD14^{high}$) and patrolling ($CD14^{low}CD16^{high}$) monocyte subpopulations were determined (28, 51). MM2 patients exhibited a significantly lower frequency of patrolling

monocytes relative to MM1 ($p<0.05$) or controls ($p<0.01$; Figure 3A-B). There was no significant difference between total monocyte frequency and lymphocyte: monocyte ratio between MM2 patients and HD (Figure 3B and Supplemental Figure 2C). Consistent with the mature neutrophil phenotype, classical monocytes from MM2 patients exhibited significantly higher expression of CD64 ($p<0.05$) and lower levels of CXCR2 ($p<0.01$) compared to MM1 (Figure 3C). Patrolling monocytes from MM2 patients exhibited higher levels of CD64 relative to MM1 patients ($p<0.001$) and controls ($p<0.0001$; Figure 3D). In contrast, CXCR2 levels on patrolling monocytes from MM2 patients were significantly higher relative to controls ($p<0.01$; Figure 3D).

An activated monocytic phenotype was observed in MM2 relative to MM1 patients indicated by a significant decrease in CD31 expression on classical and patrolling monocytes (Figure 3C-D and Supplemental Figure 3). Additionally, patrolling monocytes from MM2 patients demonstrate a significant increase in activation markers CD163 ($p<0.01$) and CD169 ($p<0.01$; Figure 3D and Supplemental Figure 3F). Patrolling monocytes from MM2 exhibited downregulation of CX3 chemokine receptor 1 (CX3CR1) ($p<0.01$) and upregulation of PD-L1 ($p<0.01$) relative to controls consistent with the features observed in an immunosuppressive environment (15, 16) (Figure 3D).

Eosinophils accelerate MM progression in synergy with microbiota-driven IL-17-producing cells in murine models (52). Decreased C-C Chemokine receptor 3 (CCR3) expression on eosinophils was observed in MM2 patients compared to controls ($p<0.05$; Figure 3E). Eosinophils from MM2 patients exhibited lower levels of cell signaling receptor tissue factor (CD142) (53) ($p<0.05$), activation marker CD66b (54) ($p<0.05$) and CD31 ($p<0.05$) relative to MM1 patients (Figure 3E and Supplemental Figure 4).

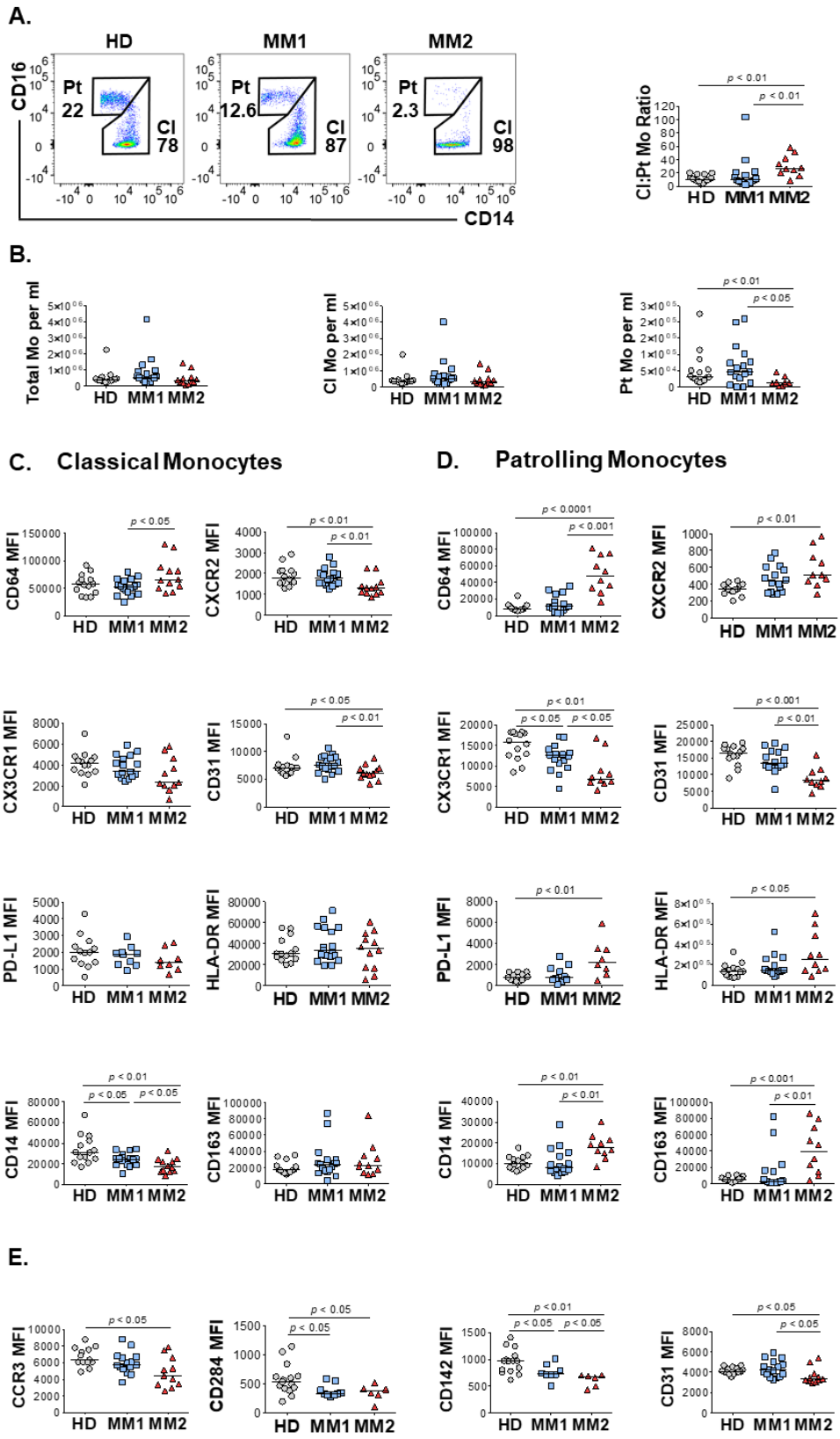
A.
HD
MM1
MM2
CD16
CD14
Pt 22
Cl 78
Pt 12.6
Cl 87
Pt 2.3
Cl 98
Cl:Pt Mo Ratio
p < 0.01
p < 0.01
HD MM1 MM2
B.
Total Mo per ml
Cl Mo per ml
Pt Mo per ml
p < 0.01
p < 0.05
C. Classical Monocytes
D. Patrolling Monocytes
CD64 MFI
CXCR2 MFI
CX3CR1 MFI
CD31 MFI
PD-L1 MFI
HLA-DR MFI
CD14 MFI
CD163 MFI
p < 0.0001
p < 0.001
p < 0.05
p < 0.01
E.
CCR3 MFI
CD284 MFI
CD142 MFI
CD31 MFI

Figure 3. MM2 patients exhibit altered monocytic and eosinophilic phenotypes. (A) Left panel: representative cytograms of $CD16^{low}CD14^{high}$ classical monocytes (Cl Mo) and $CD16^{high}CD14^{low}$ patrolling monocytes (Pt Mo) in whole blood from HD, MM1 and MM2 patients. Right panel: classical to patrolling monocyte ratios in HD, MM1, and MM2 patients. **(B)** Frequency of total, classical, and patrolling monocytes in HD, MM1, and MM2 patients. **(C, D)** Surface marker expression of monocyte markers on classical **(C)** or patrolling monocytes **(D)** of HD, MM1, and MM2 patients. **(E)** Surface marker expression of eosinophil markers of HD, MM1, and MM2 patients. MFI, median fluorescent intensity; statistical analyses were performed using the Mann-Whitney rank-sum test with *p* values indicated. Bars represent median values.

Myeloid cells in MM2 patients demonstrate altered functional activity

Next, the differences in the bioenergetic properties of myeloid cells in the subsets of patients with MM were assessed. Neutrophils from MM2 patients exhibited significantly higher mitochondrial superoxide production, detected using MitoSOX^{TM} Red fluorogenic dye in the absence and presence of PMA stimulation, compared to neutrophils from MM1 patients or controls (Figure 4A). Similar results were observed in the LDN subpopulations suggesting that neutrophils from MM2 patients have higher capacity for mitochondrial superoxide release (Figure 4B). Neutrophil subpopulations from both MM1 and MM2 patients demonstrated significantly higher mitochondrial potential detected using the cationic dye (TMRE) sequestered by mitochondria with adjustment for mitochondrial mass as indicated by MitoTracker^{TM} Green staining relative to controls ($p<0.05$; Figure 4C). Classical and patrolling monocytes from MM2 patients exhibited increased mitochondrial potential relative to controls ($p<0.01$; Figure 4D). mNs from MM2 patients demonstrated higher phagocytic capacity as determined by the phagocytosis of pHrodo^{TM} Red E. coli-conjugated BioParticles^{TM} relative to controls ($p<0.05$; Supplemental Figure 5A). No

differences were observed in the phagocytic capacity of monocyte subpopulations between MM1 and MM2 patients (Supplemental Figure 5B).

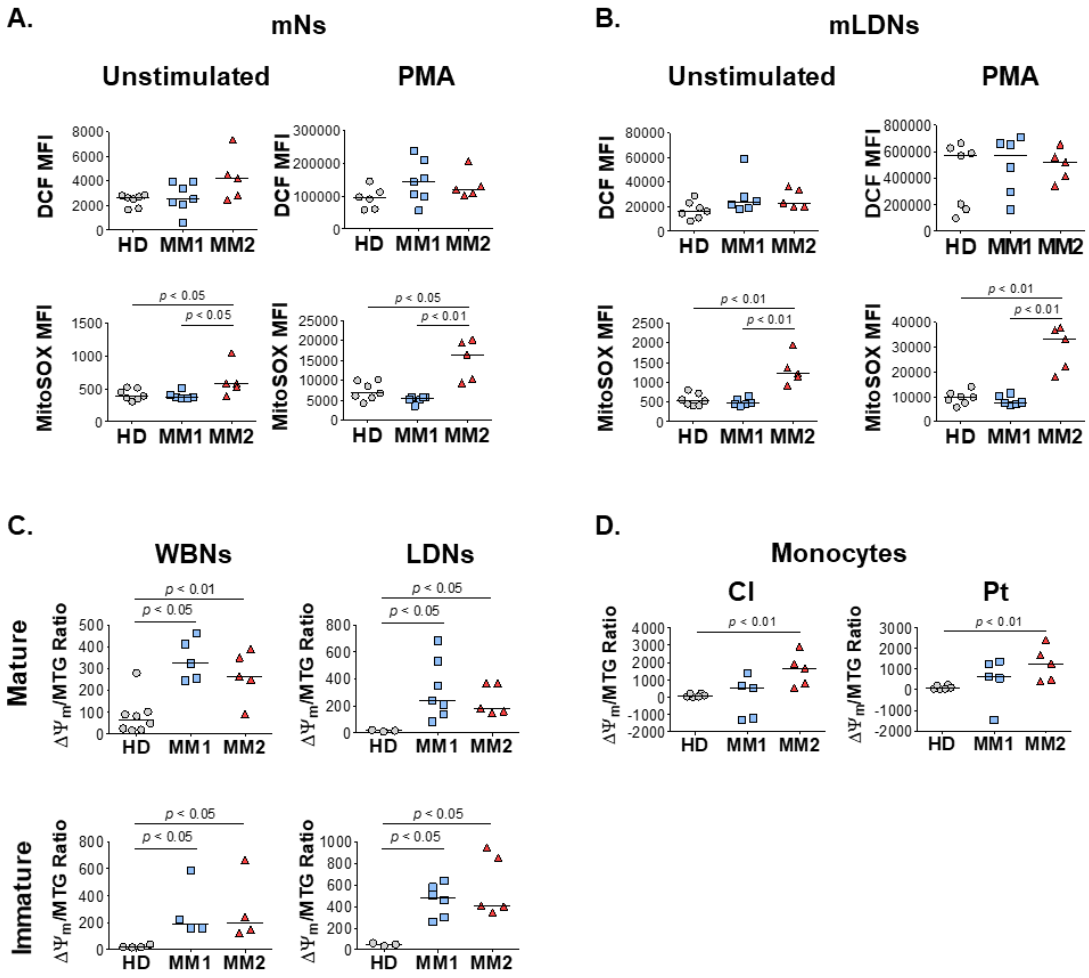

Figure 4. Myeloid cells obtained from MM2 patients exert altered functional activity. **(A-B)** ROS production determined by DCF staining and mitochondrial superoxide production by MitoSOX^{TM} Red at baseline and upon stimulation with PMA in mNs **(A)** and mLDNs **(B)** of HD and MM1 and MM2 patients. **(C, D)** Mitochondrial membrane potential was determined using TMRE staining adjusted for mitochondrial mass as detected by MitoTracker^{TM} Green (Δψm/MTG) on neutrophils **(C)** and monocytes **(D)**. MFI, median fluorescent intensity; statistical analyses were performed using the Mann-Whitney rank-sum test with *p* values indicated. Bars represent median values.

Soluble markers of myeloid cell activation are significantly elevated in MM2 patients

Serum levels of several key markers of myeloid cell activation were significantly elevated in MM patients compared to healthy donors. In particular, MM2 patients exhibited higher levels of CXCL9 (monokine induced by interferon gamma; MIG) relative to MM1 patients ($p<0.01$) or controls ($p<0.0001$; Figure 5A). Both MM1 and MM2 patients displayed higher levels of CXCL10 (IP-10) and tumor necrosis factor receptor 1 (TNF-R1) relative to controls (Figure 5A). The levels of CXCL9 and TNF-R1 positively correlated with the levels of CD64 on mature neutrophils and classical and patrolling monocytes (Figure 5B). MM1 patients demonstrated higher levels of CCL2 (monocyte chemoattractant protein-1; MCP1), eosinophil chemotactic CC-chemokine CCL11 (eotaxin-1), and neutrophil gelatinase-associated lipocalin (NGAL) relative to controls (Figure 5A). There was no significant difference in the production of granulocyte colony-stimulating factor (G-CSF), a major recruiter of neutrophils from bone marrow (55). Similarly, no significant differences in plasma levels of CRP, IL-1β, IL-6, IL-18, IFNγ, and D-dimer were identified between MM1 and MM2 patients (data not shown). To assess the level of monocyte/macrophage activation, plasma levels of soluble markers sCD14 and sCD163 were determined (56-59). The levels of sCD14 were lower in both MM1 and MM2 patients relative to controls (Figure 5A), corresponding to lower levels of cell-associated CD14 on classical but not patrolling monocytes (Figure 3C, D). In contrast, sCD163 was significantly elevated in the plasma of MM2 patients relative to controls ($p<0.05$; Figure 5A), consistent with a prior study (57). The level of sCD163 corresponded to elevated CD163 expression on patrolling monocytes (Figure 3D) and negatively correlated with the expression of CX3CR1 on patrolling and classical monocytes (Figure 5B).

MM2 phenotype components and presence of clinical features

Clinical features indicative of end-organ damage at diagnosis were assessed (Table 1). Compared to the MM1 phenotype, significantly more patients with the MM2 phenotype had involved to uninvolved FLC ratios > 100 at diagnosis after adjusting for sex, race, age, and treatment (p=0.009), suggesting that the MM2 phenotype may be reflective of myeloid dysregulation in MM patients with elevated FLC ratios (Figure 5C; Table 1). MM2 patients exhibited a trend towards increased serum calcium levels relative to controls (Figure 5D and Table 1).

Myeloma-defining events were analyzed in relation to the defining characteristics of the MM2 phenotype. The involved to uninvolved FLC ratio positively correlated with the frequency of imNs (R=0.57, p=0.001) and CD64 expression on mNs (R=0.4, p=0.03) and negatively correlated with CX3CR1 expression on patrolling monocytes (R= -0.46, p=0.04, Figure 5E). High CD64 expression on imLDNs positively correlated with elevated serum calcium related to hypercalcemia (R=0.77, p=0.0002; Figure 5F). Additionally, high CD64 expression on mNs partially correlated with lower hemoglobin values used to define anemia (R= -0.35, p=0.06; Figure 5G). Levels of CX3CR1 on patrolling monocytes negatively correlated with serum creatinine levels indicating renal involvement (R= -0.64, p=0.0008; Figure 5F).

Although CD64 expression on mNs and classical monocytes positively correlated with the start of induction therapy, aHSCT did not notably contribute to the MM2 phenotype (Supplemental Figures 6 and 7). A significant increase in CD15 expression on mNs of MM patients with dominant lambda clonal disease was observed relative to those with kappa disease (p<0.001) and an increase in CX3CR1 was observed on classical

monocytes obtained from patients with the IgG isotype ($p<0.05$). No other notable differences were observed in relation to the myeloma isotypes (Supplemental Figure 8). Lower levels of CD284 ($p<0.05$) and CD142 ($p<0.05$) were observed on eosinophils obtained from patients with a diagnosed bone disease (Supplemental Figure 9). No other significant differences with regard to MM2 phenotype components were observed (Supplemental Figure 9).

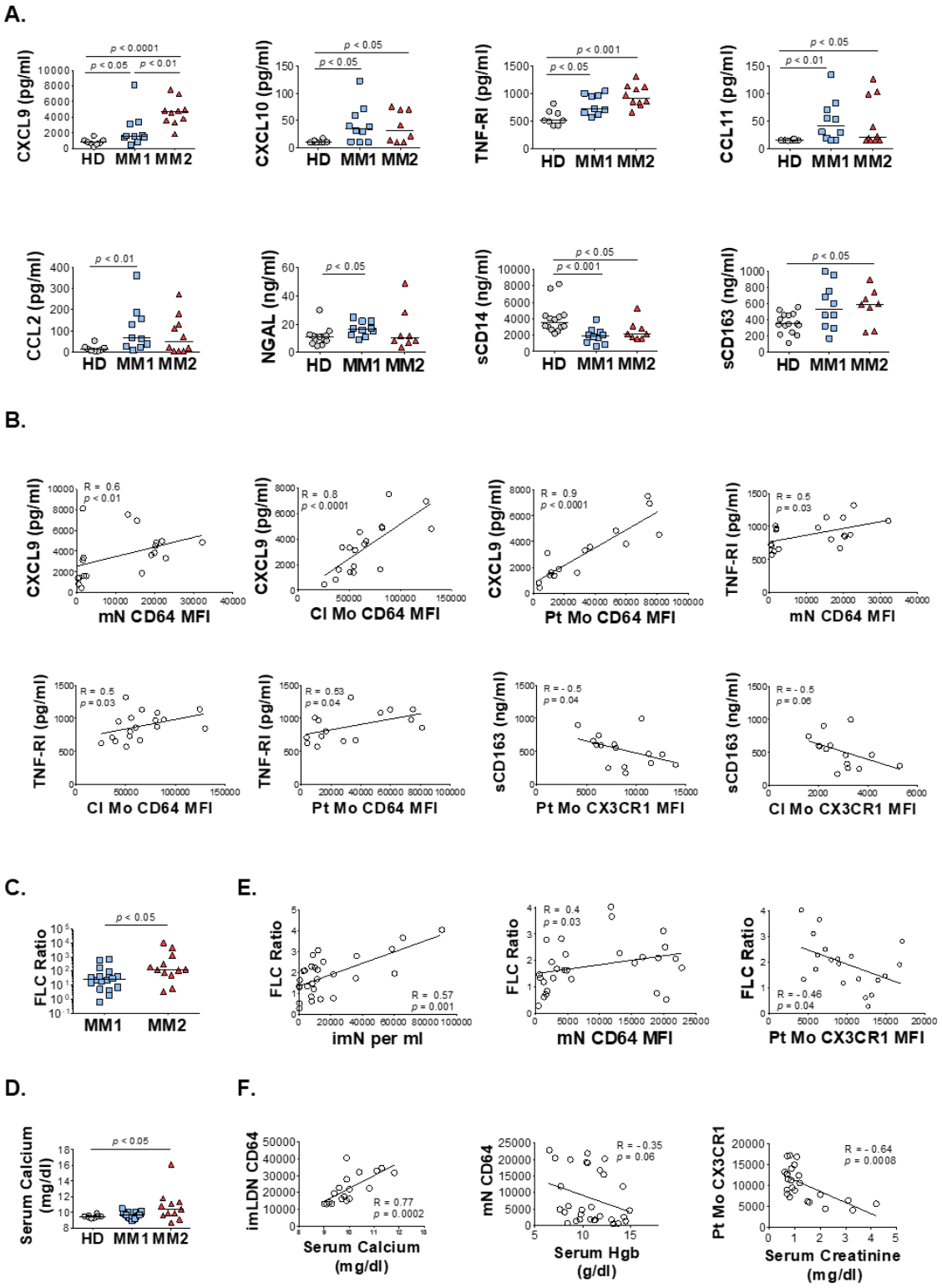
A.
CXCL9 (pg/ml)
p < 0.0001
p < 0.05
p < 0.01
HD MM1 MM2
CXCL10 (pg/ml)
p < 0.05
p < 0.05
HD MM1 MM2
TNF-RI (pg/ml)
p < 0.001
p < 0.05
HD MM1 MM2
CCL11 (pg/ml)
p < 0.05
p < 0.01
HD MM1 MM2
CCL2 (pg/ml)
p < 0.01
HD MM1 MM2
NGAL (ng/ml)
p < 0.05
HD MM1 MM2
sCD14 (ng/ml)
p < 0.05
p < 0.001
HD MM1 MM2
sCD163 (ng/ml)
p < 0.05
HD MM1 MM2
B.
CXCL9 (pg/ml)
R = 0.6
p < 0.01
mN CD64 MFI
CXCL9 (pg/ml)
R = 0.8
p < 0.0001
Cl Mo CD64 MFI
CXCL9 (pg/ml)
R = 0.9
p < 0.0001
Pt Mo CD64 MFI
TNF-RI (pg/ml)
R = 0.5
p = 0.03
mN CD64 MFI
TNF-RI (pg/ml)
R = 0.5
p = 0.03
Cl Mo CD64 MFI
TNF-RI (pg/ml)
R = 0.53
p = 0.04
Pt Mo CD64 MFI
sCD163 (ng/ml)
R = - 0.5
p = 0.04
Pt Mo CX3CR1 MFI
sCD163 (ng/ml)
R = - 0.5
p = 0.06
Cl Mo CX3CR1 MFI
C.
FLC Ratio
p < 0.05
MM1 MM2
E.
FLC Ratio
R = 0.57
p = 0.001
imN per ml
FLC Ratio
R = 0.4
p = 0.03
mN CD64 MFI
FLC Ratio
R = - 0.46
p = 0.04
Pt Mo CX3CR1 MFI
D.
Serum Calcium (mg/dl)
p < 0.05
HD MM1 MM2
F.
imLDN CD64
R = 0.77
p = 0.0002
Serum Calcium (mg/dl)
mN CD64
R = - 0.35
p = 0.06
Serum Hgb (g/dl)
Pt Mo CX3CR1
R = - 0.64
p = 0.0008
Serum Creatinine (mg/dl)

Figure 5. The MM2 phenotype is associated with changes in the plasma levels of markers of inflammation and with clinical markers of disease progression. (A) Levels of cytokines and markers of myeloid activation in plasma of HD and MM1 and MM2 patients. **(B, C)** Correlations between the plasma levels of markers of myeloid activation and surface levels of antigens on mN and patrolling monocytes. **(D)** FLC Ratio of MM1 and MM2 patients. **(E)** Serum calcium levels of HD, MM1, and MM2 patients. **(F)** Correlation between the FLC ratio and characteristic features of the MM2 phenotype. **(G)** Correlations between the characteristic features of the MM2 phenotype and myeloma-defining events. Serum calcium levels adjusted for albumin [(0.8 x (4g/dl*normal albumin – patient albumin)) + patient serum calcium level]. MFI, median fluorescent intensity. Statistical analysis was performed using the Mann-Whitney rank-sum test **(A, D, E)** or the Spearman correlation test **(B, C, F, G)**. Spearman correlation coefficients R and *p* values are indicated; bars and lines represent median values and simple linear regression analysis, respectively.

Defining characteristics of the MM2 myeloid cell phenotype are consistent with an advanced disease stage

To address the relationship between the characteristic components of the MM2 phenotype and disease stage, granulocytic and monocytic markers of MM patients and plasma markers of myeloid activation were stratified by the revised and updated International Staging System (R-ISS) criteria with R-ISS stage III indicative of advanced disease (Figure 6 and Supplemental Figure 10). Mature neutrophils from some, but not all, MM stage III patients exhibited significantly higher CD64 expression ($p<0.001$) relative to controls. Mature neutrophils from stage II patients exhibited significantly lower levels of CXCR2 ($p<0.05$) and CD10 ($p<0.01$) relative to controls (Figure 6A). No difference was observed in neutrophil activation and degranulation markers among MM patients (Figure 6A) indicating that the observed differences were not induced by neutrophil activation or degranulation. A significant decrease of CD14 expression was observed on classical monocytes ($p<0.01$) from stage III patients, while patrolling monocytes from stage III patients exhibited significantly lower levels of CX3CR1 ($p<0.01$) and CD31

($p<0.01$) relative to controls (Figure 6B-C). Further, a significant increase was observed in CD64 ($p<0.01$) and CD169 ($p<0.05$) on patrolling monocytes from stage III patients relative to controls (Figure 6C). The levels of CXCL9, TNF-RI, and sCD163 were significantly elevated in stage III patients relative to HD (Figure 6D). Similar trends in cytokine levels and myeloid marker expression were observed utilizing the Durie-Salmon (DS) staging system (Supplemental Figure 11). Overall, these data suggest that components of the MM2 myeloid phenotype, including CD64 and CX3CR1 levels on mNs and patrolling monocytes, are associated with the advanced MM disease stage.

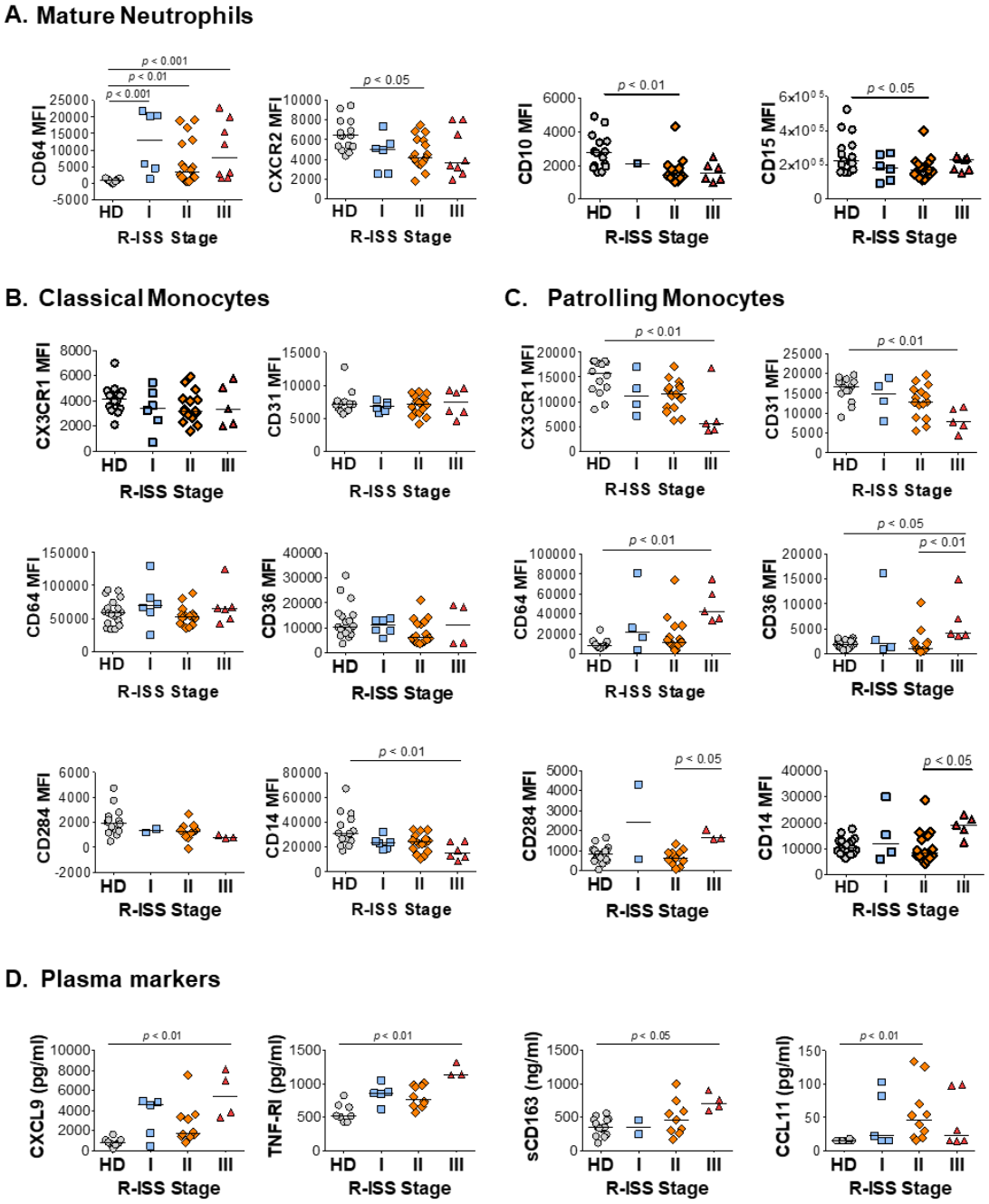

Figure 6. Characteristic features of the MM2 phenotype are associated with an advanced R-ISS stage. (A-C) Expression of surface markers on mature neutrophils **(A)**, classical monocytes **(B)**, and patrolling monocytes **(C)** stratified using R-ISS. **(D)** Levels of cytokines and plasma markers of activation stratified using R-ISS. MFI, median fluorescent intensity; statistical analyses were performed using the Kruskal-Wallis one-way ANOVA test followed by Dunn's post hoc test with *p* values as indicated. Bars represent median values.

Discussion

In this study, we report that a subset of MM patients exhibits an altered myeloid cell phenotype characterized by significant changes in the properties of circulating granulocytic, monocytic, and eosinophilic populations. Characteristic features of the observed phenotype are associated with advanced-stage disease and myeloma-defining events, including hypercalcemia and elevated involved-to-uninvolved free light chain ratio. The observed MM2 phenotype is independent of age, race, sex, and treatment type and is characterized by a significant upregulation of CD64 and downregulation of CXCR2 and CD10 on mature neutrophils indicative of their lower maturation status. Additional components of the MM2 phenotype include upregulation of CD64 and activation markers on classical and patrolling monocytes, upregulation of PD-L1 on patrolling monocytes, and downregulation of cell signaling receptors on eosinophils. Functionally, neutrophil subpopulations from MM2 patients exhibit a higher capacity for the production of mitochondrial ROS. The findings presented here are consistent with a dysregulation of myelopoiesis resulting in the release of distinct myeloid cell subsets with altered phenotypic and functional properties (6, 60-63).

The significance of assessment of neutrophil CD64 expression as a potential diagnostic tool is corroborated by previous observations demonstrating an association between upregulated CD64 and disease progression in MM patients treated with bortezomib and thalidomide (4, 64). In line with these studies, our results demonstrate that the presence of neutrophils with high CD64 expression in MM2 patients is significantly associated with the FLC ratio > 100 (Table 1). Consistent with a prior report, we did not observe an association between the level of CD64 expression on neutrophils and the

presence of specific myeloma isotypes (4). The translational relevance of quantitative assessment of CD64 levels on neutrophils in clinical settings is supported by its use in other conditions, including the discrimination between sepsis and non-septic systemic inflammatory response syndrome (65, 66).

LDNs, commonly referred to as PMN-MDSCs in cancer, represent a pathologically activated neutrophil subpopulation expanded in various malignancies (7, 67). PMN-MDSCs are implicated in regulating the immune response in cancerous conditions and exert potent immunosuppressive properties including increased arginase-1 expression and inhibition of T-cell proliferation (9, 23, 24, 62, 63). Consistent with prior studies, we observe a significant increase of LDN and imLDN frequencies in MM2 patients relative to controls (Figure 2B). imN frequency detected in whole blood is significantly elevated in the MM2 group compared to MM1 or controls (Figure 1A). In concordance with our observations, prior studies reported the expansion of PMN-MDSC in MM and demonstrated their immunosuppressive capacity and ability to protect MM cells from chemotherapy-induced toxicity (18-24). The shift in the immune cell compartments in the BME of MM results in an expansion of regulatory T cells (68) and MDSCs (18) promoting an immunosuppressive environment associated with altered function of myeloid cells (21, 23, 24). MM cells induce the development of MDSCs from healthy donor peripheral blood mononuclear cells via a bidirectional interaction between MM cells and MDSCs (19). Exosomes derived from the bone marrow stromal cells in MM patients alter myelopoiesis via an activation of STAT3 and STAT1 pathways and increase of the levels of anti-apoptotic proteins Bcl-xL and Mcl-1 resulting in immature myeloid cells with immunosuppressive activity (61). The relevance of the determination of imN/PMN-MDSC

as an indicator of myeloid dysfunction and advanced disease is supported by prior reports demonstrating strong associations between PMN-MDSC frequencies and poor clinical outcomes in cancer (7, 67, 69).

A dysregulated functional capacity of myeloid cells in MM patients, including decreased capacity for phagocytosis and oxidative burst associated with elevated neutrophil CD64 expression and STAT3 phosphorylation, has been previously reported (4). In the current study, we demonstrate an increase in the mitochondrial superoxide production in mature neutrophils of MM2 patients indicating a primed phenotype in the absence of signs of cellular activation or degranulation (Figure 4A-B). No differences in total ROS production were observed between the neutrophils of MM1 and MM2 patients (Figure 4A-B). Differences between the studies could be attributed to variances in the methods of assessment of oxidative burst.

High serum levels of CXCL9 and CXCL10, closely related inflammatory cytokines interacting with chemokine receptor CXCR3, have been proposed as potential biomarkers of MM progression associated with poor overall survival (70, 71). High concentrations of CXCL9 and CXCL10 interfere with the infiltration of natural killer (NK) cells into the MM microenvironment and limit their anti-myeloma activity (72, 73). We demonstrate that CXCL9 is significantly elevated in MM2 patients and in patients with R-ISS stage III (Figures 5 and 6), consistent with prior studies (70, 71). We further show that the levels of CXCL9 closely correlate with the expression of CD64 on myeloid cells, in particular on classical and patrolling monocytes ($R>0.8$; $p<0.0001$; Figure 5). An elevated level of sCD163 has been proposed as an independent biomarker in MM with sCD163 levels in

bone marrow aspirates and peripheral blood of MM patients shown to be associated with poor disease outcomes (57). Consistent with a prior report (57), we demonstrate that sCD163 levels are significantly elevated in the plasma of MM2 patients or patients diagnosed with R-ISS stage III disease (Figure 5A and Figure 6D).

Tumor progression, through immune editing of myeloid cells, has been demonstrated in experimental and clinical models of MM and patrolling monocytes were previously described as a potential indicator of circulating osteoclast precursors (23, 74). We did not observe a difference in the levels of classical and patrolling monocyte markers between the groups of patients with or without bone disease at the time of diagnosis (Supplemental Figure 9). The presented data provide a detailed characterization of circulating monocytic subsets, including the downregulation of CX3CR1 and upregulation of PD-L1 on patrolling monocytes in MM2 patients. To our knowledge, a detailed phenotypic characterization of circulating eosinophils has not been previously reported in patients with MM. It has been suggested that eosinophils can contribute to MM progression and demonstrate immunosuppressive properties (52, 75). Additionally, studies in allergic rhinitis (76) and pulmonary inflammation (77) demonstrate a critical role of CCR3 expression in the inflammatory pathway and recruitment of eosinophils. The data presented here demonstrating a significant downregulation of CCR3 on eosinophils in MM2 patients are consistent with prior studies and support an active involvement of eosinophils in the pathogenesis of MM.

Limitations of this study include limited sample size and younger age of controls relative to MM patients. However, healthy controls did not contribute to the interpretation

of findings from case-only analyses of patients in the MM1 and MM2 groups where no correlation with age was detected. Although MM phenotypes were primarily stratified based on neutrophil CD64 expression, other criteria including CXCR2 expression on mature neutrophils and CX3CR1 on monocytes were independently considered. Follow-up studies focusing on a detailed analysis of circulating innate immune cell subsets present in the BME pre- and post-transplantation would provide additional evidence regarding the evolving dynamics of myeloid cell populations in MM. Longitudinal investigations with serial samples collected before, during, and after treatment are warranted to closely evaluate the predictive value of markers of myeloid dysregulation in MM and associated precancerous conditions.

The novel myeloid phenotype described here improves our understanding of the phenotypic and functional changes of neutrophils, monocytes, and eosinophils in MM patients. Overall, the results of this study highlight the importance of myeloid cell subsets as a parameter in the assessment and clinical monitoring of advanced-stage disease progression in MM.

REFERENCES

1. Rajkumar SV, Dimopoulos MA, Palumbo A, Blade J, Merlini G, Mateos M-V, et al. International Myeloma Working Group Updated Criteria for the Diagnosis of Multiple Myeloma. The Lancet Oncology (2014) 15(12):e538-e48. doi: 10.1016/s1470-2045(14)70442-5.

2. Dimopoulos M, Kyle R, Fermand JP, Rajkumar SV, San Miguel J, Chanan-Khan A, et al. Consensus Recommendations for Standard Investigative Workup: Report of the International Myeloma Workshop Consensus Panel 3. Blood (2011) 117(18):4701-5. doi: 10.1182/blood-2010-10-299529.

3. Binsfeld M, Muller J, Lamour V, De Veirman K, De Raeve H, Bellahcène A, et al. Granulocytic Myeloid-Derived Suppressor Cells Promote Angiogenesis in the Context of Multiple Myeloma. Oncotarget (2016) 7(25):37931-43. doi: 10.18632/oncotarget.9270.

4. Romano A, Parrinello NL, Simeon V, Puglisi F, La Cava P, Bellofiore C, et al. High-Density Neutrophils in Mgus and Multiple Myeloma Are Dysfunctional and Immune-Suppressive Due to Increased Stat3 Downstream Signaling. Sci Rep (2020) 10(1):1983. doi: 10.1038/s41598-020-58859-x.

5. Hsu BE, Tabaries S, Johnson RM, Andrzejewski S, Senecal J, Lehuede C, et al. Immature Low-Density Neutrophils Exhibit Metabolic Flexibility That Facilitates Breast Cancer Liver Metastasis. Cell Rep (2019) 27(13):3902-15 e6. doi: 10.1016/j.celrep.2019.05.091.

6. Casbon A-J, Reynaud D, Park C, Khuc E, Gan DD, Schepers K, et al. Invasive Breast Cancer Reprograms Early Myeloid Differentiation in the Bone Marrow to Generate Immunosuppressive Neutrophils. Proceedings of the National Academy of Sciences (2015) 112(6):E566-E75. doi: 10.1073/pnas.1424927112.

7. Veglia F, Perego M, Gabrilovich D. Myeloid-Derived Suppressor Cells Coming of Age. Nature Immunology (2018) 19(2):108-19. doi: 10.1038/s41590-017-0022-x.

8. Sagiv JY, Michaeli J, Assi S, Mishalian I, Kisos H, Levy L, et al. Phenotypic Diversity and Plasticity in Circulating Neutrophil Subpopulations in Cancer. Cell Rep (2015) 10(4):562-73. doi: 10.1016/j.celrep.2014.12.039.

9. Condamine T, Dominguez GA, Youn JI, Kossenkov AV, Mony S, Alicea-Torres K, et al. Lectin-Type Oxidized Ldl Receptor-1 Distinguishes Population of Human Polymorphonuclear Myeloid-Derived Suppressor Cells in Cancer Patients. Sci Immunol (2016) 1(2). doi: 10.1126/sciimmunol.aaf8943.

10. Jimenez RV, Kuznetsova V, Connelly AN, Hel Z, Szalai AJ. C-Reactive Protein Promotes the Expansion of Myeloid Derived Cells with Suppressor Functions. Frontiers in immunology (2019):2183.

11. Vlkova M, Chovancova Z, Nechvatalova J, Connelly AN, Davis MD, Slanina P, et al. Neutrophil and Granulocytic Myeloid-Derived Suppressor Cell-Mediated T Cell Suppression Significantly Contributes to Immune Dysregulation in Common Variable Immunodeficiency Disorders. J Immunol (2019) 202(1):93-104. doi: 10.4049/jimmunol.1800102.

12. Rundgren IM, Ersvaer E, Ahmed AB, Ryningen A, Bruserud O. Circulating Monocyte Subsets in Multiple Myeloma Patients Receiving Autologous Stem Cell Transplantation - a Study of the Preconditioning Status and the Course until Posttransplant Reconstitution for a Consecutive Group of Patients. BMC Immunol (2019) 20(1):39. doi: 10.1186/s12865-019-0323-y.

13. Bolzoni M, Ronchetti D, Storti P, Donofrio G, Marchica V, Costa F, et al. Il21r Expressing Cd14(+)Cd16(+) Monocytes Expand in Multiple Myeloma Patients Leading to Increased Osteoclasts. Haematologica (2017) 102(4):773-84. doi: 10.3324/haematol.2016.153841.

14. Nicolás-Ávila JÁ, Adrover JM, Hidalgo A. Neutrophils in Homeostasis, Immunity, and Cancer. Immunity (2017) 46(1):15-28. doi: 10.1016/j.immuni.2016.12.012.

15. Bowers NL, Helton ES, Huijbregts RP, Goepfert PA, Heath SL, Hel Z. Immune Suppression by Neutrophils in Hiv-1 Infection: Role of Pd-L1/Pd-1 Pathway. PLoS Pathog (2014) 10(3):e1003993. doi: 10.1371/journal.ppat.1003993.

16. de Kleijn S, Langereis JD, Leentjens J, Kox M, Netea MG, Koenderman L, et al. Ifn-Gamma-Stimulated Neutrophils Suppress Lymphocyte Proliferation through Expression of Pd-L1. PLoS One (2013) 8(8):e72249. doi: 10.1371/journal.pone.0072249.

17. Puglisi F, Parrinello NL, Giallongo C, Cambria D, Camiolo G, Bellofiore C, et al. Plasticity of High-Density Neutrophils in Multiple Myeloma Is Associated with Increased Autophagy Via Stat3. Int J Mol Sci (2019) 20(14). doi: 10.3390/ijms20143548.

18. Favaloro J, Liyadipitiya T, Brown R, Yang S, Suen H, Woodland N, et al. Myeloid Derived Suppressor Cells Are Numerically, Functionally and Phenotypically Different in Patients with Multiple Myeloma. Leuk Lymphoma (2014) 55(12):2893-900. doi: 10.3109/10428194.2014.904511.

19. Görgün GT, Whitehill G, Anderson JL, Hideshima T, Maguire C, Laubach J, et al. Tumor-Promoting Immune-Suppressive Myeloid-Derived Suppressor Cells in the Multiple Myeloma Microenvironment in Humans. Blood, The Journal of the American Society of Hematology (2013) 121(15):2975-87.

20. Romano A, Parrinello NL, La Cava P, Tibullo D, Giallongo C, Camiolo G, et al. Pmn-Mdsc and Arginase Are Increased in Myeloma and May Contribute to Resistance to Therapy. Expert Rev Mol Diagn (2018) 18(7):675-83. doi: 10.1080/14737159.2018.1470929.

21. Perez C, Botta C, Zabaleta A, Puig N, Cedena M-T, Goicoechea I, et al. Immunogenomic Identification and Characterization of Granulocytic Myeloid-Derived Suppressor Cells in Multiple Myeloma. Blood (2020) 136(2):199-209. doi: 10.1182/blood.2019004537.

22. Giallongo C, Tibullo D, Parrinello NL, La Cava P, Di Rosa M, Bramanti V, et al. Granulocyte-Like Myeloid Derived Suppressor Cells (G-Mdsc) Are Increased in Multiple Myeloma and Are Driven by Dysfunctional Mesenchymal Stem Cells (Msc). Oncotarget (2016) 7(52):85764.

23. Ramachandran IR, Condamine T, Lin C, Herlihy SE, Garfall A, Vogl DT, et al. Bone Marrow Pmn-Mdscs and Neutrophils Are Functionally Similar in Protection of Multiple Myeloma from Chemotherapy. Cancer Lett (2016) 371(1):117-24. doi: 10.1016/j.canlet.2015.10.040.

24. Ramachandran IR, Martner A, Pisklakova A, Condamine T, Chase T, Vogl T, et al. Myeloid-Derived Suppressor Cells Regulate Growth of Multiple Myeloma by Inhibiting T Cells in Bone Marrow. J Immunol (2013) 190(7):3815-23. doi: 10.4049/jimmunol.1203373.

25. Romano A, Laura Parrinello N, Cerchione C, Letizia Consoli M, Parisi M, Calafiore V, et al. The Nlr and Lmr Ratio in Newly Diagnosed Mm Patients Treated Upfront with Novel Agents. Blood cancer journal (2017) 7(12):1-3.

26. Solmaz Medeni S, Acar C, Olgun A, Acar A, Seyhanlı A, Taskıran E, et al. Can Neutrophil-to-Lymphocyte Ratio, Monocyte-to-Lymphocyte Ratio, and Platelet-to-Lymphocyte Ratio at Day+ 100 Be Used as a Prognostic Marker in Multiple Myeloma Patients with Autologous Transplantation? Clinical Transplantation (2018) 32(9):e13359.

27. Lee G-W, Park SW, Go S-I, Kim H-G, Kim MK, Min C-K, et al. The Derived Neutrophil-to-Lymphocyte Ratio Is an Independent Prognostic Factor in Transplantation Ineligible Patients with Multiple Myeloma. Acta Haematologica (2018) 140(3):146-56.

28. Passlick B, Flieger D, Ziegler-Heitbrock HW. Identification and Characterization of a Novel Monocyte Subpopulation in Human Peripheral Blood. Blood (1989) 74(7):2527-34. doi: 10.1182/blood.V74.7.2527.2527.

29. Scavelli C, Nico B, Cirulli T, Ria R, Di Pietro G, Mangieri D, et al. Vasculogenic Mimicry by Bone Marrow Macrophages in Patients with Multiple Myeloma. Oncogene (2008) 27(5):663-74. doi: 10.1038/sj.onc.1210691.

30. VanValkenburg ME, Pruitt GI, Brill IK, Costa L, Ehtsham M, Justement IT, et al. Family History of Hematologic Malignancies and Risk of Multiple Myeloma: Differences by Race and Clinical Features. Cancer Causes Control (2016) 27(1):81-91. doi: 10.1007/s10552-015-0685-2.

31. Durie BG, Salmon SE. A Clinical Staging System for Multiple Myeloma. Correlation of Measured Myeloma Cell Mass with Presenting Clinical Features, Response to Treatment, and Survival. Cancer cytopathology (1975) 36(3):842-54. doi: 10.1002/1097-0142(197509)36:3<842::aid-cncr2820360303>3.0.co;2-u.

32. Connelly AN, Huijbregts RPH, Pal HC, Kuznetsova V, Davis MD, Ong KL, et al. Optimization of Methods for the Accurate Characterization of Whole Blood Neutrophils. Scientific Reports (2022) 12(1). doi: 10.1038/s41598-022-07455-2.

33. Elghetany MT. Surface Antigen Changes During Normal Neutrophilic Development: A Critical Review. Blood Cells, Molecules, and Diseases (2002) 28(2):260-74. doi: 10.1006/bcmd.2002.0513.

34. Lund-Johansen F, Terstappen LWMM. Differential Surface Expression of Cell Adhesion Molecules During Granulocyte Maturation. Journal of Leukocyte Biology (1993) 54(1):47-55. doi: https://doi.org/10.1002/jlb.54.1.47.

35. Kerst JM, van de Winkel JG, Evans AH, de Haas M, Slaper-Cortenbach IC, de Wit TP, et al. Granulocyte Colony-Stimulating Factor Induces Hfc Gamma Ri (Cd64 Antigen)-Positive Neutrophils Via an Effect on Myeloid Precursor Cells. Blood (1993) 81(6):1457-64. doi: 10.1182/blood.V81.6.1457.1457.

36. Marvel D, Gabrilovich DI. Myeloid-Derived Suppressor Cells in the Tumor Microenvironment: Expect the Unexpected. J Clin Invest (2015) 125(9):3356-64. doi: 10.1172/jci80005.

37. Ivetic A, Hoskins Green HL, Hart SJ. L-Selectin: A Major Regulator of Leukocyte Adhesion, Migration and Signaling. Front Immunol (2019) 10:1068. doi: 10.3389/fimmu.2019.01068.

38. Snyder KM, McAloney CA, Montel JS, Modiano JF, Walcheck B. Ectodomain Shedding by Adam17 (a Disintegrin and Metalloproteinase 17) in Canine Neutrophils. Vet Immunol Immunopathol (2021) 231:110162. doi: 10.1016/j.vetimm.2020.110162.

39. Landsberger M, Zhou J, Wilk S, Thaumuller C, Pavlovic D, Otto M, et al. Inhibition of Lectin-Like Oxidized Low-Density Lipoprotein Receptor-1 Reduces Leukocyte Adhesion within the Intestinal Microcirculation in Experimental Endotoxemia in Rats. Crit Care (2010) 14(6):R223. doi: 10.1186/cc9367.

40. Berg M, James SP. Human Neutrophils Release the Leu-8 Lymph Node Homing Receptor During Cell Activation. Blood (1990) 76(11):2381-8. doi: 10.1182/blood.V76.11.2381.2381.

41. Ekstedt S, Safholm J, Georen SK, Cardell LO. Dividing Neutrophils in Subsets Reveals a Significant Role for Activated Neutrophils in the Development of Airway Hyperreactivity. Clin Exp Allergy (2019) 49(3):285-91. doi: 10.1111/cea.13311.

42. Cassatella MA, Ostberg NK, Tamassia N, Soehnlein O. Biological Roles of Neutrophil-Derived Granule Proteins and Cytokines. Trends Immunol (2019) 40(7):648-64. doi: 10.1016/j.it.2019.05.003.

43. Borregaard N, Cowland JB. Granules of the Human Neutrophilic Polymorphonuclear Leukocyte. Blood (1997) 89(10):3503-21. doi: 10.1182/blood.V89.10.3503.

44. Mistry P, Nakabo S, O'Neil L, Goel RR, Jiang K, Carmona-Rivera C, et al. Transcriptomic, Epigenetic, and Functional Analyses Implicate Neutrophil Diversity in the Pathogenesis of Systemic Lupus Erythematosus. Proc Natl Acad Sci U S A (2019) 116(50):25222-8. doi: 10.1073/pnas.1908576116.

45. Fujimoto H, Sakata T, Hamaguchi Y, Shiga S, Tohyama K, Ichiyama S, et al. Flow Cytometric Method for Enumeration and Classification of Reactive Immature Granulocyte Populations. Cytometry (2000) 42(6):371-8.

46. Dinh HQ, Eggert T, Meyer MA, Zhu YP, Olingy CE, Llewellyn R, et al. Coexpression of Cd71 and Cd117 Identifies an Early Unipotent Neutrophil Progenitor Population in Human Bone Marrow. Immunity (2020) 53(2):319-34 e6. doi: 10.1016/j.immuni.2020.07.017.

47. Zhu YP, Padgett L, Dinh HQ, Marcovecchio P, Blatchley A, Wu R, et al. Identification of an Early Unipotent Neutrophil Progenitor with Pro-Tumoral Activity in Mouse and Human Bone Marrow. Cell Rep (2018) 24(9):2329-41 e8. doi: 10.1016/j.celrep.2018.07.097.

48. Brandau S, Trellakis S, Bruderek K, Schmaltz D, Steller G, Elian M, et al. Myeloid-Derived Suppressor Cells in the Peripheral Blood of Cancer Patients Contain a Subset of Immature Neutrophils with Impaired Migratory Properties. J Leukoc Biol (2011) 89(2):311-7. doi: 10.1189/jlb.0310162.

49. Hacbarth E, Kajdacsy-Balla A. Low Density Neutrophils in Patients with Systemic Lupus Erythematosus, Rheumatoid Arthritis, and Acute Rheumatic Fever. Arthritis & Rheumatism (1986) 29(11):1334-42. doi: https://doi.org/10.1002/art.1780291105.

50. Rice CM, Davies LC, Subleski JJ, Maio N, Gonzalez-Cotto M, Andrews C, et al. Tumour-Elicited Neutrophils Engage Mitochondrial Metabolism to Circumvent Nutrient Limitations and Maintain Immune Suppression. Nat Commun (2018) 9(1):5099. doi: 10.1038/s41467-018-07505-2.

51. Geissmann F, Jung S, Littman DR. Blood Monocytes Consist of Two Principal Subsets with Distinct Migratory Properties. Immunity (2003) 19(1):71-82.

52. Calcinotto A, Brevi A, Chesi M, Ferrarese R, Garcia Perez L, Grioni M, et al. Microbiota-Driven Interleukin-17-Producing Cells and Eosinophils Synergize to Accelerate Multiple Myeloma Progression. Nat Commun (2018) 9(1):4832. doi: 10.1038/s41467-018-07305-8.

53. Cugno M, Marzano AV, Lorini M, Carbonelli V, Tedeschi A. Enhanced Tissue Factor Expression by Blood Eosinophils from Patients with Hypereosinophilia: A Possible Link with Thrombosis. PLoS One (2014) 9(11):e111862. doi: 10.1371/journal.pone.0111862.

54. Yoon J, Terada A, Kita H. Cd66b Regulates Adhesion and Activation of Human Eosinophils. The Journal of Immunology (2007) 179(12):8454. doi: 10.4049/jimmunol.179.12.8454.

55. Pedersen CC, Borup R, Fischer-Nielsen A, Mora-Jensen H, Fossum A, Cowland JB, et al. Changes in Gene Expression During G-Csf-Induced Emergency Granulopoiesis in Humans. J Immunol (2016) 197(5):1989-99. doi: 10.4049/jimmunol.1502690.

56. Shive CL, Jiang W, Anthony DD, Lederman MM. Soluble Cd14 Is a Nonspecific Marker of Monocyte Activation. AIDS (2015) 29(10):1263-5. doi: 10.1097/QAD.0000000000000735.

57. Andersen MN, Abildgaard N, Maniecki MB, Moller HJ, Andersen NF. Monocyte/Macrophage-Derived Soluble Cd163: A Novel Biomarker in Multiple Myeloma. Eur J Haematol (2014) 93(1):41-7. doi: 10.1111/ejh.12296.

58. Hel Z, Xu J, Denning WL, Helton ES, Huijbregts RP, Heath SL, et al. Dysregulation of Systemic and Mucosal Humoral Responses to Microbial and Food Antigens as a Factor Contributing to Microbial Translocation and Chronic Inflammation in Hiv-1 Infection. PLoS pathogens (2017) 13(1):e1006087.

59. Litzman J, Nechvátalová J, Xu J, Tichá O, Vlková M, Hel Z. Chronic Immune Activation in Common Variable Immunodeficiency (Cvid) Is Associated with Elevated Serum Levels of Soluble Cd14 and Cd25 but Not Endotoxaemia. Clinical & Experimental Immunology (2012) 170(3):321-32.

60. Schultze JL, Mass E, Schlitzer A. Emerging Principles in Myelopoiesis at Homeostasis and During Infection and Inflammation. Immunity (2019) 50(2):288-301.

61. Wang J, De Veirman K, De Beule N, Maes K, De Bruyne E, Van Valckenborgh E, et al. The Bone Marrow Microenvironment Enhances Multiple Myeloma Progression by Exosome-Mediated Activation of Myeloid-Derived Suppressor Cells. Oncotarget (2015) 6(41):43992.

62. Alvarez R, Oliver L, Valdes A, Mesa C, editors. Cancer-Induced Systemic Myeloid Dysfunction: Implications for Treatment and a Novel Nanoparticle Approach for Its Correction. Seminars in Oncology; 2018: Elsevier.

63. Tcyganov E, Mastio J, Chen E, Gabrilovich DI. Plasticity of Myeloid-Derived Suppressor Cells in Cancer. Current opinion in immunology (2018) 51:76-82.

64. Ohsaka A, Saionji K, Takagi S, Igari J. Increased Expression of the High-Affinity Receptor for Igg (Fcri, Cd64) on Neutrophils in Multiple Myeloma. Hematopathology and Molecular Hematology (1996) 10:151-60.

65. Hirsh M, Mahamid E, Bashenko Y, Hirsh I, Krausz MM. Overexpression of the High-Affinity Fcgamma Receptor (Cd64) Is Associated with Leukocyte Dysfunction in Sepsis. Shock (Augusta, Ga) (2001) 16(2):102-8.

66. Groselj-Grenc M, Ihan A, Derganc M. Neutrophil and Monocyte Cd64 and Cd163 Expression in Critically Ill Neonates and Children with Sepsis: Comparison of Fluorescence Intensities and Calculated Indexes. Mediators of inflammation (2008) 2008.

67. Veglia F, Sanseviero E, Gabrilovich DI. Myeloid-Derived Suppressor Cells in the Era of Increasing Myeloid Cell Diversity. Nat Rev Immunol (2021). doi: 10.1038/s41577-020-00490-y.

68. Beyer M, Kochanek M, Giese T, Endl E, Weihrauch MR, Knolle PA, et al. In Vivo Peripheral Expansion of Naive Cd4+Cd25high Foxp3+ Regulatory T Cells in Patients with Multiple Myeloma. Blood (2006) 107(10):3940-9. doi: 10.1182/blood-2005-09-3671.

69. Zhang S, Ma X, Zhu C, Liu L, Wang G, Yuan X. The Role of Myeloid-Derived Suppressor Cells in Patients with Solid Tumors: A Meta-Analysis. PloS one (2016) 11(10):e0164514.

70. Bolomsky A, Schreder M, Hübl W, Zojer N, Hilbe W, Ludwig H. Monokine Induced by Interferon Gamma (Mig/Cxcl9) Is an Independent Prognostic Factor in Newly Diagnosed Myeloma. Leukemia & Lymphoma (2016) 57(11):2516-25. doi: 10.3109/10428194.2016.1151511.

71. Pellegrino A, Antonaci F, Russo F, Merchionne F, Ribatti D, Vacca A, et al. Cxcr3-Binding Chemokines in Multiple Myeloma. Cancer Letters (2004) 207(2):221-7. doi: https://doi.org/10.1016/j.canlet.2003.10.036.

72. Ponzetta A, Benigni G, Antonangeli F, Sciumè G, Sanseviero E, Zingoni A, et al. Multiple Myeloma Impairs Bone Marrow Localization of Effector Natural Killer Cells by Altering the Chemokine Microenvironment. Cancer Research (2015) 75(22):4766-77. doi: 10.1158/0008-5472.CAN-15-1320.

73. Bonanni V, Antonangeli F, Santoni A, Bernardini G. Targeting of Cxcr3 Improves Anti-Myeloma Efficacy of Adoptively Transferred Activated Natural Killer Cells. Journal for immunotherapy of cancer (2019) 7(1):1-16.

74. Petitprez V, Royer B, Desoutter J, Guiheneuf E, Rigolle A, Marolleau JP, et al. Cd14+ Cd16+ Monocytes Rather Than Cd14+ Cd51/61+ Monocytes Are a Potential Cytological Marker of Circulating Osteoclast Precursors in Multiple Myeloma. A Preliminary Study. International Journal of Laboratory Hematology (2015) 37(1):29-35. doi: https://doi.org/10.1111/ijlh.12216.

75. Driscoll J, Aslam I, Malek E. Eosinophils Upregulate Pd-L1 and Pd-L2 Expression to Enhance the Immunosuppressive Microenvironment in Multiple Myeloma. Blood (2017) 130(Supplement 1):4417-. doi: 10.1182/blood.V130.Suppl_1.4417.4417.

76. Fulkerson PC, Fischetti CA, McBride ML, Hassman LM, Hogan SP, Rothenberg ME. A Central Regulatory Role for Eosinophils and the Eotaxin/Ccr3 Axis in Chronic Experimental Allergic Airway Inflammation. Proceedings of the National Academy of Sciences (2006) 103(44):16418. doi: 10.1073/pnas.0607863103.

77. Fulkerson PC, Fischetti CA, Rothenberg ME. Eosinophils and Ccr3 Regulate Interleukin-13 Transgene-Induced Pulmonary Remodeling. Am J Pathol (2006) 169(6):2117-26. doi: 10.2353/ajpath.2006.06061

SUPPLEMENTAL FIGURES

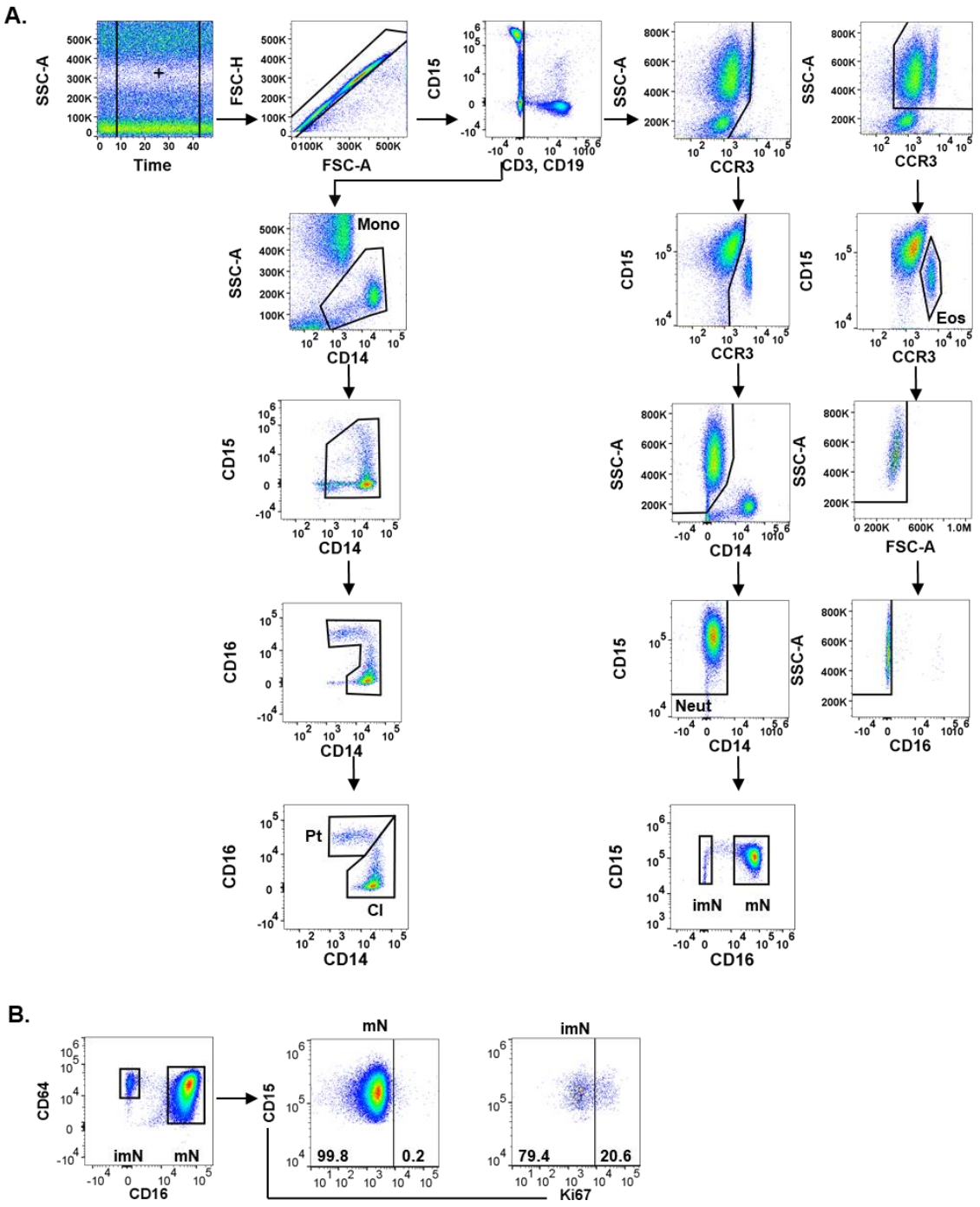

Figure S1. Gating strategies for innate immune cell subpopulations. (A) Gating strategy for the identification of monocyte, neutrophil, and eosinophil subpopulations. All cells were gated as single cells with a negative gate to remove T and B lymphocytes with lineage markers CD3 and CD19, respectively. Monocytes were gated following the removal of $CD15^{+}$ cells. Classical monocytes (Cl Mo) were identified as $CD14^{high}CD16^{low}$

and patrolling monocytes (Pt Mo) were identified as $CD14^{low}CD16^{high}$. Neutrophils were gated following the removal of eosinophils and monocytes utilizing CCR3 and CD14, respectively. Neutrophils were identified as $SSC^{high}CD15^{+}$ cells with mature neutrophils (mNs) identified as $CD15^{+}CD16^{+}$ and immature neutrophils (imNs) identified as $CD15^{+}CD16^{-}$. Eosinophils (Eos) were gated following the removal of $CD16^{+}$ cells and were identified as $CCR3^{+}CD15^{+}CD16^{-}$. **(B)** Ki67 gating of neutrophil subpopulations. All cells were gated using a previously determined FMO gate for the APC fluorochrome. Cells positive for Ki67 were determined by applying the FMO gate to the Ki67-stained cells; FMO = fluorescent minus on

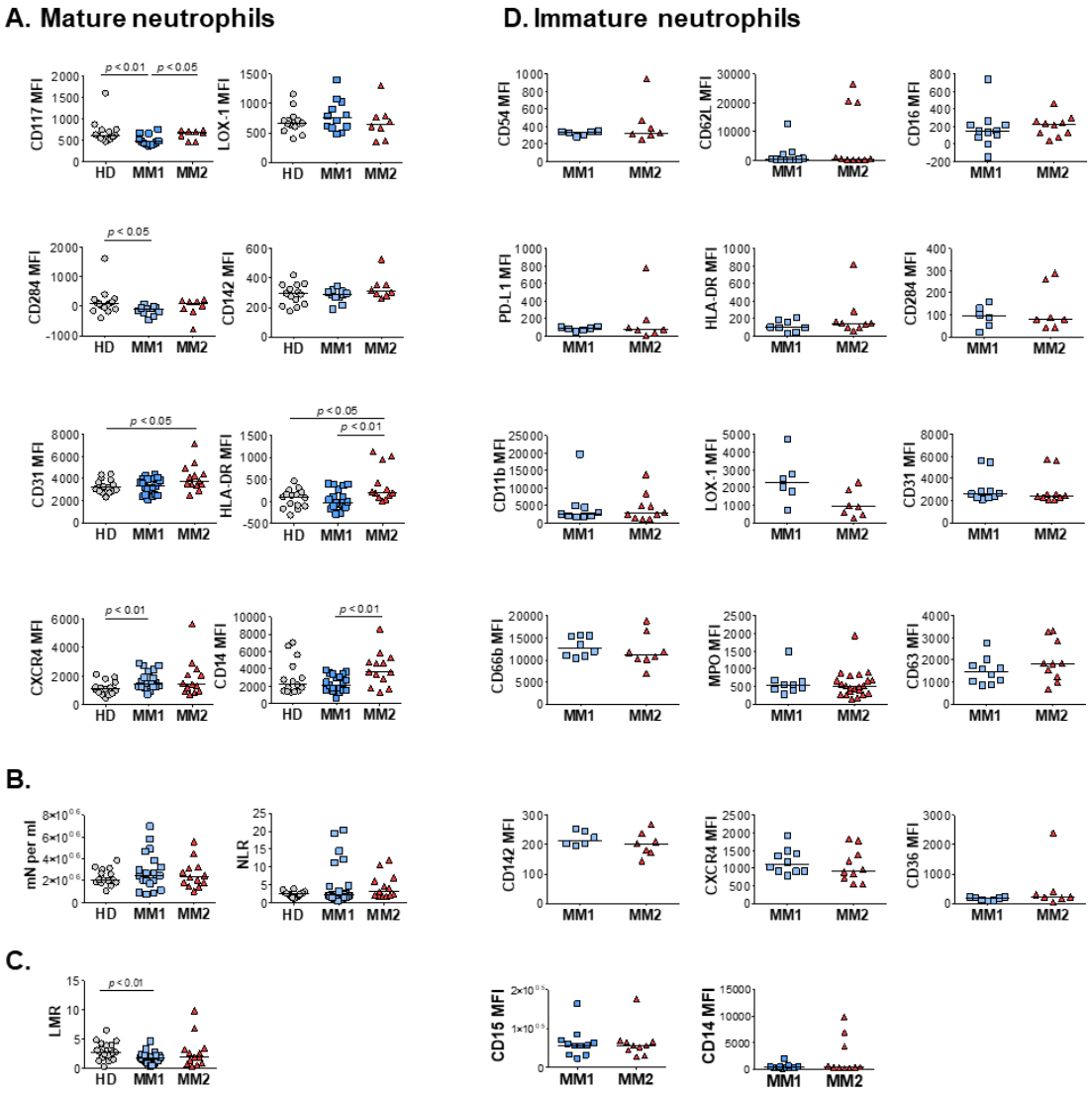

Figure S2. Analysis of the phenotype of neutrophil subpopulations and myeloid cell ratios in MM patients. (A) Expression of surface markers of neutrophil activation, cell signaling, and migration on mNs. **(B)** Frequency of mature neutrophils per ml of blood and neutrophil to T-lymphocyte ratio. **(C)** T-lymphocyte to monocyte ratio. **(D)** Expression of neutrophil surface markers on imNs. MFI, median fluorescent intensity; NLR, neutrophil to T: lymphocyte ratio; LMR, T: lymphocyte to monocyte ratio. Statistical analyses were performed using the Mann-Whitney rank-sum test with *p* values are indicated; bars and lines represent median values and simple linear regression analysis, respectively.

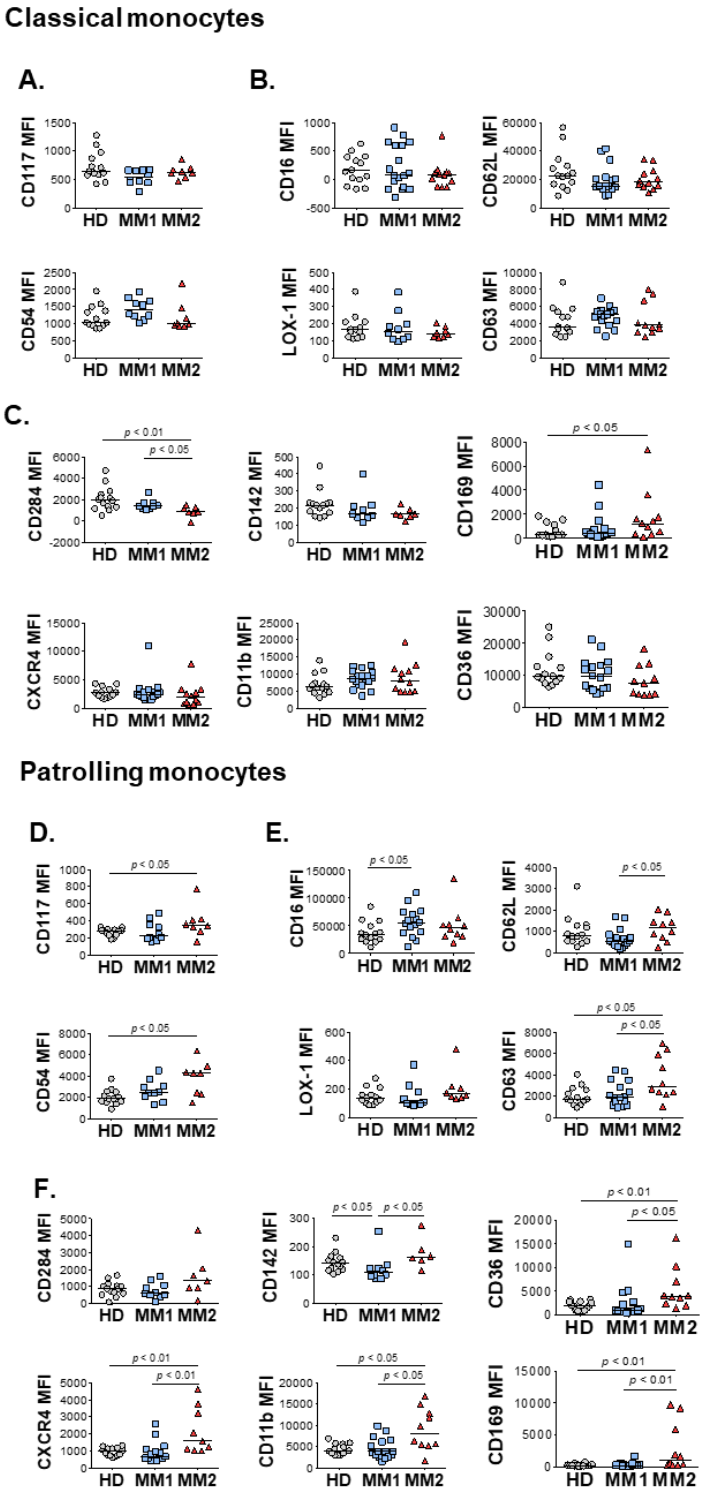

Figure S3. Analysis of monocyte phenotypes in MM patients. (A-F) Surface levels of monocyte maturation, activation, cell signaling and migration markers on classical **(A-C)** and patrolling **(D-F)** monocytes. MFI, median fluorescent intensity. Statistical analyses were performed using the Mann-Whitney rank-sum test with *p* values indicated. Bars represent median values.

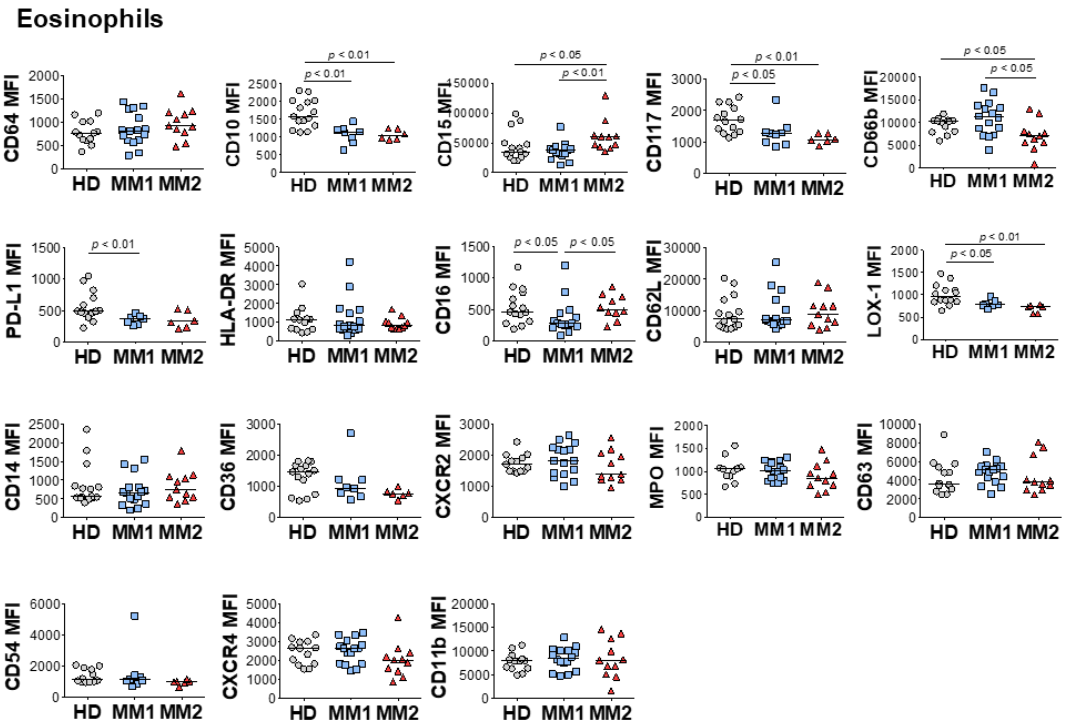

Figure S4. Analysis of the eosinophil phenotype in MM patients. Surface levels of maturation, lineage, activation, cell signaling, and migration markers on eosinophils. MFI, median fluorescent intensity. Statistical analyses were performed using the Mann-Whitney rank-sum test with *p* values indicated. Bars represent median values.

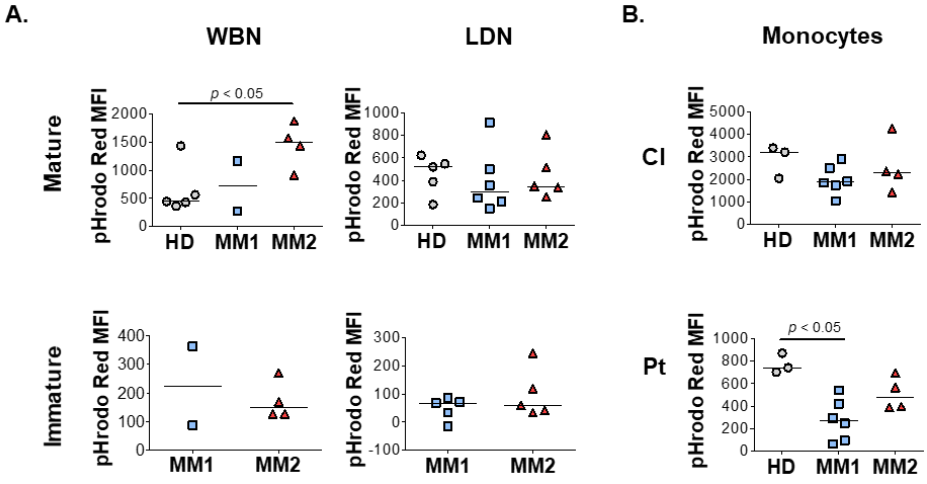

Figure S5. Phagocytic capacity of myeloid subpopulations. (A-B) Phagocytic capacity was detected by phagocytosis of pHrodo™ Red E. coli BioParticles™ on neutrophil **(A)** and monocyte **(B)** subpopulations. MFI, median fluorescent intensity. Statistical analyses were performed using the Mann-Whitney rank-sum test with *p* values indicated. Bars represent median values.

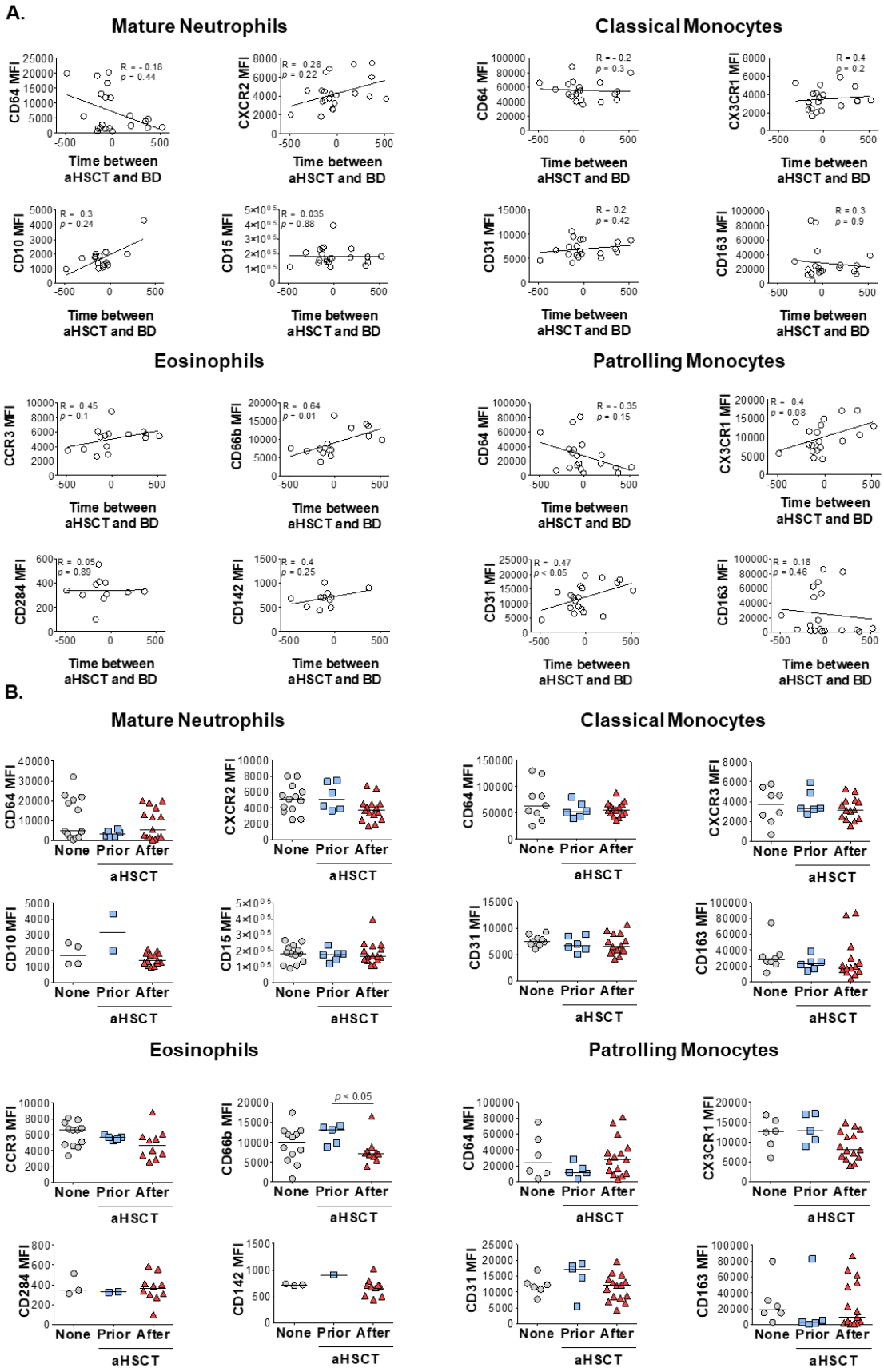
A.
Mature Neutrophils
CD64 MFI
R = - 0.18
p = 0.44
CXCR2 MFI
R = 0.28
p = 0.22
Classical Monocytes
CD64 MFI
R = - 0.2
p = 0.3
CX3CR1 MFI
R = 0.4
p = 0.2
CD10 MFI
R = 0.3
p = 0.24
CD15 MFI
R = 0.035
p = 0.88
CD31 MFI
R = 0.2
p = 0.42
CD163 MFI
R = 0.3
p = 0.9
Time between aHSCT and BD
Eosinophils
Patrolling Monocytes
CCR3 MFI
R = 0.45
p = 0.1
CD66b MFI
R = 0.64
p = 0.01
CD64 MFI
R = - 0.35
p = 0.15
CX3CR1 MFI
R = 0.4
p = 0.08
CD284 MFI
R = 0.05
p = 0.89
CD142 MFI
R = 0.4
p = 0.25
CD31 MFI
R = 0.47
p < 0.05
CD163 MFI
R = 0.18
p = 0.46
B.
Mature Neutrophils
Classical Monocytes
Eosinophils
Patrolling Monocytes
p < 0.05
None Prior After
aHSCT

Figure S6. Analysis of the potential effect of autologous stem cell transplant on MM2 myeloid phenotype components. (A) Correlation between the surface levels of characteristic markers of the MM2 phenotype on mature neutrophils, classical and patrolling monocytes, and eosinophils with the time period between autologous hematopoietic stem cell transplant (aHSCT) and blood draw (BD). **(B)** Surface levels of myeloid subpopulations separated based on aHSCT status. $aHSCT_{prior}$ is indicative of aHSCT performed > 100 days prior to BD; $aHSCT_{after}$ is indicative of aHSCT performed after BD. MFI = median fluorescent intensity. Statistical analyses were performed using the Spearman correlation test **(A)** or the Mann-Whitney ranked-sum test **(B)**. Spearman correlation coefficients R and *p* values are indicated; bars and lines represent median values and simple linear regression analysis, respectively.

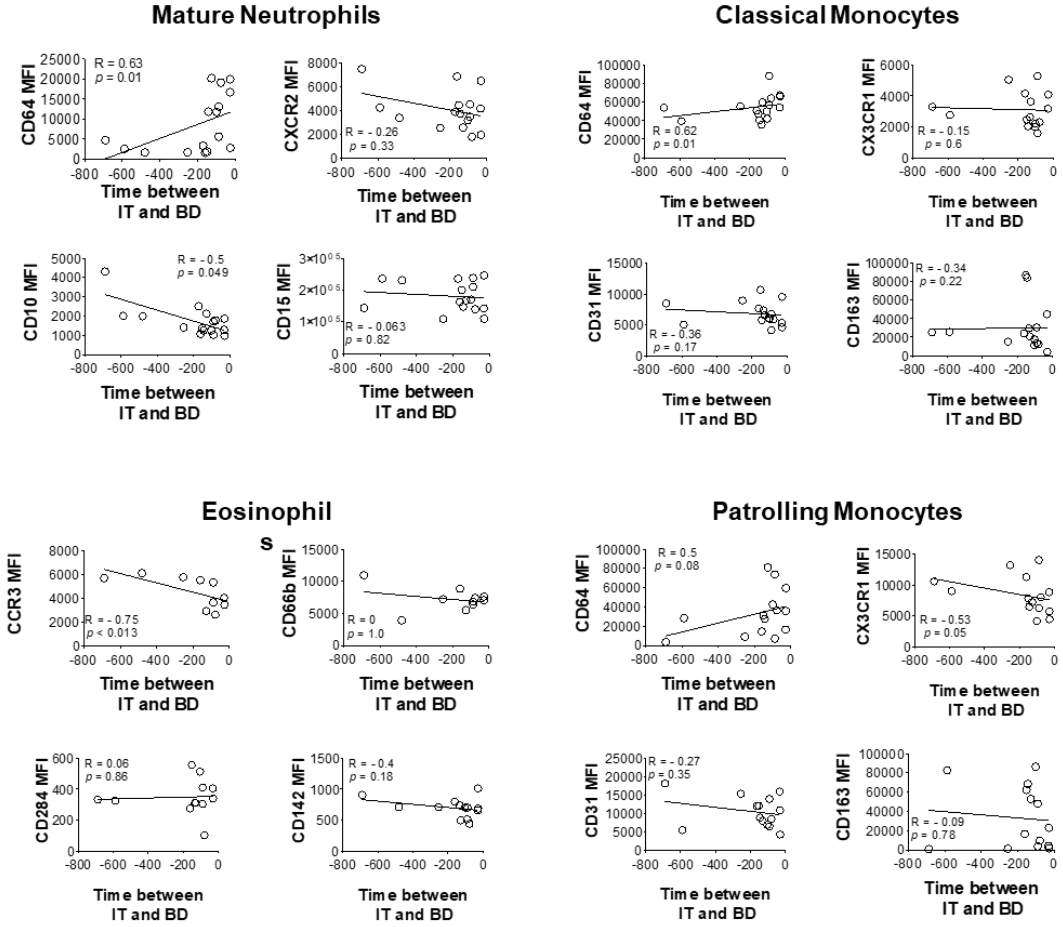

Figure S7. Analysis of the potential effect of induction therapy on MM2 myeloid phenotype components. Correlation between the time period between induction therapy (IT) and BD and the surface levels of characteristic markers of the MM2 phenotype on mature neutrophils, classical and patrolling monocytes, and eosinophils. MFI = median fluorescent intensity. Statistical analyses were performed using the Spearman correlation test. Spearman correlation coefficients R and *p* values are indicated; bars and lines represent median values and simple linear regression analysis, respectively.

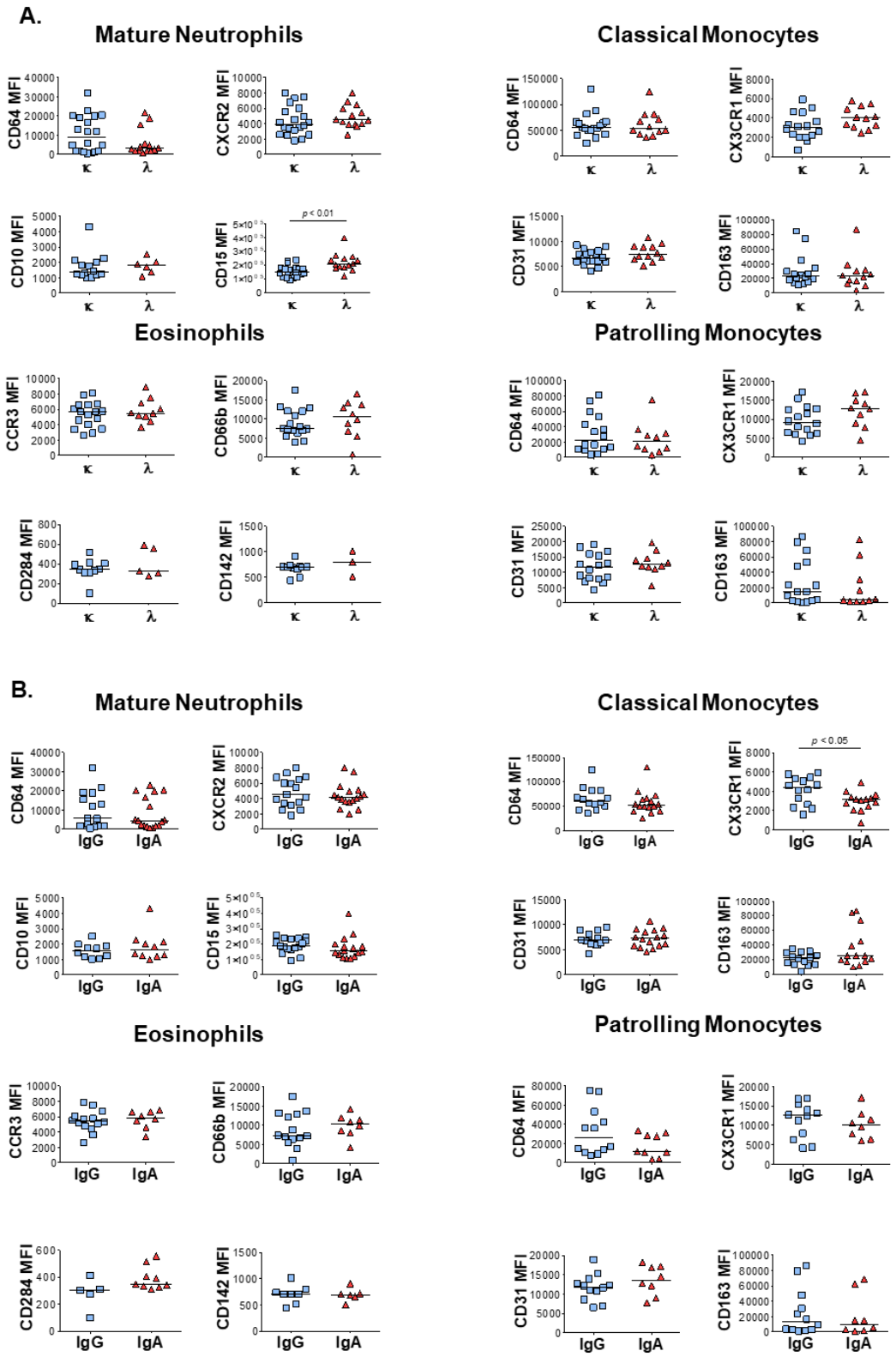

1. Seven MM patients were light-chain restricted and not included in the analyses for Supplemental figure 8A.

Figure S8. Analysis of the relationship between the characteristic features of the MM2 myeloid phenotype and MM immunoglobulin isotype. (A-B) Surface levels of characteristic markers of the MM2 phenotype on mature neutrophils, classical and patrolling monocytes, and eosinophils separated by free light chain **(A)** or immunoglobulin **(B)** isotype. MFI = median fluorescent intensity. Statistical analyses performed with the Mann-Whitney ranked-sum test with *p* values indicated. Bars represent median values

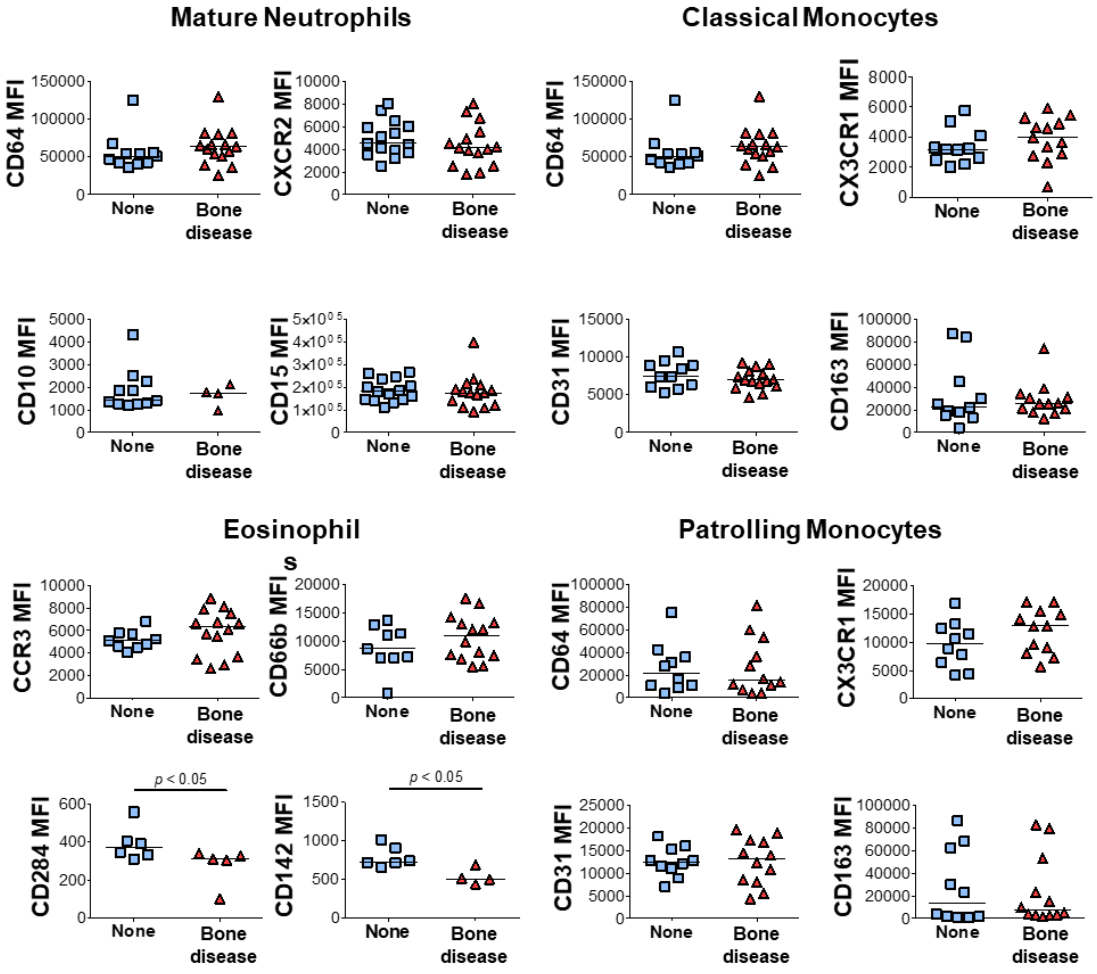

Figure S9. Analysis of the relationship between the characteristic features of the MM2 myeloid phenotype and the presence of bone disease. Surface levels of characteristic markers of the MM2 phenotype on mature neutrophils, classical monocytes, patrolling monocytes, and eosinophils separated by presence of bone disease. MFI = median fluorescent intensity. Statistical analyses performed with the Mann-Whitney ranked-sum test with *p* values indicated. Bars represent median values.

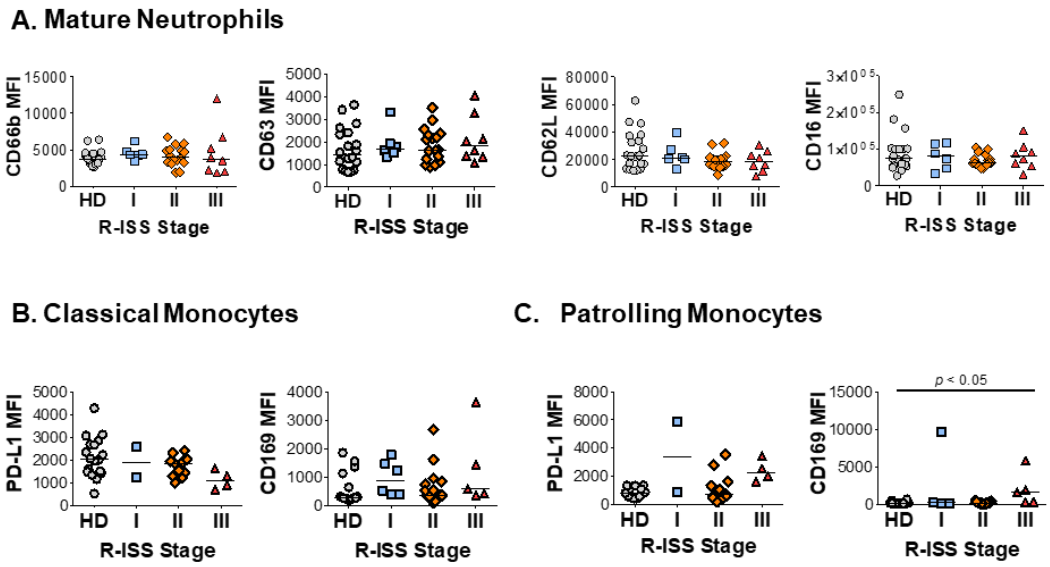

Figure S10. Characteristic features of the MM2 phenotype in relation to R-ISS staging in MM. (A-C) Expression of surface markers on mature neutrophils **(A)**, classical monocytes **(B)**, and patrolling monocytes **(C)** stratified using the R-ISS staging system. MFI, median fluorescent intensity; statistical analyses were performed using the Kruskal-Wallis one way ANOVA test followed by Dunn's post hoc test with *p* values indicated. Bars represent median values.

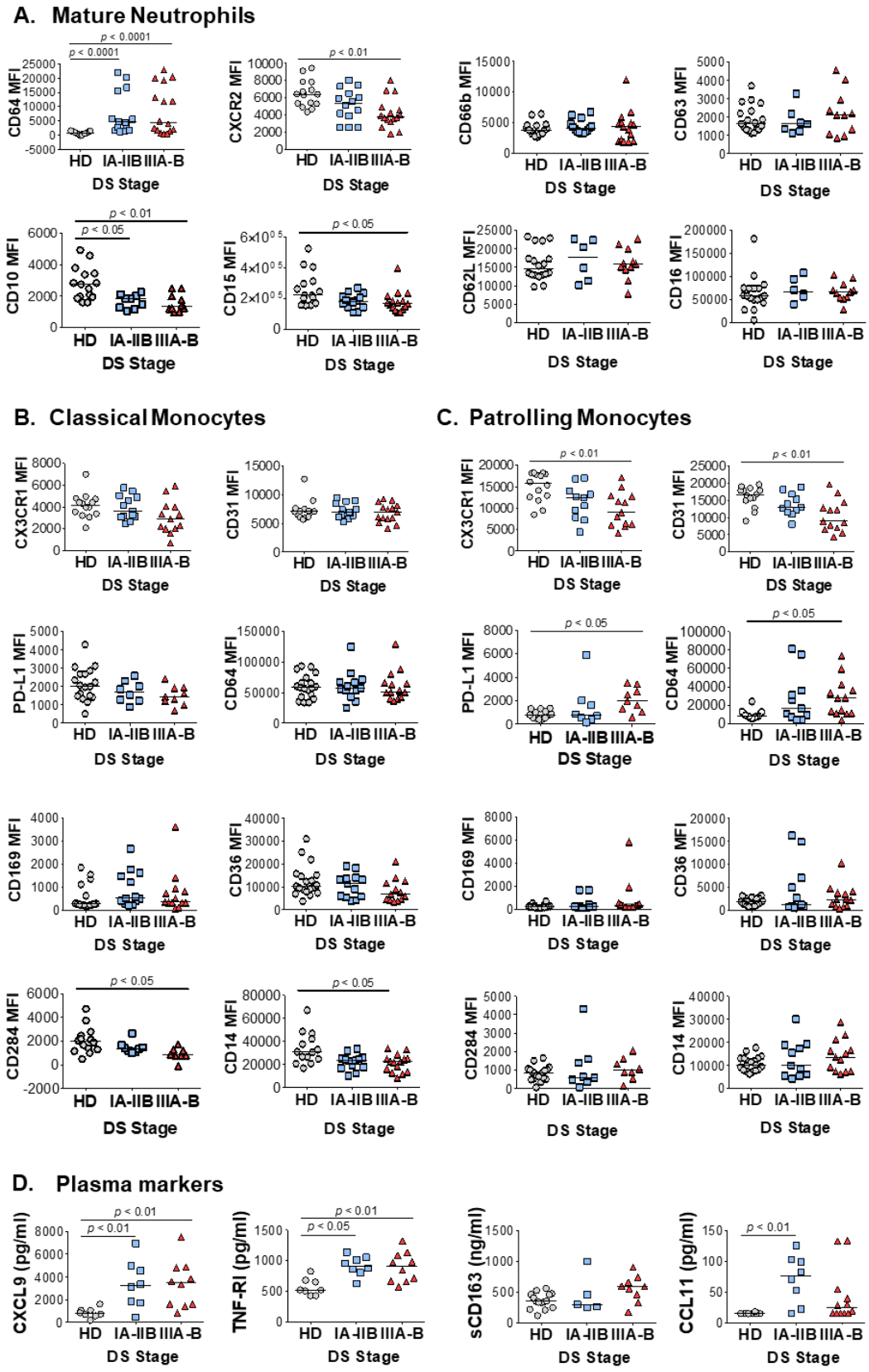
A. Mature Neutrophils
CD64 MFI
CXCR2 MFI
CD66b MFI
CD63 MFI
CD10 MFI
CD15 MFI
CD62L MFI
CD16 MFI
B. Classical Monocytes
C. Patrolling Monocytes
CX3CR1 MFI
CD31 MFI
PD-L1 MFI
CD64 MFI
CD169 MFI
CD36 MFI
CD284 MFI
CD14 MFI
D. Plasma markers
CXCL9 (pg/ml)
TNF-RI (pg/ml)
sCD163 (ng/ml)
CCL11 (pg/ml)
HD
IA-IIB
IIIA-B
DS Stage
p < 0.0001
p < 0.01
p < 0.05

Figure S11. Characteristic features of the MM2 phenotype in relation to Durie Salmon staging in MM. (A-C) Surface levels of the characteristic markers of the MM2 phenotype on mature neutrophils, **(A)** classical monocytes **(B)**, and patrolling monocytes **(C)** stratified using the DS staging system. **(D)** Levels of cytokines and myeloid markers of activation stratified using the DS staging system. MFI, median fluorescent intensity. Statistical analyses were performed using the Kruskal-Wallis one-way ANOVA test followed by Dunn's post hoc test with *p* values as indicated. Bars represent median values.

IMMATURE NEUTROPHIL SUBPOPULATIONS IN ACUTE AND CHRONIC INFECTION AND CANCER

by

KRYSTLE L. ONG*, ASHLEY N. CONNELLY*, MARCUS D. DAVIS, MIGUEL MELENDEZ-FERRO, HARISH C. PAL, CHRISTIAN X. FAY, VALERIYA KUZNETSOVA, ZDENEK HEL

Abstract

Recent identification of neutrophil subpopulations with specific functions in disease pathogenesis has sparked interest in neutrophil heterogeneity. Low-density neutrophils (LDNs), alternatively termed polymorphonuclear myeloid-derived suppressor cells (PMN-MDSCs), represent a subpopulation of neutrophils that are expanded in inflammatory diseases and exert immunosuppressive functions. We have identified a distinct immature neutrophil (imN) subpopulation characterized as $CD15^{+}CD16^{-}$ $CXCR2^{lo}CD64^{+}CD66b^{+}$ which is present in multiple inflammatory diseases, including HIV-1, coronavirus disease-19 (COVID-19), and multiple myeloma (MM). The immature neutrophil subpopulation can be readily identified in the peripheral blood mononuclear cell (PBMC) layer and in whole blood. imNs demonstrate higher proliferative capacity relative to the mature subpopulation. Assessment of nuclear morphology demonstrates that imLDNs have banded nuclei while mLDNs exhibit multi-lobular nuclei. Compared to mature neutrophils, immature neutrophil subpopulations exhibit lower levels of CXC chemokine receptor 2 (CXCR2) and CD10, a higher level of CD66b and demonstrate decreased phagocytosis and ROS production upon stimulation. The distinct phenotype and functional properties of imNs indicate specific roles for these subpopulations in disease. Further characterization of imN subpopulations is likely to contribute to novel methods to the monitoring of disease progression and design of therapeutic approaches.

Introduction

Neutrophils, the most abundant circulating leukocyte population, represent the first immune cells recruited to the sites of trauma and infection. Neutrophils are specifically equipped to detect bacterial and viral products in circulation (1, 2). Upon interactions with trauma or pathogen-associated signals neutrophils initiate potent responses including respiratory burst, release of antimicrobial proteins, and phagocytosis (3-5). Recent reports highlight neutrophil plasticity in inflammatory conditions and cancer with increasing appreciation for their functional and transcriptional heterogeneity (2-6). Emerging evidence suggests that specific neutrophil subpopulations play an active and critical role in disease pathogenesis (4-7).

LDNs or PMN-MDSCs are neutrophils that co-localize with mononuclear cells in the PBMC layer following density gradient centrifugation (8, 9). Accumulating evidence demonstrates that LDNs are associated with negative clinical outcomes of autoimmune diseases (3, 10), chronic infections (11), and cancer (4, 12). While the origin and function of LDNs remain unclear, LDNs utilize alternative metabolic pathways during hypoxic conditions (4) and exert immunosuppressive functions, including T-cell suppression via mechanisms of enhanced ROS production (13-17). We previously reported that LDNs are significantly expanded in HIV-1 and common variable immune deficiency disorder (11, 15, 16). The level of programmed death-ligand 1 (PD-L1) on LDNs significantly increased in a dose-dependent manner with co-incubation of HIV-1 virions (11).

Utilizing high-throughput single cell transcriptomics technology in combination with mass cytometry or flow cytometry, several studies have characterized novel neutrophil progenitor subpopulations, including proliferative neutrophil precursors eNeps, proNeus 1 and 2, and preNeus (5, 6, 18, 19). A revised neutrophil development pathway was proposed in which proNeu1 or eNeps are presented as the first committed neutrophil progenitors which then mature into proNeu2 and preNeu before progressing to the early neutrophil myeloblast stage. The identified neutrophil progenitor subpopulations have been suggested to play a role in disease pathogenesis with proNeus and preNeus expanded in the bone marrow during sepsis-induced stress (5, 6) with prior reports indicating that lower level of CD16 is characteristic of less differentiated neutrophils (3, 20). Additionally, Dinh et al. and Zhu et al. reported the expansion of circulating CD71-CD101- immature neutrophils in mouse models of pancreatic carcinoma and melanoma correlating with increased tumor burden (18, 19).

In this study, we characterize distinct neutrophil subpopulations in whole blood neutrophils (WBNs) and LDNs in acute and chronic inflammatory conditions including HIV-1, COVID-19, and MM. We further examine specific characteristics of the identified neutrophil subpopulations through morphologic, phenotypic, and functional analyses.

Materials and Methods

Sample collection and study approval

Blood collection of healthy donors and patients was performed by certified phlebotomists utilizing collection tubes containing acid citrate dextrose (ThermoFisher, Waltham, MA). All methods were performed in adherence with the relevant guidelines and regulations. All patients gave informed consent and all procedures were approved by the

Institutional Review Board of the University of Alabama at Birmingham (IRB protocol # 141218001).

Materials

Ethylenediaminetetraacetic acid (EDTA), Dulbecco's phosphate buffer solution (DPBS), and dimethyl sulfoxide (DMSO) were purchased from Corning (Corning, NY). A/B Human serum was purchased from ThermoFisher and fetal bovine serum (FBS) was purchased from Atlanta Biologicals (Atlanta, GA). 2',7'-dichlorodihydrofluorescein (H2-DCFDA) (Sigma Aldrich, St. Louis, MO) was dissolved in DMSO to a final concentration of 1mM. Phorbol myristate acetate (PMA) (Sigma Aldrich) was dissolved in DMSO to a final concentration of 1mg/ml. Antibodies were purchased from BioLegend (San Diego, CA) unless indicated otherwise. Antibody solutions, diluted in 10% A/B human serum in DPBS, are detailed in Appendix A: Supplemental Methods Table 1. All materials and reagents for counting were purchased from Nexcelom (Lawrence, MA).

Whole blood staining

Whole blood staining was performed as previously described (30). Briefly, neutrophil phenotype was analyzed by obtaining 50 µl of fresh whole blood (within 2 hours of collection) and stained for 30 minutes with 50 µl of pre-mixed antibody solutions made in 10% A/B human serum in DPBS at 4°C (Appendix A: Supplemental Methods Table 1). Samples were then washed with 4 ml 0.1M EDTA in DPBS and centrifuged at 200 x g for 5 minutes. Samples were lysed in 1 ml of 1x 1-step Fix/lyse buffer (Invitrogen, Waltham, MA) at room temperature (RT) for 15 minutes, washed, and suspended in equal parts 2% FBS in DPBS and intracellular fixation buffer (Invitrogen), and analyzed on the Attune

NxT flow cytometer (ThermoFisher) within 24 hours of processing. Data were then analyzed using FlowJo V 10.7 (FlowJo LLC, Ashland, OR).

Processing of peripheral blood mononuclear cells

The peripheral blood mononuclear cell (PBMC) layer was isolated by diluting equal parts of whole blood with equal parts of DPBS, which was then layered onto discontinuous Ficoll-Paque PREMIUM density gradient, 1.078g/ml, at a 1:2 dilution (GE Healthcare, Chicago, IL) and centrifuged for 30 minutes at 400 x g. The PBMC layer was isolated into DPBS, centrifuged at 300 x g for 10 minutes, washed with DPBS, centrifuged at 200 x g for 10 minutes, and suspended in 10% human A/B serum in DPBS for cell counting. 20 µl of cell suspension was stained with 20 µl Viastain^{TM} Acridine Orange/ Propidium Iodide Staining Solution, AO/PI, for 2 minutes at RT. 20 µl of stained cells were loaded onto a disposable hemacytometer and counted with the Cellometer K2 Fluorescent Viability Cell Counter. Cells were aliquoted with 1 x 10^6 cells per 50 µl in 10% human serum in DPBS and incubated for 30 minutes at 4°C. PBMCs were stained with 50 µl of pre-mixed antibody solutions at 4°C for 30 minutes. PBMCs were washed with 2% FBS in DPBS and suspended in equal parts 2% FBS in DPBS and intracellular fixation buffer (IC fix) (Invitrogen). All samples were placed at 4°C and acquired on the Attune NxT flow cytometer (ThermoFisher) within 24 hours of processing. Data were then analyzed using FlowJo V 10.7 (FlowJo LLC).

Gating strategy for phenotypic characterization

Granulocytes were visualized using Side Scatter Area and CD15 and doublets were removed using Forward Scatter Height and Area. Using CD193 (CCR3)-BV-510, CD3-

BV605™, CD19-BV605™, and CD14-APC/Fire™750 eosinophils, T and B lymphocytes, and monocytes were removed from analysis, respectively (Supplemental Figure 1A).

Sorting cells for morphological assessment

Fresh whole blood or isolated PBMCs were diluted with equal parts 2.5mM EDTA in DPBS and centrifuged for 10 minutes at 300 x g. The pellet was re-suspended and then lysed using 12.5 ml isotonic lysis buffer (25) (155 ml NH_4Cl, 10mM $KHCO_3$, 0.1mM EDTA in water sterile filtered with a Steritop 0.22µm filter) (Millipore, Burlington, MA) and set on a rotator for 5 minutes. Samples were centrifuged at 10 minutes for 300 x g and then suspended in 4 ml isolation buffer (equal parts 1% FBS 2mM EDTA in DPBS) and centrifuged for 10 minutes at 300 x g. Cells were then stained with CD3-FITC, CD14-APC, CD15-PE, and CD193 (CCR3)-FITC for 30 minutes at 4°C. Samples were washed using 4 ml of isolation buffer and immediately sorted with the Becton Dickinson FACSAria™ (Franklin Lakes, NJ). After removal of $CD14^+$ events, $CD15^+CD16^-$ and $CD15^+CD16^+$ events corresponding to imLDNs and mLDNs, respectively, were separately sorted. Imaging was performed as described in Appendix A: Supplemental Methods.

Assessment of proliferative capability

One hundred microliters of whole blood was lysed in 2 ml of isotonic lysis buffer, rotated at RT for 7 minutes, washed with 4 ml of 2% FBS in DPBS, and suspended in 500 µl of 2% FBS in DPBS for assessment in whole blood neutrophils. For assessment in LDNs, approximately 2.5 x 10^5 PBMC aliquots were suspended in 50 µl of 10% A/B human serum for 30 minutes at 4°C. Fifty microliters of the extracellular marker panel was added for 30 minutes at 4°C. Samples were washed with 2% FBS in DPBS and fixed and permeabilized using the Cytofix/Cytoperm™ Fixation/Permeabilization Kit (BD

Biosciences, Franklin Lakes, NJ) according to the manufacturer's protocol. Samples were stained with 5 µl of Ki67-APC antibody for 30 minutes at 4°C. Samples were then washed with 2% FBS in DBPS, centrifuged for 5 minutes at 200x g, and suspended in equal parts 2% FBS in DPBS and IC fix. Samples were held at 4°C and acquired on the Attune NxT (ThermoFisher) within 24 hours of processing. Analyses were performed with FlowJo V 10.7 (FlowJo LLC). A positive stain for Ki67 was determined using the fluorescent minus one (FMO) for APC. This gate was then applied to samples processed the same day and the same conditions of the FMO (Supplemental Figure 1B).

Functional Assays

Assessment of reactive oxygen species (ROS) and mitochondrial superoxide production. Fifty microliters of fresh whole blood or isolated PBMCs (1 x 10^6 aliquots) were stained with a pre-mixed antibody solution in pre-warmed tubes. Simultaneously, a final concentration of 20µM H2-DCFDA or 5µM MitoSOX^{TM} (Invitrogen) for detection of ROS and mitochondrial superoxide production, respectively, were added to samples. Samples were immediately stimulated with 10nM of PMA, and set to incubate for 30 minutes at 37°C. After, samples were lysed in 2 ml of isotonic lysis buffer, rotated at RT for 5 minutes, washed with 2% FBS in DPBS, and suspended in 500 µl of 2% FBS in DPBS. Samples were immediately acquired on the Attune NxT flow cytometer (ThermoFisher) within an hour of processing. Data were then analyzed using FlowJo V 10.7 (FlowJo LLC) measured by DCF and MitoSOX^{TM} median fluorescent intensities, for ROS and mitochondrial superoxide production, respectively.

Assessment of mitochondrial mass and mitochondrial activity. Fifty microliters of fresh whole blood or isolated PBMCs (1 x 10^6 aliquots) were stained with a pre-mixed antibody solution in pre-warmed tubes. Simultaneously, a final concentration of 1μM MitoTracker™ Green FM (MTG) (Invitrogen) and 500nM of tetramethylrhodamine ethyl ester (TMRE) (BD Biosciences) were added to samples. Samples were set to incubate for 30 minutes at 37°C, and then treated the same as the protocol discussed in "Assessment of reactive oxygen species (ROS) and mitochondrial superoxide production". Mitochondrial mass was determined by MTG median fluorescent intensity. The functional status of mitochondria was defined as mitochondrial membrane potential ($\Delta\Psi_m$) measured by TMRE adjusted for mitochondrial mass and presented as $\Delta\Psi_m$/MTG ratio.

Assessment of phagocytic activity. Fifty microliters of fresh whole blood or isolated PBMCs (1 x 10^6 aliquots) were stained with a pre-mixed antibody solution in pre-warmed tubes. Simultaneously, 10 μl of pHrodo™ Red *E. coli* BioParticles™ (ThermoFisher) was added to determine phagocytic capacity of neutrophil subpopulations as indicated by a decrease in pH and output as pHrodo median fluorescent intensity. Samples incubated at 37°C for 30 minutes. Samples were then treated as described above in, "whole blood staining."

Quantification of neutrophil subpopulations

Calculating total neutrophils and neutrophil subpopulation frequencies. Fifty microliters of fresh whole blood were stained with 50 μl of a pre-mixed antibody absolute count panel for 30 minutes at 4°C. 1 ml of 1x 1-step Fix/lyse buffer was added to samples for red blood cell lysis and fixation at RT for 15 minutes. Using a predetermined concentration reported by the manufacturer, 50 μl of CountBright™ Absolute Counting

Beads (ThermoFisher) were added to samples. Samples were held at 4°C prior to acquisition and acquired on the Attune NxT flow cytometer (ThermoFisher) within 24 hours of processing. Analyses was performed with FlowJo V 10.7 (FlowJo LLC). Using the manufacturer's protocol, the bead adjustment factor was calculated by dividing the number of beads gated by the pre-determined concentration of beads per volume. Leukocytes were gated with side scatter and forward scatter area and total neutrophils were gated using $CD15^{+}CD14^{-}$ gate with adjustment performed by multiplying cell counts by the bead adjustment factor. Percentages from imN and mN gates were multiplied by the number of total neutrophils calculated.

Quantification of neutrophils in the PBMC layer. PBMC counts from the cellometer were used to determine the amount of PBMCs per ml of blood recalculated to the amount of blood used for isolation of PBMCs. Then the percentage of total neutrophils or neutrophil subpopulations gated from flow cytometry was used to determine amount of neutrophils per volume of blood.

Statistical analysis

Tests for statistical significance were determined with a two-sided p-value of $p<0.05$ conducted with the non-parametric Mann-Whitney rank-sum test as the majority of the data were not normally distributed. Specific analyses are reported in the text and figure legends. All calculations were performed with GraphPad Prism V.5.04 (GraphPad Software Inc., La Jolla, CA

Results

A proliferative immature neutrophil subpopulation is identifiable in whole blood and PBMCs of patients with acute or chronic inflammatory conditions

LDNs were analyzed utilizing pre-determined antibody panels designed to assess neutrophil differentiation and activation including CD64 (FcγRI), a glycoprotein expressed by promyelocytes, myelocytes, and metamyelocytes (20, 21) (Appendix A: Supplemental Methods Table 1). Comprehensive analyses revealed two distinct neutrophil subpopulations, $CD15^{+}CD16^{-}CD64^{+}$ and $CD15^{+}CD16^{+}CD64^{int}$, corresponding to immature (imLDN) and mature (mLDN) neutrophil phenotypes, respectively, in PBMCs obtained from HD, HIV-1, COVID-19, or MM patients (3, 20) (Figure 1A). The immature $CD15^{+}CD16^{-}CD64^{+}$ neutrophil (imN) subpopulation was readily identifiable in whole blood (Figure 1A). Eosinophils are reported to exhibit lower level of CD16 and variable levels of CD15 relative to neutrophils (22, 23). To ensure the purity of imNs in the analyses, eosinophils were separately gated and superimposed with WBN subpopulations (Supplemental Figure 1A-B). Separate eosinophil, imN, and mN subpopulations were observed, with eosinophils exhibiting lower surface marker expression of CD64 relative to imNs (Supplemental Figure 1B).

Neutrophil progenitors and immature neutrophils have been previously reported to be expanded in chronic inflammatory conditions including autoimmune diseases and cancer (3, 19, 24). The percentage of imLDNs of total LDNs was significantly higher in COVID-19 and MM with a significant expansion of imLDNs observed in all disease cohorts relative to HD (Figure 1B). The percentage of imNs of total neutrophils were

significantly higher in HIV-1 (p<0.0001) and COVID-19 (p<0.001) with significantly higher imN frequencies observed in all disease cohorts relative to HD (Figure 1C).

Bone marrow neutrophil progenitors have a lower differentiation state indicated by their proliferative capacity (5); however, it remains unclear whether this is retained in circulating immature neutrophils. imLDNs obtained from COVID-19 (p<0.01) or MM (p<0.01) patients exhibited proliferative capacity indicated by significantly higher levels of proliferative marker Ki67 relative to mLDNs (Figure 1D). Similarly, imNs from COVID-19 (p<0.001) or MM (p<0.05) patients demonstrated increased proliferative capacity relative to mNs (Figure 1E). These data demonstrate that immature neutrophil subpopulations can be readily identified in whole blood and PBMCs, are expanded in acute and chronic inflammatory conditions, and exhibit higher proliferative capacity.

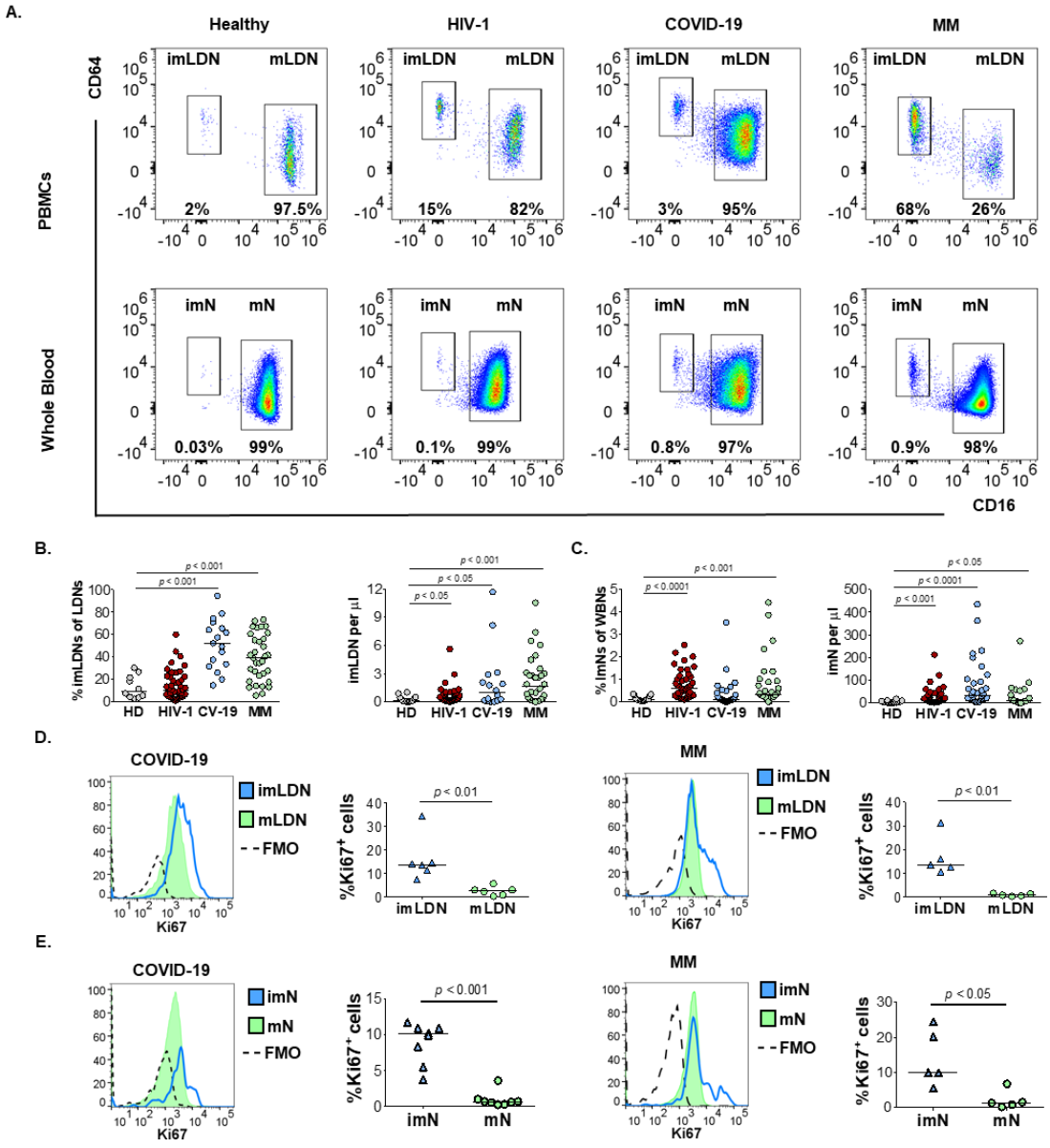

Figure 1. Identification of immature neutrophils in PBMCs and whole blood. (A) Representative cytograms of neutrophil subpopulations in PBMCs and whole blood of HD, HIV-1, COVID-19, and MM patients. **(B-C)** Percentage and frequency of immature neutrophil subpopulations in PBMCs **(B)** and whole blood neutrophils (WBN) **(C)** of HD (*n*=19-31), HIV-1 (*n*=33-46), CV-19 (*n*=33-40), and MM (*n*=31-33) patients. **(D-E)** Representative histogram overlay of Ki67 intracellular expression and percentage of $Ki67^+$ cells in imLDNs **(D)** and imNs **(E)** from COVID-19 (*n*=6-7) and MM (*n*=5) patients. MFI, median fluorescent intensity; FMO, fluorescence minus one. Statistical analyses were performed using the Mann-Whitney rank-sum test. Bars represent median values with *p* values indicated.

ImLDN and mLDN subpopulations are morphologically and phenotypically distinct

To address the characteristics of the imLDN and mLDN subpopulations, the nuclear morphology of sorted LDN subpopulations obtained from HIV-1-infected individuals were assessed (Figure 2A). Neutrophils from the sorted $CD15^{+}CD16^{-}CD14^{-}CCR3^{-}$ imLDN subpopulation demonstrated round and banded nuclei, consistent with the characteristics of myeloblasts and promyelocytes (25) (Figure 2A). Conversely, neutrophils from the sorted $CD15^{+}CD16^{+}CD14^{-}CCR3^{-}$ mLDN subpopulation exhibited multi-segmented nuclei, indicative of terminally mature neutrophils (3, 25) (Figure 2A). Majority of neutrophils in the imLDN subpopulation exhibited a single nuclear lobe while the neutrophils in the mLDN subpopulation displayed a morphology characterized by three or more nuclear lobes (Figure 2B).

The lower maturation status of neutrophils in the imLDN subpopulation was supported by lower levels of CXC chemokine receptor 2 (CXCR2) and CD10 relative to neutrophils in the mLDN subpopulation in HIV-1-infected individuals (Figure 2C and Supplemental Figure 2). imLDNs from HIV-1-infected individuals displayed a higher level of carcinoembryonic antigen-related cell adhesion molecule 8 (CD66b). The level of oxidized low-density lipoprotein receptor 1 (Lox-1), a proposed marker associated with PMN-MDSC in cancer (12), was significantly higher on imLDNs relative to mLDNs from HIV-1-infected individuals ($p<0.01$; Figure 2C).

LDNs from COVID-19 or MM patients demonstrated significant trends between imLDNs and mLDNs consistent with the neutrophil phenotypes observed in HIV-1. imLDNs obtained from COVID-19 patients exhibited lower levels of CD16 ($p<0.0001$), CXCR2 ($p<0.0001$) and higher levels of CD64 ($p<0.0001$) and CD66b ($p<0.05$) relative to

mLDNs (Figure 2D). imLDNs obtained from patients with MM demonstrated similar trends with the exception of Lox-1 expression (Figure 2E).

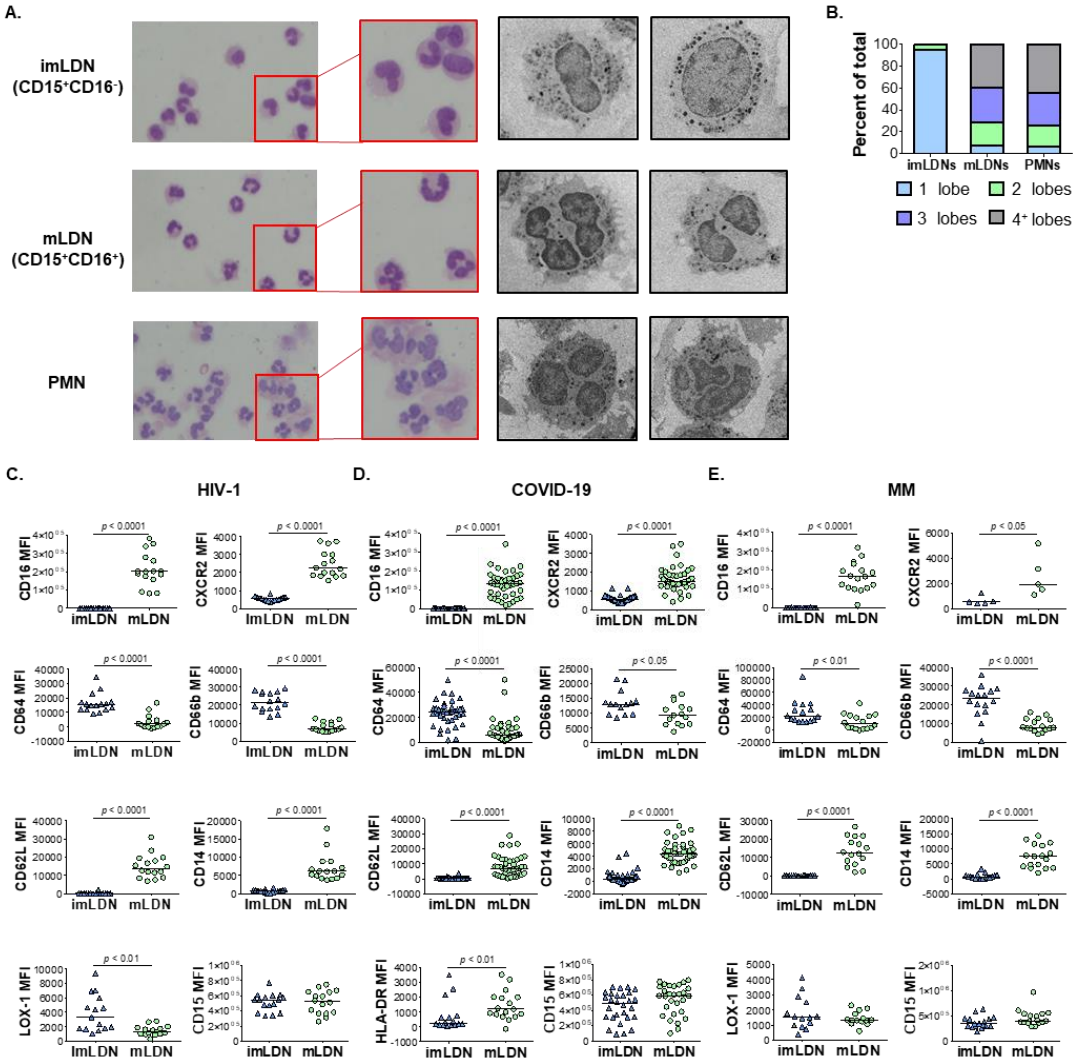

Figure 2. LDNs are comprised of morphologically and phenotypically distinct subpopulations. (A) Representative Giemsa staining and electron microscopy images of sorted $CD15^{+}CD16^{-}$ and $CD15^{+}CD16^{+}$ LDN subpopulations and isolated cells from the PMN layer (*n*=92-100) **(B)** Quantification of nuclear lobes from LDN subpopulations and PMNs (*n*=92). **(C-E)** Surface marker expression of imLDNs and mLDNs in HIV-1 (*n*=14) **(C)** COVID-19 (*n*=14-40) **(D)** and MM patients (*n*=5-21) **(E)**. MFI, median fluorescent intensity. Statistical analyses were performed using the Mann-Whitney rank-sum test. Bars represent median values with *p* values indicated.

Neutrophil heterogeneity in whole blood immature neutrophils

To address neutrophil heterogeneity between the imN and mN subpopulations in whole blood, neutrophil maturation, differentiation, and activation markers were assessed (Figure 3 and Supplemental Figure 3). Neutrophils from the imN subpopulation exhibited significantly lower levels of CD16 ($p<0.0001$), CXCR2 ($p<0.0001$), and CD10 ($p<0.0001$) compared to neutrophils from the mN subpopulation obtained from HIV-1-infected individuals (Figure 3A). imNs exhibited significantly higher levels of CD64 ($p<0.0001$), CD66b ($p<0.0001$), Lox-1 ($p<0.001$) and CD14 ($p<0.0001$) consistent with an immature neutrophil phenotype (Figure 3A and Supplemental Figure 3A). CD117, a marker expressed by neutrophils in advanced stage of differentiation in the bone marrow (26), was significantly increased on mNs relative to imNs ($p<0.001$; Figure 3A). The phenotype of imNs from COVID-19 patients closely resembled the phenotype of imNs obtained from HIV-1-infected individuals (Figure 3B and Supplemental 3B). imNs obtained from MM patients displayed a slightly different phenotype with no significant differences observed in the expression levels of CD64, Lox-1, or CD63 relative to mNs (Figure 3C).

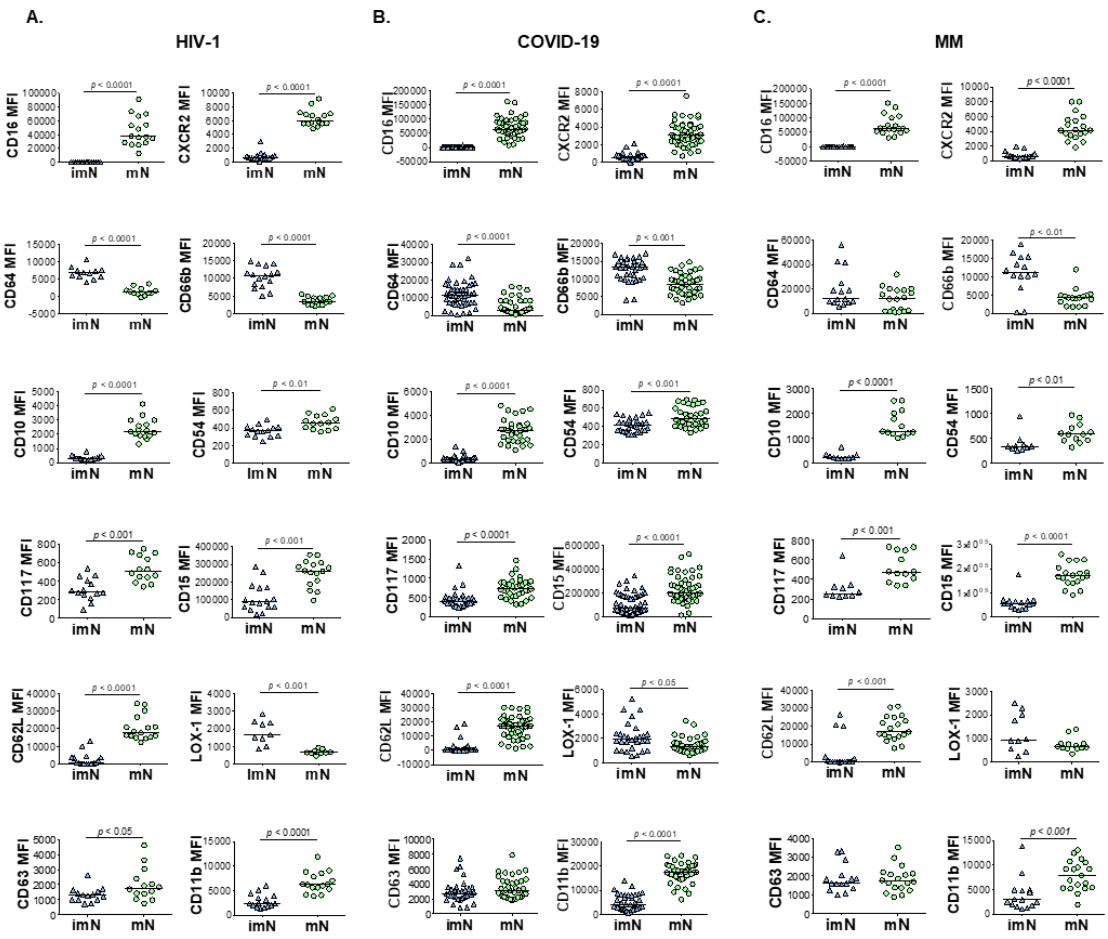

Figure 3. Heterogeneity of neutrophil subpopulations in whole blood. (A-C) Surface marker expression of maturation, degranulation, and activation markers on imNs and mNs of HIV-1 (*n*=14) **(A)**, COVID-19 (*n*=40) **(B)**, and MM (*n*=10-16) **(C)** patients. MFI, median fluorescent intensity. Statistical analyses were performed using the Mann-Whitney rank-sum test. Bars represent median values with *p* values indicated.

Neutrophil subpopulations demonstrate significant differences in functional capacity

To address functional differences in LDN and WBN subpopulations the capacity for ROS production and mitochondrial potential were assessed. mNs obtained from COVID-19 patients demonstrated a significantly higher ROS capacity at basal levels relative to the imN subpopulation (Figure 4A). Significantly higher capacities for ROS production were observed in mNs compared to imNs from COVID-19 ($p<0.0001$) and MM ($p<0.001$) patients upon stimulation of blood with PMA as indicated by significantly higher

dichlorofluorescein (DCF) staining (Figure 4A-B). mLDNs from MM patients demonstrated significantly higher ROS production at basal levels and upon PMA stimulation relative to imLDNs (Supplemental Figure 4A). Mitochondrial superoxide production, detected using MitoSOX^{TM} Red fluorogenic dye, was significantly higher in mNs relative to imNs following PMA stimulation in COVID-19 and MM patients (Figure 4A-B). No significant differences were observed in mitochondrial mass as indicated by MitoTracker^{TM} Green staining or mitochondrial potential detected by tetramethylrhodamine ethyl ester (TMRE) after adjustment for mitochondrial mass between imN and mN subpopulations in whole blood. imNs obtained from MM patients demonstrated a significant increase in mitochondrial potential (Figure 4C-D and Supplemental Figure 4B).

mNs from COVID-19 or MM patients exhibited increased phagocytic capacity as detected by the phagocytosis of pHrodo^{TM} Red E. coli-conjugated BioParticles^{TM} relative to imNs (Figure 4E-F). mLDNs demonstrated higher phagocytic capacity from MM patients (p<0.01) relative to imLDNs (Supplemental Figure 4C). Overall, these data suggest mature neutrophil subpopulations exhibit higher capacity for ROS production and phagocytosis compared to immature neutrophil subpopulations.

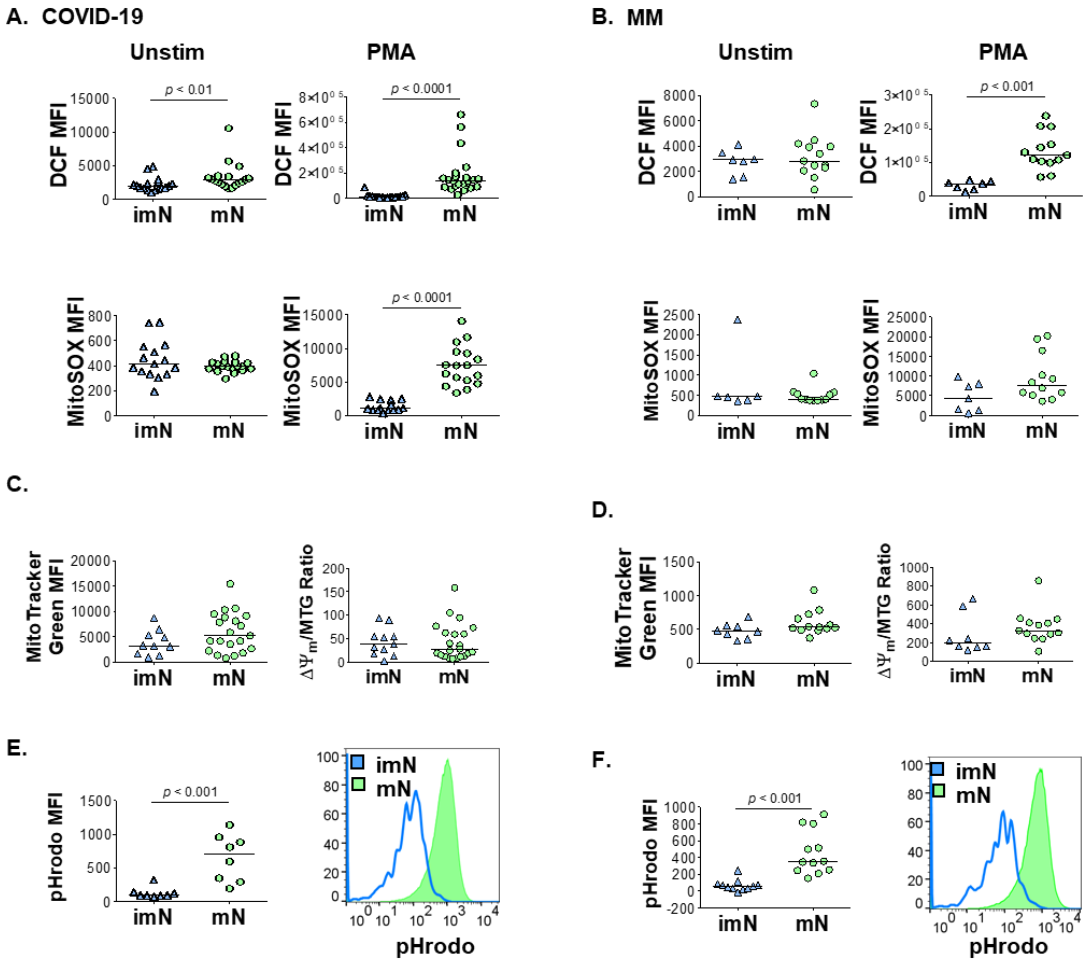

Figure 4. Neutrophil subpopulations exert altered functional activity. (A-B) ROS production and mitochondrial superoxide production, determined by DCF staining and MitoSOX™ Red, respectively at baseline and upon stimulation with PMA of LDN subpopulations in COVID-19 (*n*=16-18) **(A)**, and MM (*n*=7-10) **(B)** patients. **(C-D)** Mitochondrial mass as indicated by MitoTracker™ Green and membrane potential determined with TMRE staining adjusted for mitochondrial mass ($\Delta\psi_m$/MTG) of LDN subpopulations in COVID-19 (*n*=7-16) **(C)**, and MM (*n*=12) **(D)** patients. **(E-F)** Phagocytic capacity was determined by phagocytosis of pHrodo™ Red E. coli BioParticles™ on LDN subpopulations in COVID-19 (*n*=14) **(E)**, and MM (*n*=7) **(F)** patients. MFI, median fluorescent intensity. Statistical analyses were performed using the Mann-Whitney rank-sum test. Bars represent median values with *p* values indicated.

Discussion

Accumulating evidence implicates specific neutrophil subpopulations in the pathogenesis of acute and chronic inflammatory diseases; however, the knowledge regarding their phenotypic and functional heterogeneity remains under-investigated. In this study we identify distinct LDN subpopulations consistent with different neutrophil maturation stages in patients with HIV-1, COVID-19, or MM. Importantly, we show that the immature neutrophil subpopulation can be detected in whole blood using CD16 and CD64 expression. Immature neutrophil subpopulations are significantly elevated in HIV-1, COVID-19, and MM patients. Characteristic features of the immature neutrophil phenotype include uni-lobular nuclei, higher expression of CD64 and CD66b, and higher proliferative capacity relative to mLDNs. The immature neutrophil phenotype exhibited significantly lower capacities for ROS production and phagocytosis.

The significance of immature neutrophil subpopulations as potentially pathogenic is supported by prior reports demonstrating an expansion of distinct imN subpopulations during conditions of immune stress caused by sepsis, tumor-related factors, or autoimmune diseases (3, 5, 6, 18, 19). Here we report a significant expansion of $CD15^{+}CD16^{-}$ imLDNs in the circulation of HIV-1, COVID-19, and MM patients (Figure 1). The quantification of LDNs as an indicator of neutrophil dysregulation in disease is supported by prior studies demonstrating associations between LDN frequency and clinical features of disease observed in autoimmune and cardiovascular diseases and cancer (3, 10, 12).

Recent reports have identified several immature neutrophil subpopulations including $CXCR2^{-}CD101^{-}$ and $CD71^{+}CD117^{+}$ neutrophil progenitor subpopulations (5, 18). In line with these studies, we describe a distinct immature LDN subpopulation characterized by $CD16^{-}CXCR2^{lo}CD64^{+}CD66b^{+}$ that exhibits less-segmented nuclei and is

identifiable in whole blood with CD64 expression. Although the imN subpopulation described in this study exhibits lower CXCR2 level relative to mNs, to our knowledge CD64 has not been reported to be expressed by immature neutrophils prior to the promyelocyte stage (20). Comparatively, comprehensive analyses of maturation and activation surface antigens reveal the imLDN morphology and phenotype is consistent with that of promyelocyte and myeloblast neutrophil maturation stages, including high expression of CD64 and CD66b, and low expression of CD16 (20). Consistent with our findings, studies have characterized immature LDN subpopulations including $CD10^-$ immature LDNs that display less segmented and rounded nuclei (3, 4, 27, 28).

imN subpopulations have been previously characterized as cells that promote T-cell survival and proliferation with impaired neutrophil extracellular trap (NET) formation, decreased phagocytosis, and decreased chemotaxis (3, 28). Consistent with prior studies, we demonstrate decreased phagocytic capacity in imNs relative to mNs. Additionally, a decrease in the capacity for ROS and mitochondrial superoxide production in imNs was observed at basal levels and upon PMA stimulation (Figure 4). Interestingly, imLDNs demonstrated elevated mitochondrial potential relative to mLDNs in MM patients (Supplemental Figure 4D). Our observations are further supported by a prior report demonstrating that imLDNs utilize alternative metabolic pathways including glutamate and proline catabolism in glucose-deficient environments (4).

The identified immature LDN and WBN subpopulations described in this study enhance our knowledge of neutrophil heterogeneity in acute and chronic diseases. The specific properties of imLDNs and imNs described in this study may pre-determine them as active players in acute and chronic inflammatory diseases.

REFERENCES

1. Nicolás-Ávila JÁ, Adrover JM, and Hidalgo A. Neutrophils in Homeostasis, Immunity, and Cancer. Immunity. 2017;46(1):15-28.

2. Leliefeld PHC, Pillay J, Vrisekoop N, Heeres M, Tak T, Kox M, et al. Differential antibacterial control by neutrophil subsets. Blood Adv. 2018;2(11):1344-55.

3. Mistry P, Nakabo S, O'Neil L, Goel RR, Jiang K, Carmona-Rivera C, et al. Transcriptomic, epigenetic, and functional analyses implicate neutrophil diversity in the pathogenesis of systemic lupus erythematosus. Proc Natl Acad Sci U S A. 2019;116(50):25222-8.

4. Hsu BE, Tabaries S, Johnson RM, Andrzejewski S, Senecal J, Lehuede C, et al. Immature Low-Density Neutrophils Exhibit Metabolic Flexibility that Facilitates Breast Cancer Liver Metastasis. Cell Rep. 2019;27(13):3902-15 e6.

5. Evrard M, Kwok IWH, Chong SZ, Teng KWW, Becht E, Chen J, et al. Developmental Analysis of Bone Marrow Neutrophils Reveals Populations Specialized in Expansion, Trafficking, and Effector Functions. Immunity. 2018;48(2):364-79 e8.

6. Kwok I, Becht E, Xia Y, Ng M, Teh YC, Tan L, et al. Combinatorial Single-Cell Analyses of Granulocyte-Monocyte Progenitor Heterogeneity Reveals an Early Uni-potent Neutrophil Progenitor. Immunity. 2020;53(2):303-18 e5.

7. Ng LG, Ostuni R, and Hidalgo A. Heterogeneity of neutrophils. Nat Rev Immunol. 2019;19(4):255-65.

8. Hacbarth E, and Kajdacsy-Balla A. Low density neutrophils in patients with systemic lupus erythematosus, rheumatoid arthritis, and acute rheumatic fever. Arthritis & Rheumatism. 1986;29(11):1334-42.

9. Gabrilovich DI. Myeloid-Derived Suppressor Cells. Cancer Immunol Res. 2017;5(1):3-8.

10. Carlucci PM, Purmalek MM, Dey AK, Temesgen-Oyelakin Y, Sakhardande S, Joshi AA, et al. Neutrophil subsets and their gene signature associate with vascular inflammation and coronary atherosclerosis in lupus. JCI Insight. 2018;3(8).

11. Bowers NL, Helton ES, Huijbregts RP, Goepfert PA, Heath SL, and Hel Z. Immune suppression by neutrophils in HIV-1 infection: role of PD-L1/PD-1 pathway. PLoS Pathog. 2014;10(3):e1003993.

12. Condamine T, Dominguez GA, Youn JI, Kossenkov AV, Mony S, Alicea-Torres K, et al. Lectin-type oxidized LDL receptor-1 distinguishes population of human polymorphonuclear myeloid-derived suppressor cells in cancer patients. Sci Immunol. 2016;1(2).

13. Corzo CA, Cotter MJ, Cheng P, Cheng F, Kusmartsev S, Sotomayor E, et al. Mechanism regulating reactive oxygen species in tumor-induced myeloid-derived suppressor cells. J Immunol. 2009;182(9):5693-701.

14. Ohl K, and Tenbrock K. Reactive Oxygen Species as Regulators of MDSC-Mediated Immune Suppression. Front Immunol. 2018;9:2499.

15. Jimenez RV, Kuznetsova V, Connelly AN, Hel Z, and Szalai AJ. C-Reactive Protein Promotes the Expansion of Myeloid Derived Cells With Suppressor Functions. Front Immunol. 2019;10:2183.

16. Vlkova M, Chovancova Z, Nechvatalova J, Connelly AN, Davis MD, Slanina P, et al. Neutrophil and Granulocytic Myeloid-Derived Suppressor Cell-Mediated T Cell Suppression Significantly Contributes to Immune Dysregulation in Common Variable Immunodeficiency Disorders. J Immunol. 2019;202(1):93-104.

17. Groth C, Hu X, Weber R, Fleming V, Altevogt P, Utikal J, et al. Immunosuppression mediated by myeloid-derived suppressor cells (MDSCs) during tumour progression. Br J Cancer. 2019;120(1):16-25.

18. Dinh HQ, Eggert T, Meyer MA, Zhu YP, Olingy CE, Llewellyn R, et al. Coexpression of CD71 and CD117 Identifies an Early Unipotent Neutrophil Progenitor Population in Human Bone Marrow. Immunity. 2020;53(2):319-34 e6.

19. Zhu YP, Padgett L, Dinh HQ, Marcovecchio P, Blatchley A, Wu R, et al. Identification of an Early Unipotent Neutrophil Progenitor with Pro-tumoral Activity in Mouse and Human Bone Marrow. Cell Rep. 2018;24(9):2329-41 e8.

20. Elghetany MT. Surface antigen changes during normal neutrophilic development: a critical review. Blood Cells Mol Dis. 2002;28(2):260-74.

21. Kerst JM, van de Winkel JG, Evans AH, de Haas M, Slaper-Cortenbach IC, de Wit TP, et al. Granulocyte colony-stimulating factor induces hFc gamma RI (CD64 antigen)-positive neutrophils via an effect on myeloid precursor cells. Blood. 1993;81(6):1457-64.

22. Davoine F, Lavigne S, Chakir J, Ferland C, Boulay ME, and Laviolette M. Expression of FcgammaRIII (CD16) on human peripheral blood eosinophils increases in allergic conditions. J Allergy Clin Immunol. 2002;109(3):463-9.

23. Hellmark T, Ohlsson S, Pettersson A, Hansson M, and Johansson ACM. Eosinophils in anti-neutrophil cytoplasmic antibody associated vasculitis. BMC Rheumatol. 2019;3:9.

24. Brandau S, Trellakis S, Bruderek K, Schmaltz D, Steller G, Elian M, et al. Myeloid-derived suppressor cells in the peripheral blood of cancer patients contain a subset of immature neutrophils with impaired migratory properties. J Leukoc Biol. 2011;89(2):311-7.

25. Bainton DF, Ullyot JL, and Farquhar MG. The development of neutrophilic polymorphonuclear leukocytes in human bone marrow. J Exp Med. 1971;134(4):907-34.

26. Rice CM, Davies LC, Subleski JJ, Maio N, Gonzalez-Cotto M, Andrews C, et al. Tumour-elicited neutrophils engage mitochondrial metabolism to circumvent nutrient limitations and maintain immune suppression. Nat Commun. 2018;9(1):5099.

27. Sagiv JY, Michaeli J, Assi S, Mishalian I, Kisos H, Levy L, et al. Phenotypic diversity and plasticity in circulating neutrophil subpopulations in cancer. Cell Rep. 2015;10(4):562-73.

28. Marini O, Costa S, Bevilacqua D, Calzetti F, Tamassia N, Spina C, et al. Mature CD10(+) and immature CD10(-) neutrophils present in G-CSF-treated donors display opposite effects on T cells. Blood. 2017;129(10):1343-56.

29. Connelly AN, Huijbregts RPH, Pal HC, Kuznetsova V, Davis MD, Ong KL, et al. Optimization of methods for the accurate characterization of whole blood neutrophils. Scientific Reports. 2022;12(1).

30. de Kleijn S, Langereis JD, Leentjens J, Kox M, Netea MG, Koenderman L, et al. IFN-gamma-stimulated neutrophils suppress lymphocyte proliferation through expression of PD-L1. PLoS One. 2013;8(8):e72249.

31. Tak T, Wijten P, Heeres M, Pickkers P, Scholten A, Heck AJR, et al. Human CD62L(dim) neutrophils identified as a separate subset by proteome profiling and in vivo pulse-chase labeling. Blood. 2017;129(26):3476-85.

.

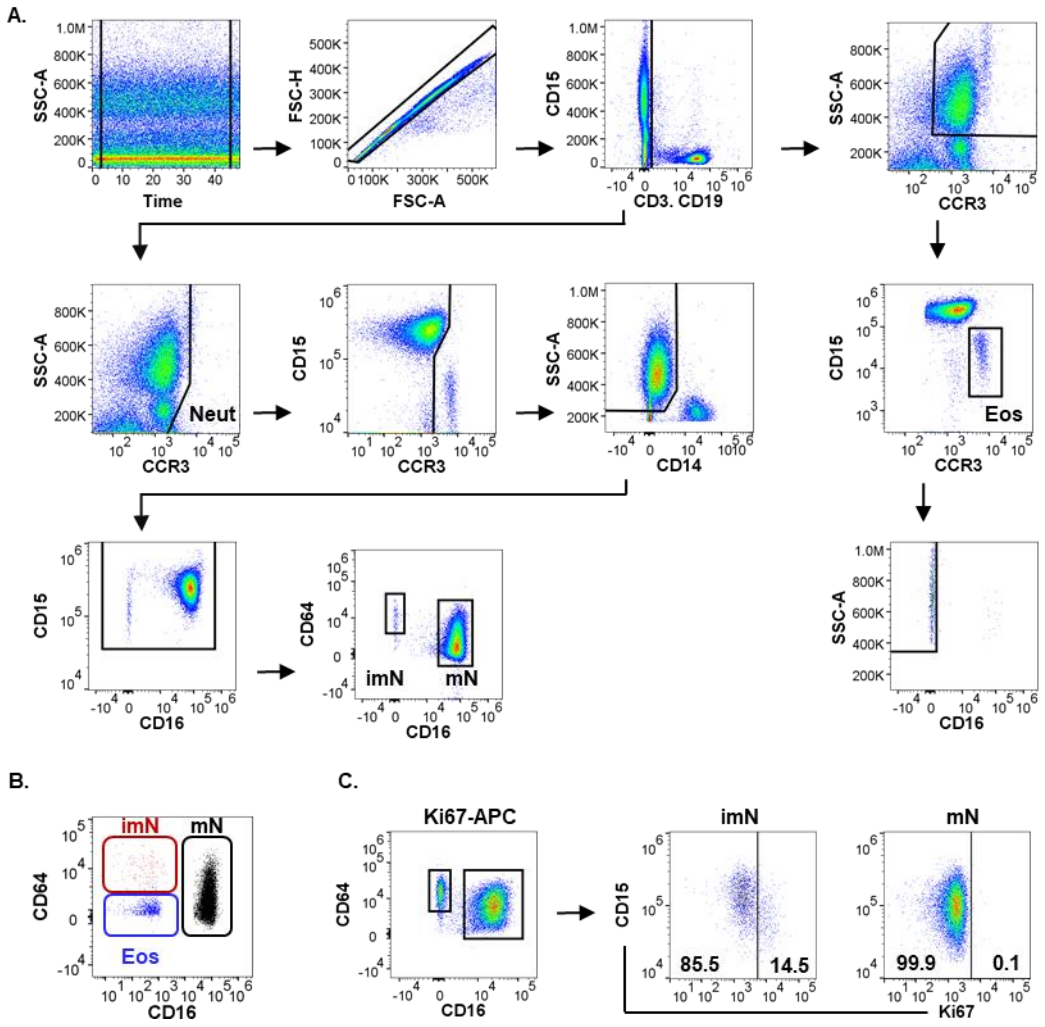

Figure S1. Gating strategy for the identification of neutrophil subpopulations.
(A) Neutrophils were gated as single cells with negative gates to remove doublets, T and B lymphocytes using lineage markers CD3 and CD19 eosinophils using CCR3, and monocytes using CD14 from the analyses, respectively. Immature neutrophil subpopulations were identified as $CD15^{+}CD16^{-}$. Mature neutrophil subpopulations were identified as $CD15^{+}CD16^{+}$. **(B)** Cytogram of imN, mN, and eosinophil cell populations. **(C)** Ki67-APC gating of neutrophil subpopulations with positive cells identified by applying a gate determined using the FMO. FMO, fluorescence minus one.

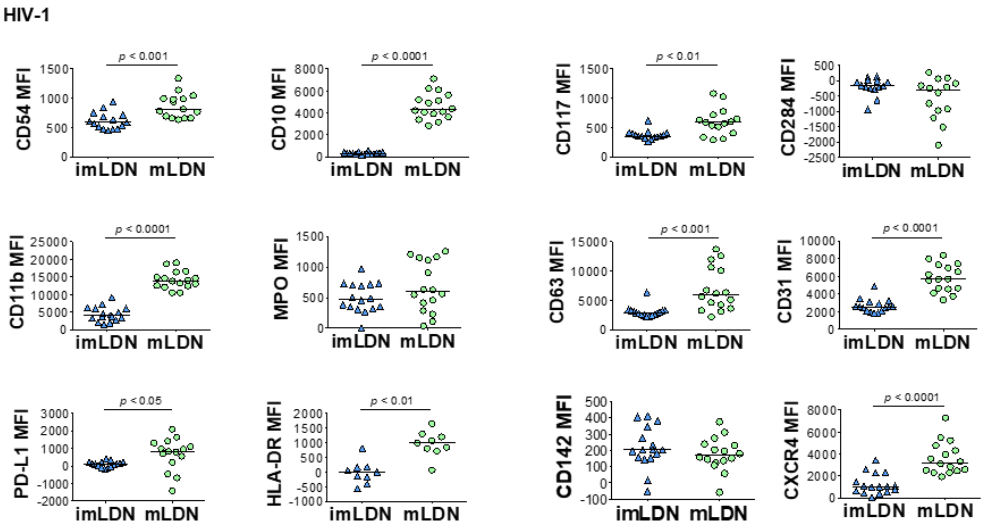

Figure S2. LDNs are comprised of phenotypically distinct subpopulations. Surface marker expression of neutrophil maturation, degranulation, and activation markers on imLDNs and mLDNs of HIV-1 patients (n=16). MFI, median fluorescent intensity. Statistical analyses were performed using the Mann-Whitney rank-sum test. Bars represent median values with *p* values indicated.

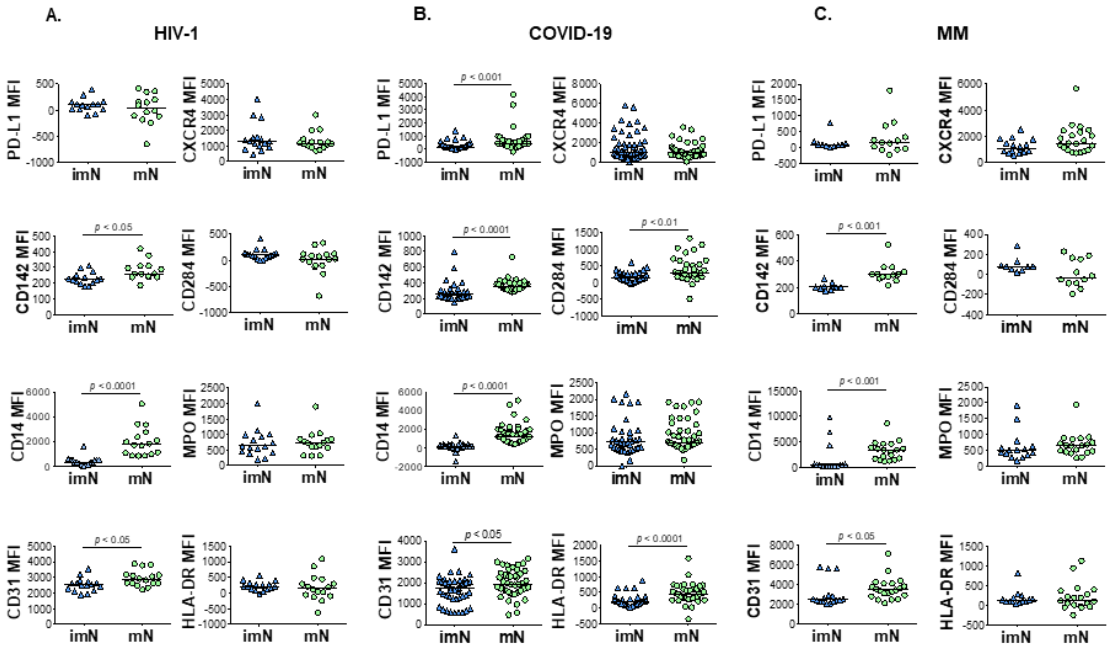

Figure S3. Phenotypic heterogeneity of neutrophil subpopulations in whole blood. (A-C) Surface marker expression of maturation, degranulation, and activation markers on imNs and mNs of HIV-1 (*n*=14) **(A)**, COVID-19 (*n*=40) **(B)**, and MM (*n*=10-16) **(C)** patients. MFI, median fluorescent intensity. Statistical analyses were performed using the Mann-Whitney rank-sum test. Bars represent median values with *p* values indicated.

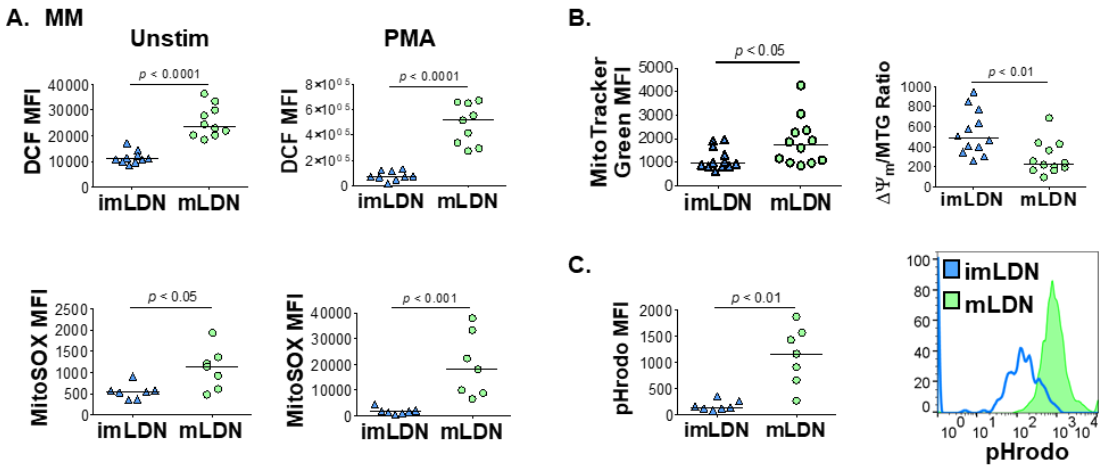

Figure S4. LDN subpopulations exert altered functional activity. (A) ROS production and mitochondrial superoxide production, determined by DCF staining and MitoSOX™ Red, respectively at baseline and upon stimulation with PMA of LDN subpopulations of MM patients (*n*=7-10). **(B)** Mitochondrial mass as indicated by MitoTracker™ Green and membrane potential as determined with TMRE staining adjusted for mitochondrial mass ($\Delta\psi_m$/MTG) of LDN subpopulations of MM patients (*n*=12). **(C)** Phagocytic capacity was determined by phagocytosis of pHrodo™ Red E. coli BioParticles™ on LDN subpopulations of MM patients (*n*=7). MFI, median fluorescent intensity. Statistical analyses were performed using the Mann-Whitney rank-sum test. Bars represent median values with *p* values indicated.

NEUTROPHIL-PLATELET INTERACTIONS PARTIALLY CONTRIBUTE TO THE INDUCTION OF THE LOW-DENSITY NEUTROPHIL PHENOTYPE

by

KRYSTLE L. ONG*, HARISH C. PAL*, ASHLEY N. CONNELLY, MARCUS D. DAVIS, ZDENEK HEL

(* these authors contributed equally to the work)

In preparation for *The Journal of Leukocyte Biology: Brief Reports*

Format adapted for dissertation

Abstract

Neutrophil-platelet complexes (NPCs) and monocyte-platelet complexes (MPCs) are hallmarks of different pathologic conditions. Recently, distinct neutrophil subsets have become appreciated for their diverse phenotype and function in disease. A subset of neutrophils that co-localize with mononuclear cells, known as low-density neutrophils (LDNs), are found at increased frequencies in patients with inflammatory conditions including chronic infections and malignancies. LDNs are shown to exert immunosuppressive functions, including suppression of T-cell-mediated responses by reactive oxygen species (ROS), release of arginase-1, and induction of T regulatory cells. Several inflammatory mediators and bacterial components including TGF-β, lipopolysaccharide (LPS), and N-Formylmethionyl-leucyl-phenylalanine (fMLF) have been previously reported to induce LDNs. However, the mechanisms responsible for the induction of the LDN phenotype is unclear. Here, we demonstrate that thrombin receptor activator peptide-6 (TRAP-6)-activated platelets induce the transformation of neutrophils to LDNs in whole blood through the binding of P-selectin (CD62P) to P-selectin glycoprotein ligand-1 (PSGL-1). Neutrophils in whole blood interact with activated platelets resulting in a rapid expansion of LDNs. Pre-treatment with αPSGL-1 or actin polymerization inhibitor Cytochalasin D significantly reduces the frequency of LDNs stimulated by TRAP-6. Treatment with fMLF does not significantly increase platelet-neutrophil interactions, but separately induces the LDN phenotype. The data presented here indicate that neutrophil-platelet interactions significantly contribute to the induction of LDNs in acute inflammatory conditions.

Keywords: Platelets, low-density neutrophils, TRAP-6, PSGL-1

Introduction

Platelets actively regulate immunologic processes, including wound healing and thrombus formation, and are essential in the recruitment of immune cells (1-3). Increased frequencies of circulating NPCs and MPCs have been reported during infection, sepsis, atherosclerosis, coronary syndromes, and other inflammatory conditions (4-8). The physical interactions between platelets and leukocytes occur by direct binding of CD62P expressed on platelets to PSGL-1 expressed on neutrophils and monocytes (9, 10). The CD62P/PSGL-1 complex activates Src and MAP kinases in leukocytes and induces expression of integrin αLβ2 (LFA-1) and αMβ2 integrin CD11b/CD18 (Mac-1), further promoting platelet-leukocyte interactions activating neutrophils and monocytes (11, 12). These interactions are enhanced by binding of soluble CD40 ligand (sCD40L) secreted by activated platelets to CD40 receptor expressed on neutrophils (13, 14). Physical interaction of platelets and neutrophils modulates inflammatory responses by enhancing the extravasation of neutrophils, ROS production, phagocytic capacity, and release of neutrophil extracellular traps (NETosis) (15-18). Interestingly, P-selectin-deficient platelets fails to induce NETosis due to hampered NPC formation, whereas platelets with enhanced P-selectin expression resulted in increased NETosis when co-cultured with neutrophils (15).

LDNs or polymorphonuclear myeloid-derived suppressor cells (PMN-MDSCs) are a subpopulation of neutrophils which co-localize with monocytes and lymphocytes in the peripheral blood mononuclear cell (PBMC) layer following density gradient centrifugation (19). LDNs have critical roles in the inhibition of T-cell signaling and function, are expanded in many diseases including chronic infections and malignancy, and associated

with poor clinical outcomes in cancer (20-24). Several inflammatory mediators have been demonstrated to promote the low-density phenotype, including fMLF, TGF-β, tumor necrosis factor (TNF), and LPS. However, the specific mechanisms of LDN induction remains to be elucidated (21, 25, 26).

In the present study, we investigated LDN and NPC frequency in relation to disease state and aimed to characterize the interactions between activated platelets and leukocytes. We investigated how neutrophil-platelet interactions affected the induction of the low-density phenotype utilizing platelet-specific and non-specific activators. The results presented here are suggestive of an alternative mechanism of LDN induction involving the interactions between neutrophils and activated platelets (Supplemental Figure 1).

Materials and methods

Ethics statement

All procedures involving human subjects were approved by the Institutional Review Board of the University of Alabama at Birmingham (IRB protocols: 141218001 and 300004485). Informed consent was obtained from all participants in this study, all of whom were eighteen years and older. Blood samples were collected in acid citrate dextrose (ACD) tubes (ThermoFisher, Waltham MA) by certified phlebotomists.

Materials

Fetal bovine serum (FBS) and A/B human serum were purchased from Atlanta Biologicals (Atlanta, GA) and ThermoFisher, respectively. All reagents and materials for cell counting, including the Viastain^{TM}Acridine Orange/ Propidium Iodide (AO/PI) Staining Solution and the Nexcelom cell counter were purchased by Nexcelom (Lawrence, MA). Dulbecco's phosphate buffer solution (DPBS), Ethylenediaminetetraacetic acid

(EDTA), Roswell Park Memorial Institute (RPMI) medium 1640 with 2mM L-glutamine, and Dimethyl sulfoxide (DMSO), were purchased from Corning (Corning, NY). N-formyl-methionyl-leucyl-phenylalanine (fMLF) was purchased from Sigma Aldrich (Sigma Aldrich, St. Louis, MO) and dissolved in DMSO to a concentration of 10nM. Thrombin receptor activator peptide 6 (TRAP-6) purchased from Sigma Aldrich, was dissolved in DMSO at a concentration of 25mM.

Platelet isolation

Whole blood was centrifuged at 200 x g for 10 minutes and platelet rich plasma (PRP) was collected. The PRP was then centrifuged at 200 x g for 10 minutes to pellet red blood cells (RBCs) and other immune cells. The supernatant was transferred to a new tube and centrifuged for 600 x g for 10 minutes. The resulting platelet pellet was suspended in DPBS and stained with carboxyfluorescein succinimidyl ester-green (CFSE) (Sigma Aldrich) for seven minutes at 37°C. Twenty microliters of stained platelets were loaded onto a hemocytometer and counted using the Cellometer K2 Fluorescent Viability Cell Counter.

Microscopy staining and imaging

Wright-Giemsa staining. For platelet activation TRAP-6 or fMLF were added to 50 µl of whole blood at indicated time points. Twenty microliters of blood were used to create thin blood smears on Fishbrand™ Superfrost™ Plus Microscopic Slides (ThermoFisher). Smears were air dried and fixed in chilled methanol for five minutes and stored at room temperature (RT) prior to Giemsa staining. Slides were stained with 1 ml Giemsa bright stain (Electron Microscopy Sciences, Hatfield, PA) for 4 minutes at RT. Excess Giemsa stain was removed by adding 2 ml of 0.1M phosphate-buffer (Electron Microscopy

Sciences) on top of the Giemsa stain and incubated at RT for 8 minutes. Slides were gently washed with water for 1 minute, air dried, then mounted with Fisher Chemical™ Permount™ Mounting Medium (ThermoFisher) and cover slipped. The Keyence microscope 20X and 60X lenses (Keyence, Itasca, IL) were used for analyses. Manual quantification of neutrophil-platelet interactions was performed with the assistance of the ImageJ software (National Institutes of Health, Bethesda, MD).

Immunofluorescent staining of whole blood. Whole blood was stained with CD14-PE/Cy5.5 (Biolegend, San Diego, CA), CD15-PE (Biolegend) and CD41-FITC (Biolegend) for 30 minutes and stimulated with TRAP-6 or fMLF at different time points. After incubation, blood was fixed and lysed using 1 ml of 1-step 1x 1-step Fix/lyse buffer (Invitrogen, Waltham, MA) for 15 minutes at RT in the dark. Cells were washed with chilled wash buffer (DPBS containing 2% FBS) by centrifugation at 200 x g for 5 minutes. The cell pellet was suspended in equal parts intracellular fixation buffer (IC fix) (Invitrogen) and 2% FBS. Cell suspensions were then cytospun at 800rpm for 4 minutes using medium acceleration on glass slides. Cells were mounted with vectashield mounting medium containing DAPI (Vector Laboratories, Burlingame, CA) prior to applying the coverslip. Images were captured at 40X using the Keyence microscope. Cell suspensions were also acquired on the Attune NxT flow cytometer (ThermoFisher) within 24 hours and analyzed utilizing FlowJo V 10.7 (FlowJo LLC, Ashland, OR).

Co-culture of TRAP-6 activated platelets with whole blood. Platelets from whole blood were isolated as described above and stained with CFSE in 500 µl DPBS for 15 minutes at 37°C. Stained platelets were washed twice with DPBS containing 2% FBS by centrifugation for 10 minutes at 800 x g. Platelets were suspended in RPMI medium and

counted. $CFSE^{+}$ platelets and TRAP-6 were added to isotonically-lysed whole blood stained prior to co-incubation with CD15-PE (Biolegend) and CD41-FITC, as previously described, for indicated time periods (27). After incubation, stained blood was processed for blood smears or separately in 1-step Fix/Lyse for 15 minutes at RT for flow cytometry and then cytospun for microscopy. Slides were mounted with vectashield mounting medium containing DAPI and cytospun for microscopy using the Shandon™ Cytospin3 cytocentrifuge (ThermoFisher).

Sample preparation for flow cytometry analysis

Whole blood samples were stained with the platelet antibody stain mix consisting of CD3-BV605 (Biolegend), CD19-BV605 (Biolegend), CD14-APCFire™ (Biolegend), CD15-eF450 (eBioscience™), CD16-APC (eBioscience™), CD62L-BV711 (BD Biosciences), CD193 (CCR3)-BV510 (BD Biosciences), CD41-FITC (Biolegend) and CD62P-PE-Cy7 (Biolegend) in10% A/B human serum in DPBS for 30 minutes in the dark at 4°C. After, TRAP-6 or fMLF were added at different time points and samples were incubated at 37°C. Samples were washed in chilled DPBS containing 1mM EDTA and centrifuged at 200 x g for 5 minutes and fixed with RBC lysis in 1 ml of 1-step 1x Fix/lyse solution for 15 minutes in the dark at RT. Samples were washed with 1 ml chilled DPBS containing 1mM EDTA and centrifuged at 200 x g for 5 minutes and suspended in equal parts of 2% FBS in DPBS and IC fix. Samples were acquired on the Attune NxT flow cytometer (ThermoFisher) within 24 hours and analyzed utilizing FlowJo V 10.7 (FlowJo LLC, Ashland, OR).

To acquire peripheral blood mononuclear cells (PBMCs), equal parts of whole blood was diluted with equal parts DPBS, and then layered onto a discontinuous Ficoll-

Paque PREMIUM density gradient (GE Healthcare, Chicago, IL) at a 2:1 ratio, 1.078g/ml, and centrifuged for 30 minutes at 400 x g. The resulting PBMC layer was isolated into 10 ml of DPBS and centrifuged at 300 x g for 10 minutes. The PBMCs were then suspended in 10% A/B human serum in DPBS to block nonspecific binding of antibodies for 30 minutes at 4°C. During blocking, 20 ml of PBMCs were stained with 20 ml of AO/PI for 5 minutes at 25°C, and then loaded onto the Cellometer K2 Fluorescent Viability Cell Counter for counting. After blocking, PBMCs were stained with 50 ml of the platelet antibody mix for 30 minutes at 4°C, washed with 2% FBS in DPBS, and suspended in equal parts of 2% FBS in DPBS and IC fix. The same protocol for whole blood sample acquisition and analysis was utilized for PBMC acquisition.

Blocking interaction assays

Whole blood or co-cultures were pre-treated with 10 μg/ml αCD62P (BioLegend), 10 μg/ml αCD162 (PSGL-1) (BioLegend), 10 μM Cytochalasin D (CytoD) (Sigma Aldrich) or 10 mM ammonium chloride (NH_4Cl) for 30 minutes at RT prior to TRAP-6 or fMLF stimulation. Samples were stimulated for 5 minutes before washing after αCD62P and αCD162 (αPSGL-1) treatment, or 30 minutes for Cyto D or NH_4Cl treatments. Samples were then processed as described above.

Gating for flow cytometry

For all analyses, $CD3^+$ and $CD19^+$ events corresponding to T and B lymphocytes, respectively, were removed. For neutrophil analyses, $CD193^+$ (CCR3) and $CD14^+$ events were removed. For monocyte analyses, $CD15^+$ and $CCR3^+$ events were removed. NPCs and MPCs were defined as $CD15^+CD41^+$ and $CD14^+CD41^+$, respectively. Activated

leukocyte-platelet complexes were determined by $CD62P^+$. This gating strategy was utilized for whole blood and PBMC samples (Supplemental Figure 2).

Low-density neutrophil quantification

PBMCs and PMNs were counted from the cellometer to determine the amount of total neutrophils per volume of blood. The percentage of LDNs or PMNs gated from flow cytometry was multiplied by the total number of neutrophils to determine the frequency of LDNs.

Statistical analysis

Tests for statistical significance of NPC and LDN frequencies, and extracellular antigen expression on neutrophils, were conducted with paired t-tests. Statistical significance was determined at a standard level of $p<0.05$. GraphPad Prism (GraphPad Software Inc., La Jolla, CA) was utilized for all calculations.

For original data, please contact zdenekhel@uabmc.edu

Results and Discussion

Activated NPCs and MPCs are upregulated in COVID-19

The frequencies of total NPCs, defined as $CD15^+CD41^+$, and MPCs, defined as $CD14^+CD41^+$, were determined on neutrophils and monocytes obtained from healthy donors (HD) and patients with acute or chronic infection (Figure 1A and Supplemental Figure 2). Total NPCs and MPCs and level of CD41 on neutrophils or monocytes were not significantly increased in inflammatory disease conditions relative to HD (Figure 1A-D). In contrast, complexes of neutrophils and monocytes with activated platelets were significantly elevated in patients with coronavirus 19 (COVID-19) relative to HD (Figure

1E-F). Expression of CD62P was significantly increased on activated NPCs and MPCs in COVID-19 and human immunodeficiency virus-1 (HIV-1) relative to HD (Figure 1E-F). Analyses of LDNs reveal that patients with COVID-19 (p<0.05) or HIV-1 (p<0.001) exhibited higher LDN frequencies relative to HD with total NPC frequency observed to be significantly increased in LDNs relative to WB (Figure 1G-H).

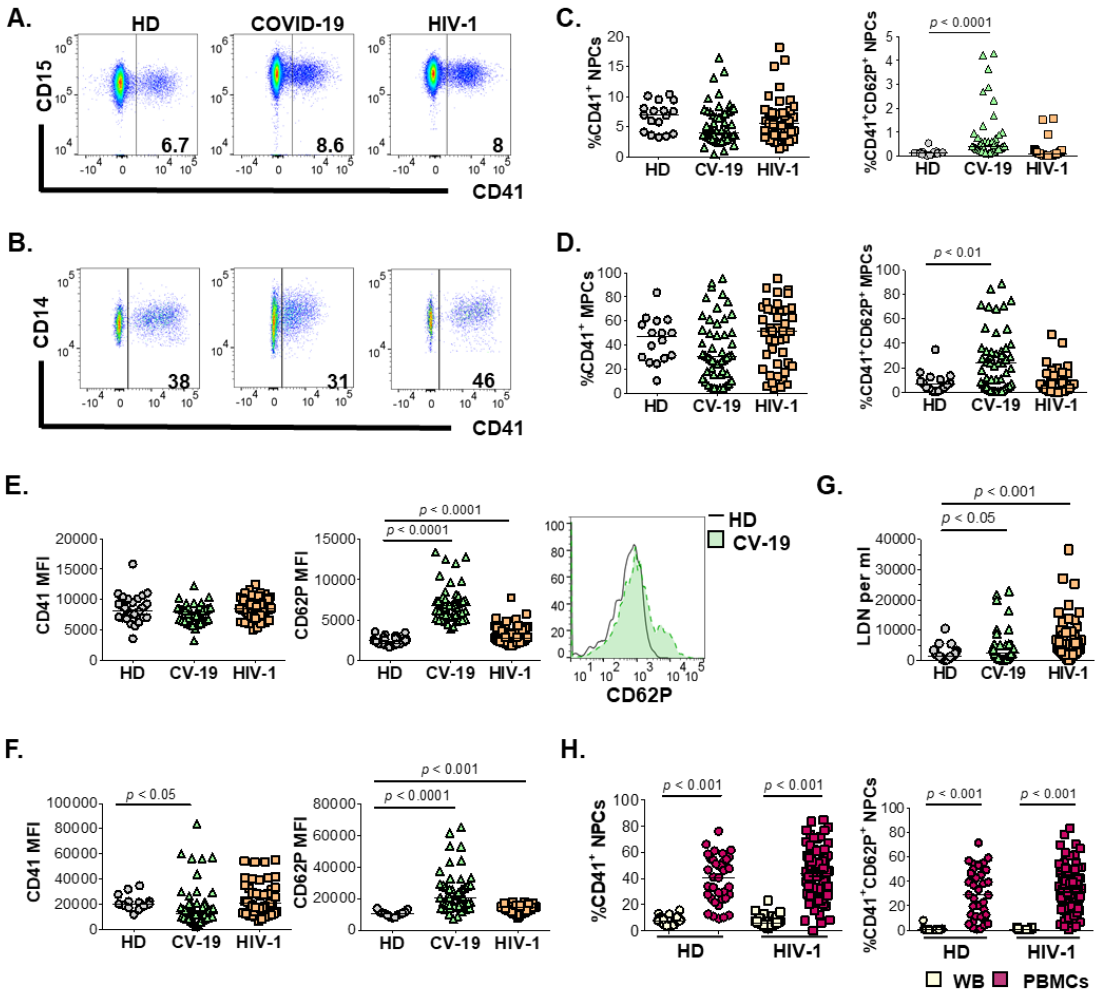

Figure 1. Platelet-leukocyte complexes and LDNs are increased in patients with COVID-19. (A-B) Cytograms of CD15$^+$CD41$^+$ NPCs **(A)** or CD14$^+$CD41$^+$ MPCs **(B)** from a healthy donor (HD) or individuals infected with SARS-CoV-2 (CV-19) or HIV-1. **(C-D)** Expression of CD41 and frequency of total NPCs **(C)** and MPCs **(D)** in whole blood. **(E-F)** Frequency of CD41$^+$CD62P$^+$ activated NPCs **(E)** and MPCs **(F)** and expression of CD62P in whole blood. **(G)** LDN frequency of HD, CV-19, and HIV-1. **(H)** Frequency of

NPCs in whole blood (WB) and PBMCs of HD and HIV-1. HD (*n*=28) CV-19 (*n*=31-50) HIV-1 (*n*=56). Statistical analyses were performed using the Mann-Whitney rank-sum test with *p* values as indicated. Bars represent median values.

TRAP-6 stimulation induces the formation of activated NPCs

To investigate the effect of platelet activation on neutrophil-platelet interactions thrombin-receptor activator peptide-6 (TRAP-6), a hexapeptide fragment that acts as a protease-activated receptor 1 (PAR1) agonist was utilized (28). Stimulation with TRAP-6 resulted in a time-dependent increase in the formation of $CD41^{+}CD15^{+}$NPCs as indicated by immunofluorescent staining and flow cytometry in whole blood (Figure 2A-B). Platelet-neutrophil interactions were observed within two minutes of TRAP-6 stimulation with a maximum interaction frequency observed within 5 minutes, after which the interaction frequency and expression of CD41 declined (Figure 2B-C). There was a significant, transient increase in the percentage of activated $CD41^{+}CD62P^{+}CD15^{+}$NPCs, as indicated by the upregulation of CD62P expression, in TRAP-6-stimulated whole blood ($p<0.05$; Figure 1D-E).

To analyze if platelet-neutrophil interactions were specifically due to the activation of platelets, whole blood was stimulated with fMLF; a bacterial peptide which predominantly binds to the formyl peptide receptor on neutrophils (29, 30). There was a slight increase in NPC frequency with fMLF stimulation, however, there were no significant differences in activated NPC frequency between unstimulated and fMLF-stimulated blood (Figure 1B, D, F).

We observe a significant increase in NPC frequency after TRAP-6 stimulation and further show that non-specific leukocyte activator, fMLF, did not demonstrate the same level of potency. Our observations are corroborated by a prior study demonstrating rapid

formation of NPCs upon TRAP-6 stimulation (17). The lower platelets-neutrophil interactions in fMLF-stimulated relative to TRAP-6-stimulated blood may be the result of partial activation of platelets.

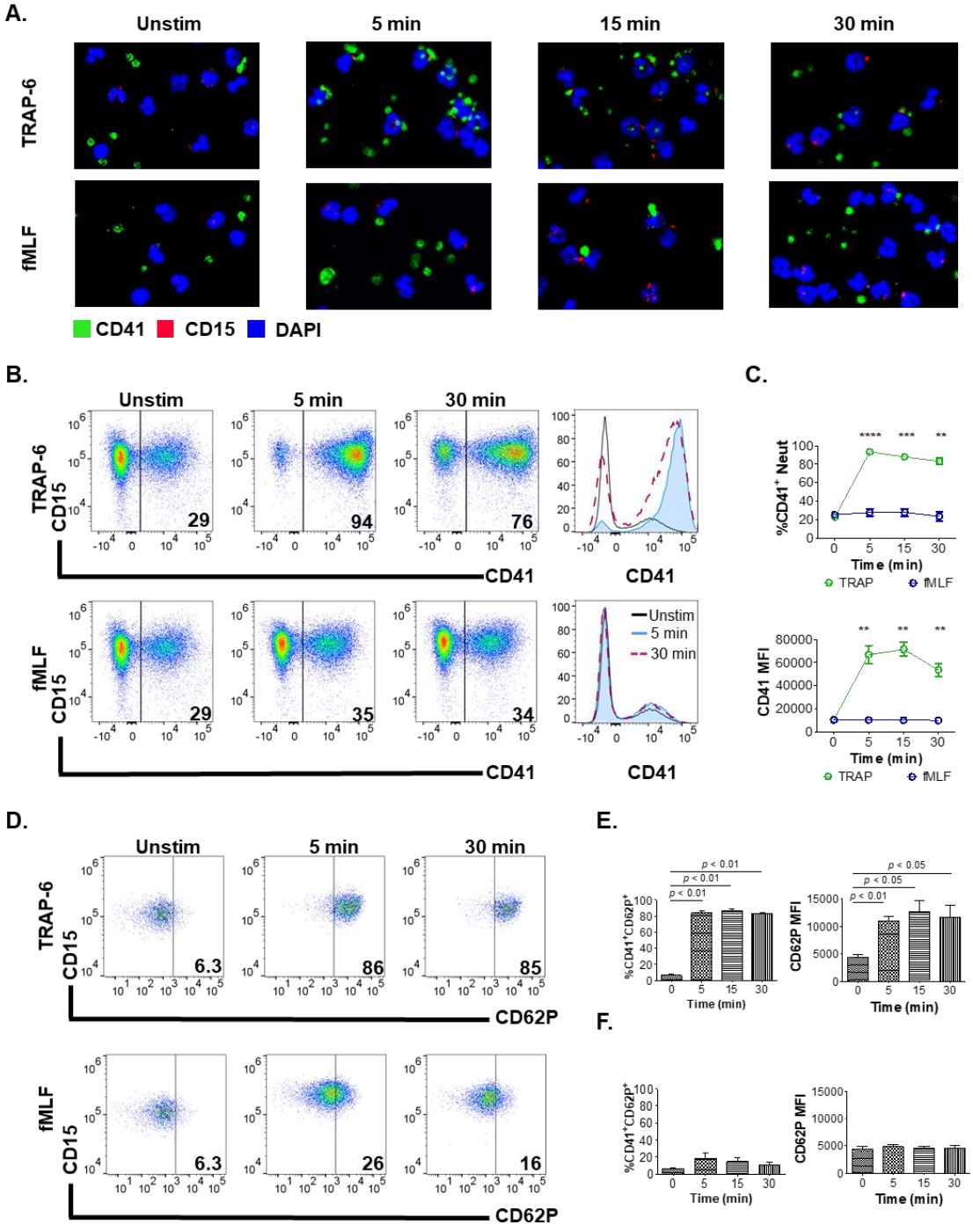

Figure 2. Stimulation of whole blood by TRAP-6 increases the frequency of activated NPCs. (A) Representative immunofluorescence microscopy images of NPCs in stimulated whole blood from HD (*n*=6). Platelets were indicated by CD41, green; neutrophils were indicated by CD15, pink, with DAPI, blue, used to counterstain nuclei. **(B)** Left panel- representative cytograms of NPCs in stimulated whole blood; right panel- histogram overlay of CD41 expression. **(C)** Percentage of CD41+ NPCs and expression of CD41 at different time points with TRAP-6 or fMLF stimulation. **(D)** Representative cytograms of activated NPCs as determined by $CD15^{+}CD41^{+}CD62P^{+}$ neutrophils in stimulated whole blood. **(E-F)** Percentage of activated NPCs and expression of CD62P on activated NPCs at different time points with TRAP-6 **(E)** or fMLF **(F)** stimulation. Statistical analyses were performed using the Mann-Whitney rank-sum test with *p* values as indicated. Bars represent standard error of the means.

Neutrophils rapidly interact with TRAP-6-activated platelets

Consistent with immunofluorescent microscopy observations, Giemsa staining of TRAP-6-stimulated whole blood reveal a rapid accumulation of platelets interacting with neutrophils, which was observed in monocytes (Figure 3A and Supplemental 3A). To assess the transfer of platelet contents to neutrophils, platelets pre-stained with CFSE were co-cultured with neutrophils from isotonically-lysed blood and stimulated with TRAP-6 (Figure 3B-C). There was a rapid accumulation of CFSE staining with the addition of TRAP-6 suggesting that platelets were binding extracellularly to neutrophils or internalized into the cytoplasm (Figure 3C). A rapid increase in the percent of CFSE-positive neutrophils was observed reaching a maximum at 30 minutes with greater than fifty percent of neutrophils exhibiting CFSE positivity (Figure 3D). Pre-treatment with ammonium chloride (NH4Cl), which has been previously reported to block the formation of the phago-lysosome, did not result in an increase in CFSE accumulation with neutrophils (Figure 3E) (31-33).

Giemsa staining of whole blood suggest that platelet particles are encapsulated within neutrophils and upon TRAP-6 stimulation (Figure 2A). This observation is

consistent with prior reports demonstrating neutrophil engulfment of activated platelets in disease (34, 35). Our observations support that platelet content is actively transferred to neutrophils upon TRAP-6 stimulation. Maugeri et al. previously demonstrated the phagocytosis of activated platelets by neutrophils in neutrophil-platelet co-cultures (17). They proposed that leukocyte phagocytosis of platelets is dependent on binding of CD62P to PSGL-1 on neutrophils which is stabilized by LFA and Mac-1 interactions (17). Previous clinical reports have suggested neutrophil engulfment of platelets is occurring in inflammatory diseases including coronary artery syndrome and system sclerosis (17, 34, 35). The data presented indicates that after adherence of activated platelets on neutrophils, platelet contents can be transferred to neutrophils.

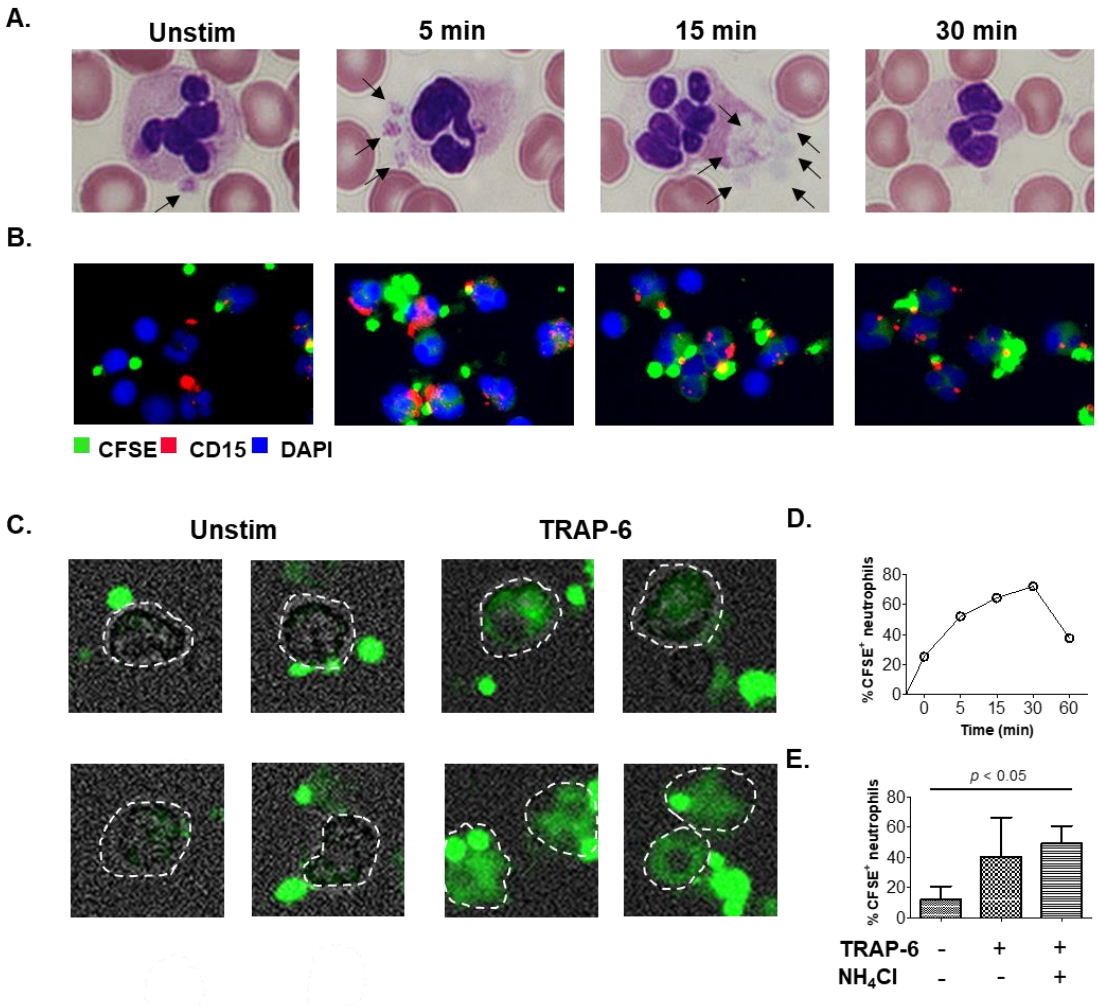

Figure 3. Neutrophil-platelet interactions are enhanced with TRAP-6 stimulation
(A) Giemsa-stained whole blood stimulated with TRAP-6 depicting neutrophil-platelet interactions. **(B)** Immunofluorescent microscopy images of isotonically-lysed whole blood co-cultured with platelets pre-stained with CFSE stimulated with TRAP-6 at different time points; CFSE (green), CD15 (red), and neutrophil nuclei counterstained with DAPI (blue). **(C)** Representative immunofluorescent microscopy images of whole blood neutrophils interacting with platelets pre-stained with CFSE. **(D)** Frequency of CFSE-positive neutrophils with TRAP-6 stimulation (one of four experiments shown). **(E)** Percentage of CFSE-positive neutrophils after stimulation with TRAP-6 and/or pretreatment with ammonium chloride (NH_4Cl) (n=4). Images of Giemsa staining were enhanced equally with increasing color brightness and contrast which did not change or compromise the original images. Statistical analyses were performed using paired t-test with p values as indicated. Bars represent standard error of the means.

TRAP-6 and fMLF stimulation of whole blood induce LDNs

To determine whether platelet-neutrophil interactions induced the low-density neutrophil phenotype, LDNs were quantified from TRAP-6-stimulated-whole blood at different time points. There was a rapid, but transient, expansion of LDNs observed within five minutes of TRAP-6 or fMLF stimulation relative to unstimulated blood (Figure 4A-B). To determine if the interaction between neutrophils and activated platelets affects LDN frequency, whole blood was treated with TRAP-6 or fMLF for 5 minutes after pretreatment with αCD62P or αPSGL-1 preventing interaction of the CD62P/PSGL-1 axis, or inhibiting actin rearrangement with Cytochalasin D (Cyto D) (36). Pretreatment with αPSGL-1 (p<0.05) or Cyto D (p<0.05) significantly reduced LDN frequency with αPSGL-1 pre-treatment resulting in decreased formation of NPCs in whole blood (Figure 4D). Pretreatment with αCD62P resulted in partial inhibition of LDN frequency, but did not reach a level of statistical significance (data not shown). Overall, these findings suggest that the transfer of platelet contents to neutrophils mediated by PSGL-1 play a role in the induction of LDNs by TRAP-6 stimulation.

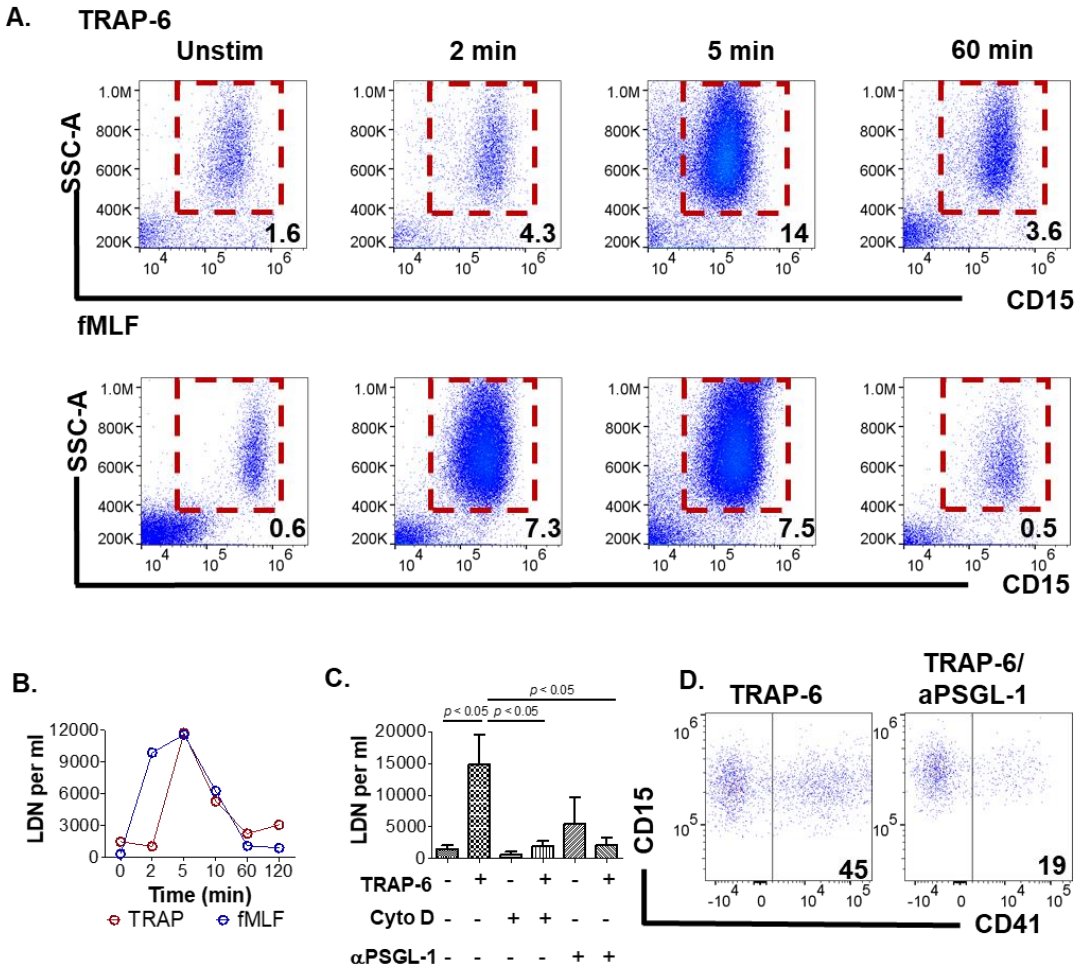

Figure 4. TRAP-6 and fMLF stimulation of whole blood induces LDNs. (A) Cytograms of LDNs in PBMCs from TRAP-6-stimulated or fMLF-stimulated whole blood at indicated time points. **(B)** Time course of LDN induction from TRAP-6 or fMLF-stimulated blood; one of four experiments shown. **(C)** Frequency of LDNs obtained from whole blood stimulated for 5 minutes with TRAP-6 with pretreatment conditions including αPSGL-1 or Cytochalasin D for 30 minutes as indicated (*n*=3-11). **(D)** Cytogram of neutrophils in whole blood with TRAP-6 stimulation with and without pre-treatment with αPSGL-1. Statistical analyses were performed using paired t-test with *p* values as indicated. Bars represent standard error of the means.

Summary and study limitations

The present study provides a potential mechanism involving neutrophil-platelet interactions for the induction of LDNs. We demonstrate the rapid formation of activated

NPCs with TRAP-6 stimulation in whole blood. Interestingly, TRAP-6 or fMLF stimulation of whole blood resulted in the rapid expansion of LDNs. The induction of LDNs by TRAP-6 was reduced with pre-treatment with αPSGL-1 or Cytochalasin D. Although several inflammatory mediators have been demonstrated to promote the low-density phenotype, our findings provide novel evidence for a specific platelet-involved mechanism of LDN induction (21, 25, 26).

The effect of the interactions between activated platelets with specific neutrophil subsets is under-investigated in disease conditions. A recent study in psoriasis reported that LDNs were found to co-localize with platelets in circulatory blood (37). Further, that LDN-platelet complexes are strongly associated with early atherosclerotic non-calcified coronary burden suggesting that LDN-platelet complexes may significantly contribute to the disease severity and the development of cardiovascular-related comorbidities (37). Future studies focused on comprehensive analyses of neutrophil-platelet interactions on the induction of LDNs are suggested to understand the effect of LDN-platelet complexes in the development of co-morbidities and relation to disease progression.

Limitations of the study include the small sample size. Additionally, detailed phenotypic characterization and comparison of functional properties were not possible due to the transient nature of the experimental low-density phenotype. Utilizing density gradient centrifugation for isolated neutrophils from whole blood resulted in poor recovery of LDNs suggesting a component in whole blood may be necessary for the TRAP-6-induction of LDNs. Though fMLF has independently been observed to increase LDN frequency our data suggest fMLF is involved in separate mechanism(s) of LDN induction in addition to indirect platelet activation (21). Overall our data demonstrate how platelet-

neutrophil interactions are involved in promoting the low-density phenotype and are suggestive of a novel mechanism of LDN induction.

REFERENCES

1. Kral, J. B., Schrottmaier, W. C., Salzmann, M., Assinger, A. (2016) Platelet Interaction with Innate Immune Cells. Transfus Med Hemother 43, 78-88.

2. Smyth, S. S., McEver, R. P., Weyrich, A. S., Morrell, C. N., Hoffman, M. R., Arepally, G. M., French, P. A., Dauerman, H. L., Becker, R. C., Platelet Colloquium, P. (2009) Platelet functions beyond hemostasis. J Thromb Haemost 7, 1759-66.

3. Sreeramkumar, V., Adrover, J. M., Ballesteros, I., Cuartero, M. I., Rossaint, J., Bilbao, I., Nacher, M., Pitaval, C., Radovanovic, I., Fukui, Y., McEver, R. P., Filippi, M. D., Lizasoain, I., Ruiz-Cabello, J., Zarbock, A., Moro, M. A., Hidalgo, A. (2014) Neutrophils scan for activated platelets to initiate inflammation. Science 346, 1234-8.

4. Zhang, D., Xu, C., Manwani, D., Frenette, P. S. (2016) Neutrophils, platelets, and inflammatory pathways at the nexus of sickle cell disease pathophysiology. Blood 127, 801-9.

5. Totani, L. and Evangelista, V. (2010) Platelet-leukocyte interactions in cardiovascular disease and beyond. Arterioscler Thromb Vasc Biol 30, 2357-61.

6. Lisman, T. (2018) Platelet-neutrophil interactions as drivers of inflammatory and thrombotic disease. Cell Tissue Res 371, 567-576.

7. Mauler, M., Herr, N., Schoenichen, C., Witsch, T., Marchini, T., Hardtner, C., Koentges, C., Kienle, K., Ollivier, V., Schell, M., Dorner, L., Wippel, C., Stallmann, D., Normann, C., Bugger, H., Walther, P., Wolf, D., Ahrens, I., Lammermann, T., Ho-Tin-Noe, B., Ley, K., Bode, C., Hilgendorf, I., Duerschmied, D. (2019) Platelet Serotonin Aggravates Myocardial Ischemia/Reperfusion Injury via Neutrophil Degranulation. Circulation 139, 918-931.

8. Allen, N., Barrett, T. J., Guo, Y., Nardi, M., Ramkhelawon, B., Rockman, C. B., Hochman, J. S., Berger, J. S. (2019) Circulating monocyte-platelet aggregates are a robust marker of platelet activity in cardiovascular disease. Atherosclerosis 282, 11-18.

9. Gardiner, E. E., De Luca, M., McNally, T., Michelson, A. D., Andrews, R. K., Berndt, M. C. (2001) Regulation of P-selectin binding to the neutrophil P-selectin counter-receptor P-selectin glycoprotein ligand-1 by neutrophil elastase and cathepsin G. Blood, The Journal of the American Society of Hematology 98, 1440-1447.

10. Wang, Y., Gao, H., Shi, C., Erhardt, P. W., Pavlovsky, A., D, A. S., Bledzka, K., Ustinov, V., Zhu, L., Qin, J., Munday, A. D., Lopez, J., Plow, E., Simon, D. I. (2017) Leukocyte integrin Mac-1 regulates thrombosis via interaction with platelet GPIbalpha. Nat Commun 8, 15559.

11. Evangelista, V., Pamuklar, Z., Piccoli, A., Manarini, S., Dell'elba, G., Pecce, R., Martelli, N., Federico, L., Rojas, M., Berton, G., Lowell, C. A., Totani, L., Smyth, S. S. (2007) Src family kinases mediate neutrophil adhesion to adherent platelets. Blood 109, 2461-9.

12. Piccardoni, P., Sideri, R., Manarini, S., Piccoli, A., Martelli, N., de Gaetano, G., Cerletti, C., Evangelista, V. (2001) Platelet/polymorphonuclear leukocyte adhesion: a new role for SRC kinases in Mac-1 adhesive function triggered by P-selectin: Presented in part at the 42nd Annual Meeting of the American Society of Hematology, December 1-5, 2000, San Francisco, CA. Blood 98, 108-116.

13. Jin, R., Yu, S., Song, Z., Zhu, X., Wang, C., Yan, J., Wu, F., Nanda, A., Granger, D. N., Li, G. (2013) Soluble CD40 ligand stimulates CD40-dependent activation of the β2 integrin Mac-1 and protein kinase C zeda (PKCζ) in neutrophils: implications for neutrophil-platelet interactions and neutrophil oxidative burst. PLoS One 8, e64631.

14. Setianto, B. Y., Hartopo, A. B., Gharini, P. P. R., Anggrahini, D. W., Irawan, B. (2010) Circulating soluble CD40 ligand mediates the interaction between neutrophils and platelets in acute coronary syndrome. Heart and Vessels 25, 282-287.

15. Caudrillier, A., Kessenbrock, K., Gilliss, B. M., Nguyen, J. X., Marques, M. B., Monestier, M., Toy, P., Werb, Z., Looney, M. R. (2012) Platelets induce neutrophil extracellular traps in transfusion-related acute lung injury. Journal of Clinical Investigation 122, 2661-2671.

16. Kim, S. J. and Jenne, C. N. (2016) Role of platelets in neutrophil extracellular trap (NET) production and tissue injury. Semin Immunol 28, 546-554.

17. Maugeri, N., Rovere-Querini, P., Evangelista, V., Covino, C., Capobianco, A., Bertilaccio, M. T., Piccoli, A., Totani, L., Cianflone, D., Maseri, A., Manfredi, A. A. (2009) Neutrophils phagocytose activated platelets in vivo: a phosphatidylserine, P-selectin, and [225]2 integrin-dependent cell clearance program. Blood 113, 5254-65.

18. Zucoloto, A. Z. and Jenne, C. N. (2019) Platelet-Neutrophil Interplay: Insights Into Neutrophil Extracellular Trap (NET)-Driven Coagulation in Infection. Front Cardiovasc Med 6, 85.

19. Hacbarth, E. and Kajdacsy-Balla, A. (1986) Low density neutrophils in patients with systemic lupus erythematosus, rheumatoid arthritis, and acute rheumatic fever. Arthritis & Rheumatism 29, 1334-1342.

20. Bowers, N. L., Helton, E. S., Huijbregts, R. P., Goepfert, P. A., Heath, S. L., Hel, Z. (2014) Immune suppression by neutrophils in HIV-1 infection: role of PD-L1/PD-1 pathway. PLoS Pathog 10, e1003993.

21. Vlkova, M., Chovancova, Z., Nechvatalova, J., Connelly, A. N., Davis, M. D., Slanina, P., Travnickova, L., Litzman, M., Grymova, T., Soucek, P., Freiberger, T., Litzman, J., Hel, Z. (2019) Neutrophil and Granulocytic Myeloid-Derived Suppressor Cell-Mediated T Cell Suppression Significantly Contributes to Immune Dysregulation in Common Variable Immunodeficiency Disorders. J Immunol 202, 93-104.

22. Pillay, J., Kamp, V. M., van Hoffen, E., Visser, T., Tak, T., Lammers, J. W., Ulfman, L. H., Leenen, L. P., Pickkers, P., Koenderman, L. (2012) A subset of neutrophils in human systemic inflammation inhibits T cell responses through Mac-1. J Clin Invest 122, 327-36.

23. Schmielau, J. and Finn, O. J. (2001) Activated granulocytes and granulocyte-derived hydrogen peroxide are the underlying mechanism of suppression of t-cell function in advanced cancer patients. Cancer research 61, 4756-4760.

24. Diaz-Montero, C. M., Salem, M. L., Nishimura, M. I., Garrett-Mayer, E., Cole, D. J., Montero, A. J. (2009) Increased circulating myeloid-derived suppressor cells correlate with clinical cancer stage, metastatic tumor burden, and doxorubicin–cyclophosphamide chemotherapy. Cancer immunology, immunotherapy 58, 49-59.

25. Sagiv, J. Y., Michaeli, J., Assi, S., Mishalian, I., Kisos, H., Levy, L., Damti, P., Lumbroso, D., Polyansky, L., Sionov, R. V., Ariel, A., Hovav, A. H., Henke, E., Fridlender, Z. G., Granot, Z. (2015) Phenotypic diversity and plasticity in circulating neutrophil subpopulations in cancer. Cell Rep 10, 562-73.

26. Hardisty, G. R., Llanwarne, F., Minns, D., Gillan, J. L., Davidson, D. J., Gwyer Findlay, E., Gray, R. D. (2021) High purity isolation of low density neutrophils casts doubt on their exceptionality in health and disease. Frontiers in Immunology 12, 2057.

27. Connelly, A. N., Huijbregts, R. P. H., Pal, H. C., Kuznetsova, V., Davis, M. D., Ong, K. L., Fay, C. X., Greene, M. E., Overton, E. T., Hel, Z. (2022) Optimization of methods for the accurate characterization of whole blood neutrophils. Scientific Reports 12.

28. Vassallo, R. R., Kieber-Emmons, T., Cichowski, K., Brass, L. F. (1992) Structure-function relationships in the activation of platelet thrombin receptors by receptor-derived peptides. Journal of Biological Chemistry 267, 6081-6085.

29. Schiffmann, E., Corcoran, B. A., Wahl, S. M. (1975) N-formylmethionyl peptides as chemoattractants for leucocytes. Proceedings of the National Academy of Sciences 72, 1059-1062.

30. Becker, E. (1979) A multifunctional receptor on the neutrophil for synthetic chemotactic oligopeptides. Journal of the Reticuloendothelial Society 26, 701-709.

31. Shawcross, D. L., Wright, G. A., Stadlbauer, V., Hodges, S. J., Davies, N. A., Wheeler-Jones, C., Pitsillides, A. A., Jalan, R. (2008) Ammonia impairs neutrophil phagocytic function in liver disease. Hepatology 48, 1202-12.

32. Unanue, E. R. (1993) Macrophages, antigen-presenting cells, and the phenomena of antigen handling and presentation. Fundamental Immumology 111.

33. Hart, P. D. and Young, M. R. (1991) Ammonium chloride, an inhibitor of phagosome-lysosome fusion in macrophages, concurrently induces phagosome-endosome fusion, and opens a novel pathway: studies of a pathogenic mycobacterium and a nonpathogenic yeast. Journal of Experimental Medicine 174, 881-889.

34. Manfredi, A. A., Ramirez, G. A., Godino, C., Capobianco, A., Monno, A., Franchini, S., Tombetti, E., Corradetti, S., Distler, J. H., Bianchi, M. E., Rovere-Querini, P., Maugeri, N. (2021) Platelet phagocytosis via PSGL1 and accumulation of microparticles in systemic sclerosis. Arthritis Rheumatol.

35. Maugeri, N., Capobianco, A., Rovere-Querini, P., Ramirez, G. A., Tombetti, E., Valle, P. D., Monno, A., D'Alberti, V., Gasparri, A. M., Franchini, S., D'Angelo, A., Bianchi, M. E., Manfredi, A. A. (2018) Platelet microparticles sustain autophagy-associated activation of neutrophils in systemic sclerosis. Science Translational Medicine 10, eaao3089.

36. Cooper, J. A. (1987) Effects of cytochalasin and phalloidin on actin. The Journal of cell biology 105, 1473-1478.

37. Teague, H. L., Varghese, N. J., Tsoi, L. C., Dey, A. K., Garshick, M. S., Silverman, J. I., Baumer, Y., Harrington, C. L., Stempinski, E., Elnabawi, Y. A., Dagur, P. K., Cui, K., Tunc, I., Seifuddin, F., Joshi, A. A., Stansky, E., Purmalek, M. M., Rodante, J. A., Keel, A., Aridi, T. Z., Carmona-Rivera, C., Sanda, G. E., Chen, M. Y., Pirooznia, M., McCoy, J. P., Jr., Gelfand, J. M., Zhao, K., Gudjonsson, J. E., Playford, M. P., Kaplan, M. J., Berger, J. S., Mehta, N. N. (2019) Neutrophil Subsets, Platelets, and Vascular Disease in Psoriasis. JACC Basic Transl Sci 4, 1-14.

SUPPLEMENTAL FIGURES

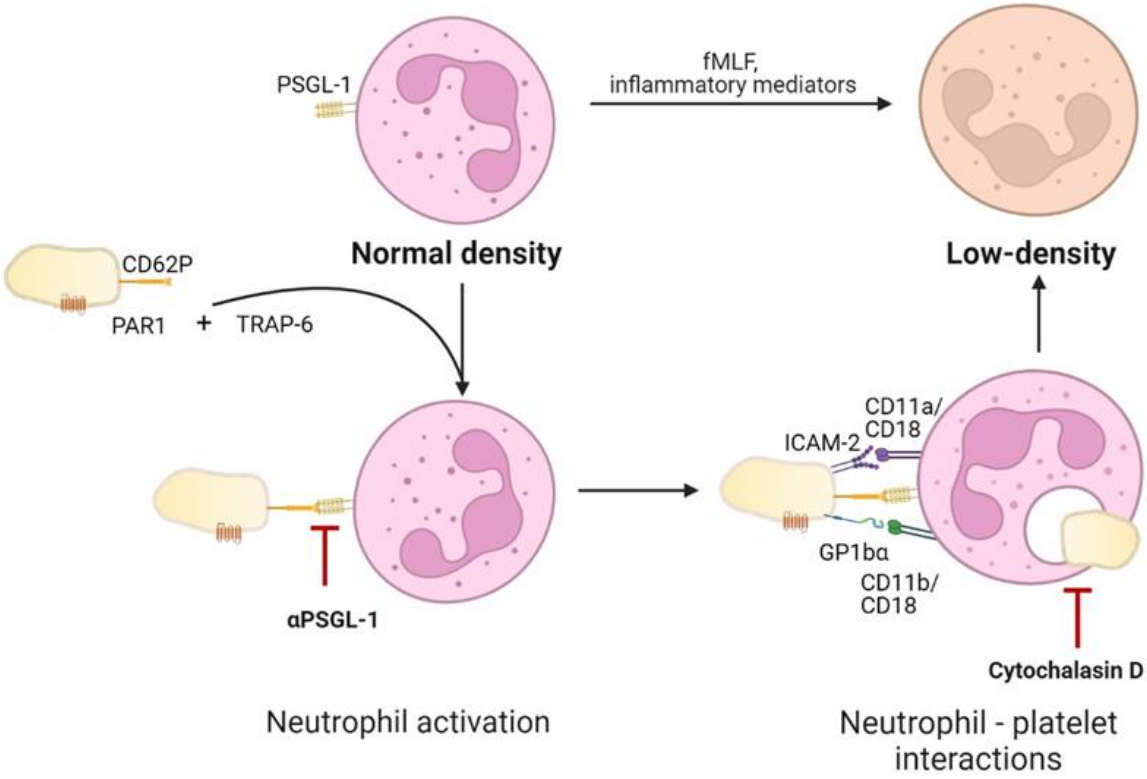

Figure S1. Graphical abstract. Platelets are activated through the PAR-1 receptor with Thrombin receptor activator peptide 6 (TRAP-6). Activated platelets then bind neutrophils though the P-selectin/PSGL-1 axis activating neutrophils. Once activated, neutrophils rapidly interact with platelets through Mac-1 binding of ICAM-2 and GP1bα promoting the low-density phenotype. Pre-treatment blocking PSGL-1 binding or actin rearrangement with Cytochalasin D hampers the development of the low-density phenotype. fMLF and inflammatory mediators utilize an independent mechanism of induction. Created with BioRender.com.

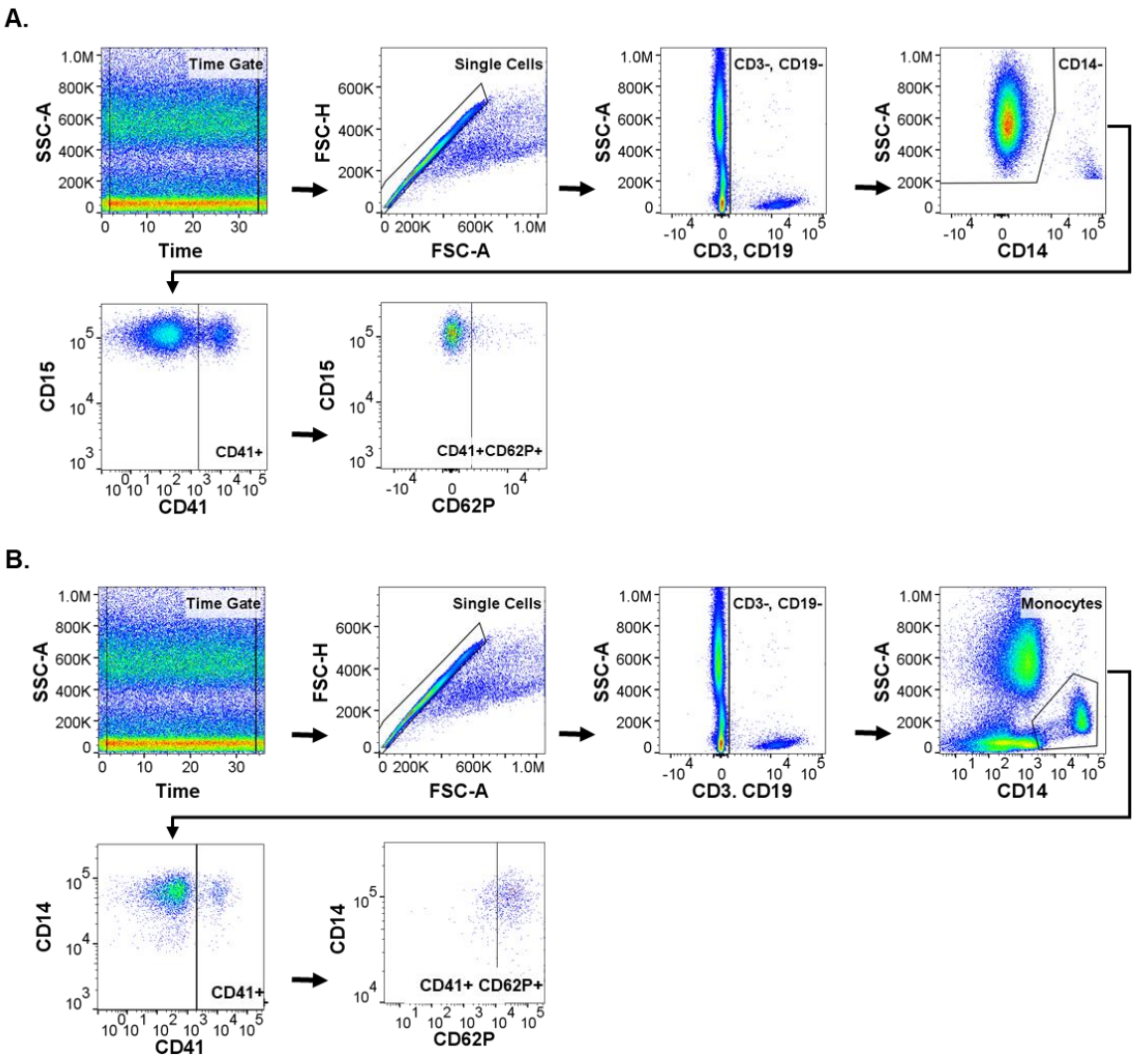

Figure S2. Gating strategy for leukocyte-platelet complexes. (A-B) Neutrophils **(A)** and monocytes **(B)** were gated as single cells with negative gates to remove doublets, T and B lymphocytes with lineage markers CD3 and CD19 and eosinophils with CCR3. MPCs and NPCs were identified as $CD14^{+}CD41^{+}$ and $CD15^{+}CD41^{+}$ respectively. CD62P expression was used to determine activation of platelet-leukocyte complexes.

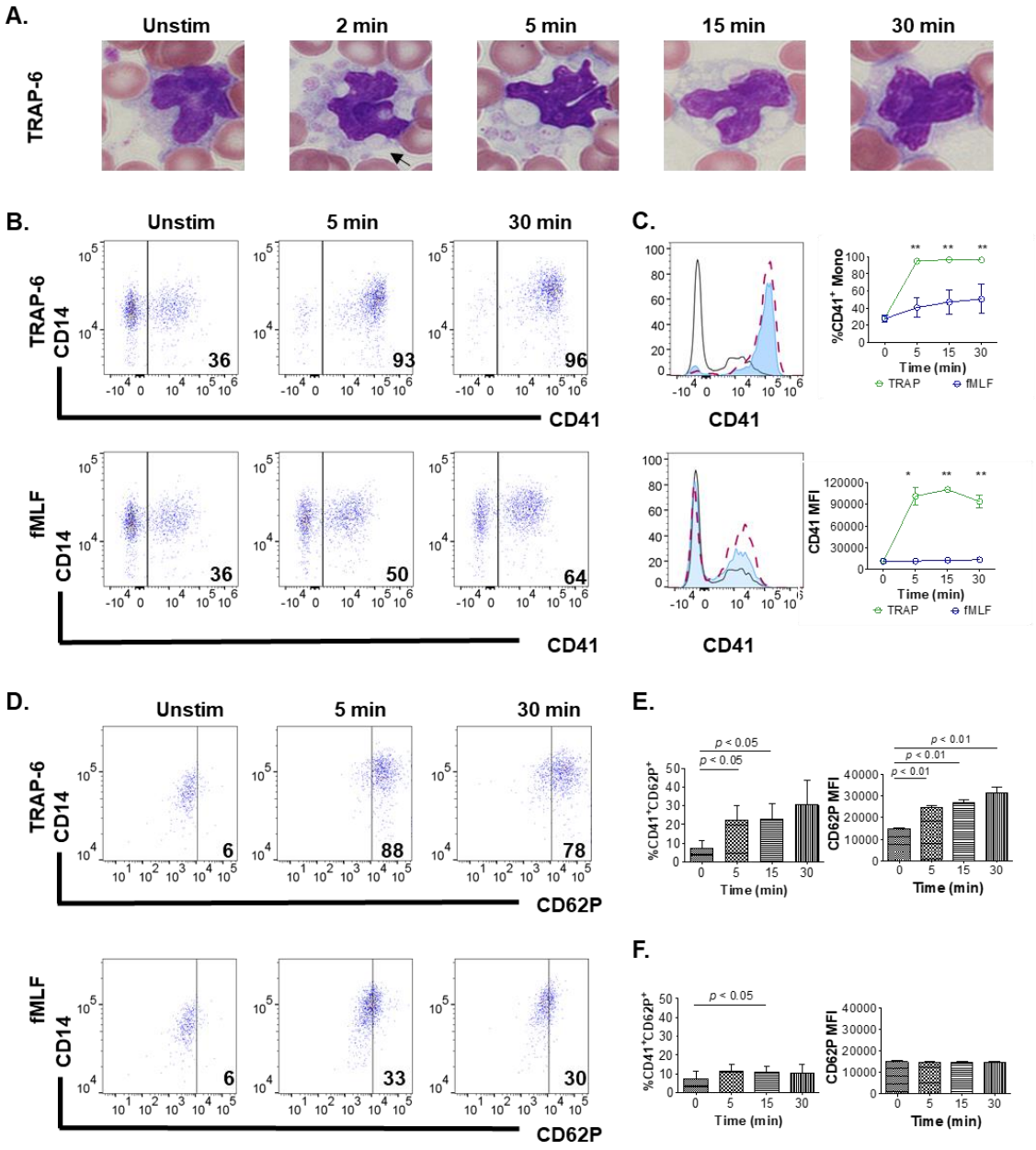

Figure S3. Monocyte interactions with platelets. (A) Giemsa-stained whole blood stimulated with TRAP-6 depicting monocyte-platelet interactions. **(B)** Left panel- representative cytograms of MPCs in stimulated whole blood; right panel- histogram overlay of CD41 expression. **(C)** Percentage of $CD41^+$ MPCs and expression of CD41 at different time points with TRAP-6 or fMLF stimulation. **(D)** Representative cytograms of activated MPCs as determined by $CD14^+CD41^+CD62P^+$ monocytes in stimulated whole blood. **(E-F)** Percentage of activated MPCs and expression of CD62P on activated MPCs at different time points with TRAP-6 **(E)** or fMLF **(F)** stimulation. Statistical analyses were performed using the Mann-Whitney rank-sum test with *p* values as indicated. Bars represent standard error of the means.

DISCUSSION

The cells of the myeloid compartment are essential to maintaining homeostasis through wound healing, controlling infection and recruitment of adaptive immune cells; however, the full spectrum of their functional potential remains to be discovered. A growing body of evidence suggests specific neutrophil subpopulations are strongly associated with disease pathogenesis and severity. The work presented in this dissertation reveals the following findings regarding myeloid cell subsets in infection and cancer:

1. Neutrophils are comprised of immature and mature neutrophils with distinct phenotypes and functions;
2. Circulating immature neutrophils are readily identified in whole blood, demonstrate proliferative activity, and are expanded in inflammatory conditions including HIV-1, COVID-19, and MM;
3. An alternatively differentiated myeloid phenotype, MM2, exists in a subset of multiple myeloma patients;
4. The MM2 myeloid cell phenotype strongly correlates with myeloma-defining events and is associated with advanced disease;
5. LDN, NPC, and MPC frequencies are significantly upregulated in SARS-CoV-2 infection;

6. The low-density neutrophil phenotype can be transiently induced by TRAP-6-activated platelets, potentially dependent upon a phagocytic mechanism mediated by PSGL-1.

THE ROLE OF MYELOID CELLS IN THE PREDICTION AND MONITORING OF MULTIPLE MYELOMA

Despite advancements in the clinical monitoring and treatment of MM, it remains an inevitably fatal cancer with most patients experiencing relapsed or refractory disease [230, 231]. Multiple studies have reported associations between PMN-MDSC frequency or NLR with poor outcomes in MM [173, 176, 232]. However, the clinical significance of the functions of circulatory myeloid cells has been under-investigated. The present study provides comprehensive insight into the specific myeloid phenotypes of circulatory neutrophils, monocytes, and eosinophils associated with immune dysregulation in MM. We identify a specific subset of MM patients that display myeloid dysregulation related to myeloma-defining events. The MM2 phenotype is defined by a profound upregulation of CD64 and significant downregulation of CXCR2 and CD10 on mature neutrophils. Other components of the MM2 phenotype include the downregulation of monocytic markers CX3CR1 and CD31 on patrolling monocytes and a downregulation of cell signaling receptors on eosinophils. Our results indicate that features of the MM2 phenotype including CD64 expression on neutrophils will be instrumental when incorporated into future predictive and prognostic models of MM and its precursory conditions.

Our findings are consistent with a prior study observing that CD64 expression is significantly higher on neutrophils from MM relative to MGUS patients, whereas no significant difference was observed in CD32 (FcγRII) or CD16 (FcγRIII) expression [233].

A positive relationship was observed between high CD64 expression on neutrophils and poor overall survival in MM patients receiving first-line therapies [181]. Quantification of CD64 levels on neutrophils is indicative of leukocyte dysfunction and has been investigated as a method of discrimination between non-septic and septic inflammatory responses in clinical settings [234, 235].

Altered myelopoiesis occurring in MM results in increased frequency of T-regulatory cells and MDSCs associated with immunosuppressive myeloid cell function [179, 180, 236]. We report a significant expansion of immature neutrophil subpopulation in patients with the MM2 phenotype. Mature neutrophil subpopulations were primed for mitochondrial ROS release and displayed increased mitochondrial potential indicative of an immature neutrophil phenotype. In line with these findings, Perez, Botta et al. reported an upregulation of genes characteristic of PMN-MDSCs in mature neutrophils in MM patients due to varied chromatin accessibility [232]. Previous studies have demonstrated that PMN-MDSC display higher arginase-1 expression and phagocytic capacity [176, 181].

The current study reports a strong association between the MM2 phenotype and the involved to uninvolved FLC ratio. Components of the MM2 phenotype including CD64 level on mNs and CX3CR1 level on patrolling monocytes negatively correlated with serum hemoglobin and creatinine levels, respectively. Our observations that features of the MM2 phenotype are significantly associated with advanced disease stages in MM are consistent with prior studies demonstrating high CD64 on neutrophils are associated with poor disease outcome in MM patients [181]. Although the MM2 phenotype was not found to be significantly associated with treatment status, several investigations have been performed to determine how current MM therapies affect myeloid cells [176, 181]. PMN-MDSC

frequency and arginase-1 levels were reduced *in vivo* after lenalidomide treatment, but not with treatment with bortezomib [176]. Future investigations are needed to better understand how treatment affects immune dysregulation to assist in the development of more optimal treatment strategies.

The results described in this study present a novel myeloid phenotype improving our understanding of dysregulated myelopoiesis in granulocytic and monocytic subpopulations in MM patients. Our findings highlight the importance of myeloid cells as a parameter in monitoring MM. We propose that the myeloid markers described in this study can be used to identify patients that are at an increased risk of developing advanced-stage disease.

ADDRESSING NEUTROPHIL HETEROGENEITY IN CHRONIC DISEASES

Despite detailed investigations into neutrophil heterogeneity, our understanding of the relationship between neutrophil subpopulations and disease severity in acute and chronic inflammatory conditions is limited. The present study reports detailed phenotypic profiles of immature and mature neutrophil subpopulations in WB and PBMCs in HIV-1, COVID-19, and MM. We demonstrate that the immature neutrophil subpopulation is readily identifiable in whole blood and expanded in inflammatory diseases. imNs displays higher proliferative capacity and increased mitochondrial potential. Mature neutrophil subpopulations demonstrate higher phagocytic capacity and are primed for ROS production.

Consistent with the identification and characterization of imNs in whole blood, several novel neutrophil progenitor subpopulations and immature neutrophil subpopulations, including preNeus and proNeus, have been identified [76-78, 237]. PreNeu, proNeu1, and proNeu2 are proliferative neutrophil progenitor subpopulations first

characterized in the bone marrow. PreNeu and proNeu1 subpopulations were observed to be expanded in sepsis models during conditions of immune stress. Recently characterized immature neutrophil subpopulations include a $CD101^-$ mouse neutrophil subpopulation associated with increased pancreatic tumor burden, and a $CD71^+$ human neutrophil subpopulation observed to be expanded in blood obtained from melanoma patients [76, 78].

There has been an increasing interest in the phenotype and function of distinct LDN subpopulations due to their relevance in chronic inflammatory settings. In line with the present study the differences in nuclear morphology [70, 74], transcription factors [73, 74, 89], and phenotypic markers [74, 88] within the LDN subpopulation have been demonstrated. In 2019, Hsu et al. were the first to show the metabolic flexibility of LDN subpopulations and the distinct bioenergetic processes they employ [89]. imLDNs were shown to produce ATP through mitochondrial-dependent pathways and maintain functionality under nutrient-limited conditions.

Although immunosuppressive functions have been ascribed to LDNs, the roles and functions of specific LDN subpopulations have yet to be fully elucidated. In the present study we demonstrate that mature neutrophil subpopulations have increased capacity for ROS production and phagocytosis relative to immature neutrophil subpopulations. Consistent with our study, Mistry et al. show that imLDNs from SLE patients had a lower capacity for phagocytosis and spontaneous NET production relative to mLDNs [74]. Interestingly, Hsu et al. demonstrate that imLDNs, through sustained NETosis, can promote breast-to-liver metastases further suggesting that the functional capacities of neutrophil subpopulations differ between disease conditions [89].

In the study presented we provide a comprehensive analysis of neutrophil subpopulations present in acute and chronic inflammatory diseases. Moving forward, it will be important to continue to identify and characterize neutrophil subpopulations to understand their specific roles in various diseases.

CURRENT KNOWLEDGE REGARDING THE ORIGIN OF LOW-DENSITY NEUTROPHILS

Despite many studies demonstrating an association between LDN frequency and poor outcomes in disease [70, 73, 75], there is currently no method available that could allow for the identification and targeting of LDNs. This remains a significant barrier in determining and mapping the origin and fate of LDNs. The central question remains: are a subset of neutrophils predestined to become LDNs once released from the bone marrow or do normal-density neutrophils (NDN) acquire the LDN phenotype following exposure to factors in the extracellular environment?

Our study proposes a novel mechanism for transient LDN induction through platelet-neutrophil interactions. We determine that direct activation of platelets through the PAR-1 receptor stimulates platelet-leukocyte interactions and engulfment of platelets by neutrophils. In addition, we demonstrate that whole blood stimulation rapidly induces LDNs, and that this induction can be abrogated through the inhibition of actin polymerization.

Although the relationship between the LDN frequency and disease pathogenesis is well-supported, critical knowledge gaps remain regarding the origin and kinetics of LDNs. Several hypotheses have been developed regarding the mechanisms of LDN induction. Inflammatory components, including cytokines and bacterial peptides, have become

increasingly studied as potential mediators of LDN induction. In 2015, Sagiv et al. proposed that TGF-β found in the extracellular environment could induce LDNs [70]. They demonstrate that dose-dependent exposure to TGF-β increased the LDN to NDN ratio *ex vivo*, and treatment with a TGF-β inhibitor reduced the proportion of LDNs to NDNs in tumor-bearing mice [70]. While the evidence is compelling, it was concluded that the effects of TGF-β were confined to NDNs and not naïve neutrophils, warranting further investigation [70]. Furthermore, the study did not comment on the time kinetics of LDN induction.

A recent study showed that NDN activation by inflammatory mediators TNF, lipopolysaccharide (LPS), or fMLF promoted LDN induction [81, 238]. Interestingly, they report different neutrophil morphologies with LPS-induced LDNs demonstrating membrane ruffling and fMLF-induced LDNs becoming vacuolated [238]. Altogether, the evidence suggests that inflammatory mediators play an important role in LDN induction; however, the mechanism involved has not been elucidated.

Multiple studies have investigated the effect of degranulation on the dynamics of neutrophil cell density, hypothesizing that the release of granule content decreases density and increases buoyancy [239, 240]. Jan et al. demonstrated that the release of α-defensins triggered by β-chemokines, such as RANTES, resulted in increased frequency of LDNs [239]. A recent study in sepsis observed positive correlations between supernatant MPO and MMP9 concentrations with the frequency of $CD66b^+$ LDNs [240]. Though both studies report an association between LDN frequency and degranulation, this mechanism has not been confirmed. Gaining deeper insight into the involved mechanisms will provide novel approaches to clinical interventions.

CONCLUSIONS AND FUTURE DIRECTIONS

The work described herein provides a detailed characterization of myeloid subpopulations in chronic inflammatory diseases. These findings may have important implications in the clinical monitoring of disease progression in MM and associated pre-cancerous conditions. We provide a comprehensive analysis of different myeloid cell compartment phenotypes, MM1 and MM2, in which MM2 is correlated with myeloma-defining events independent of previous treatment. We propose that the findings of our study can improve clinical monitoring of MM and provide instrumental tools to identify patients who are at a higher risk for developing advanced-stage disease. In addition, we describe a novel mechanism of transient LDN induction which may be further expanded in future studies.

The present study in MM provides a detailed characterization of an alternative myeloid phenotype strongly associated with myeloma-defining events and potentially the development of advanced disease stage. We propose that future investigations of the MM2 phenotype be conducted with paired blood and bone marrow samples through longitudinal studies in patients diagnosed with MM and pre-MM conditions. This will enable us to determine the clinical relevance of the MM2 phenotype concerning disease progression in pre-cancerous MM conditions. We hypothesize that these findings will provide additional insights with implications for future therapeutic approaches.

The work described in this dissertation identifies novel neutrophil subpopulations with distinct phenotype and function in the WB and PBMCs of HIV-1, COVID-19, and

MM patients. Our studies demonstrate the presence of immature and mature neutrophil subpopulations characterized as $CD16^{-}CD64^{+}$ and $CD16^{+}CD64^{int}$, respectively. The advancement of high-throughput transcriptomics technology has enabled us with new tools to identify and characterize novel myeloid and myeloid progenitor subpopulations and their clinical associations [76, 77]. Cellular Indexing of Transcriptomes and Epitopes by Sequencing (CITE-seq) combines single-cell RNA-sequencing (scRNA) with DNA-barcoded antibodies allows for immunophenotyping of cells with transcriptome analyses [241]. Since its inception, CITE-seq has arguably revolutionized proteomic and transcriptomic analyses.

Though outside the scope of this dissertation, we have initiated the utilization of CITE-seq technology focusing on the identification of novel neutrophil subpopulations. We have identified two immature and six mature neutrophil subpopulations in HIV-1 and COVID-19. This technology will provide deeper analyses and new avenues for therapeutic approaches. Additionally, studies aimed at identifying critical differences in metabolic and bioenergetic processes and functions, including NETosis and T-cell suppression, should be performed in conjunction with proteomic and transcriptomic analyses.

Accumulating evidence on the origin of LDNs implies that more than one mechanism of the induction of LDNs from NDNs exists. To corroborate our findings, *in vivo* studies assessing LDN induction with the inhibition of PSGL-1 and CD62P is suggested. Exploring mechanisms involved in LDN induction will improve our understanding of LDNs in different inflammatory conditions and potentially reveal novel therapeutic approaches for clinical intervention.

In closing, the studies described herein contributes to our understanding of myeloid subpopulations in MM, HIV-1, and COVID-19. The presented studies provide a framework for future investigations focused on elucidating the role of myeloid cells and chronic inflammatory changes in MM pathogenesis and comprehensive analyses of the kinetics of LDNs for the development of novel therapeutic approaches.

GENERAL REFERENCES

1. Ehrlich, P., *Methodologische Beiträge zur Physiologie und Pathologie der verschiedenen Formen der Leukocyten*. 1880, Z Klin Med. p. 553-560.
2. Nicolás-Ávila, J.Á., J.M. Adrover, and A. Hidalgo, *Neutrophils in Homeostasis, Immunity, and Cancer.* Immunity, 2017. **46**(1): p. 15-28.
3. Metchnikoff, E., *Lecon sur la pathologie comparee de inflammation*. 1893, Ann Inst Pasteur.
4. Niels, B., *Neutrophils, from Marrow to Microbes.* Immunity, 2010. **33**(5): p. 657-670.
5. Bainton, D.F., J.L. Ullyot, and M.G. Farquhar, *The development of neutrophilic polymorphonuclear leukocytes in human bone marrow.* The Journal of experimental medicine, 1971. **134**(4): p. 907-934.
6. Borregaard, N. and J.B. Cowland, *Granules of the Human Neutrophilic Polymorphonuclear Leukocyte.* Blood, 1997. **89**(10): p. 3503-3521.
7. Bainton, D.F. and M.G. Farquhar, *Origin of granules in polymorphonuclear leukocytes: two types derived from opposite faces of the Golgi complex in developing granulocytes.* The Journal of cell biology, 1966. **28**(2): p. 277-301.
8. Welsh, I. and J. Spitznagel, *Distribution of lysosomal enzymes, cationic proteins, and bactericidal substances in subcellular fractions of human polymorphonuclear leukocytes.* Infection and immunity, 1971. **4**(2): p. 97-102.
9. Baggiolini, M., *The enzymes of the granules of polymorphonuclear leukocytes and their functions.* Enzyme, 1972. **13**: p. 132-160.
10. Pütsep, K., et al., *Deficiency of antibacterial peptides in patients with morbus Kostmann: an observation study.* The Lancet, 2002. **360**(9340): p. 1144-1149.
11. Leffell, M.S. and J.K. Spitznagel, *Association of lactoferrin with lysozyme in granules of human polymorphonuclear leukocytes.* Infection and immunity, 1972. **6**(5): p. 761-765.
12. Leppert, D., et al., *T cell gelatinases mediate basement membrane transmigration in vitro.* The Journal of Immunology, 1995. **154**(9): p. 4379-4389.
13. Bakowski, B. and H. Tschesche, *Migration of polymorphonuclear leukocytes through human amnion membrane--a scanning electron microscopic study.* Biological chemistry Hoppe-Seyler, 1992. **373**(7): p. 529-546.

14. Lok, L.S. and M.R. Clatworthy, *Neutrophils in secondary lymphoid organs.* Immunology, 2021. **164**(4): p. 677-688.

15. Maletto, B.A., et al., *Presence of neutrophil-bearing antigen in lymphoid organs of immune mice.* Blood, 2006. **108**(9): p. 3094-3102.

16. Fournier, B. and C. Parkos, *The role of neutrophils during intestinal inflammation.* Mucosal immunology, 2012. **5**(4): p. 354-366.

17. Eash, K.J., et al., *CXCR2 and CXCR4 antagonistically regulate neutrophil trafficking from murine bone marrow.* The Journal of clinical investigation, 2010. **120**(7): p. 2423-2431.

18. Martin, C., et al., *Chemokines Acting via CXCR2 and CXCR4 Control the Release of Neutrophils from the Bone Marrow and Their Return following Senescence.* Immunity, 2003. **19**: p. 583-593.

19. Phillipson, M. and P. Kubes, *The neutrophil in vascular inflammation.* Nature medicine, 2011. **17**(11): p. 1381-1390.

20. Crooks, S. and R. Stockley, *Leukotriene B4.* The international journal of biochemistry & cell biology, 1998. **30**(2): p. 173-178.

21. Ford-Hutchinson, A., et al., *Leukotriene B, a potent chemokinetic and aggregating substance released from polymorphonuclear leukocytes.* Nature, 1980. **286**(5770): p. 264-265.

22. Silva, M.T., M.N. Silva, and R. Appelberg, *Neutrophil-macrophage cooperation in the host defence against mycobacterial infections.* Microbial pathogenesis, 1989. **6**(5): p. 369-380.

23. Farrera, C. and B. Fadeel, *Macrophage clearance of neutrophil extracellular traps is a silent process.* The Journal of Immunology, 2013. **191**(5): p. 2647-2656.

24. Bennouna, S. and E.Y. Denkers, *Microbial antigen triggers rapid mobilization of TNF-α to the surface of mouse neutrophils transforming them into inducers of high-level dendritic cell TNF-α production.* The Journal of Immunology, 2005. **174**(8): p. 4845-4851.

25. van Gisbergen, K.P., et al., *Interactions of DC-SIGN with Mac-1 and CEACAM1 regulate contact between dendritic cells and neutrophils.* FEBS letters, 2005. **579**(27): p. 6159-6168.

26. van Gisbergen, K.P., et al., *Neutrophils mediate immune modulation of dendritic cells through glycosylation-dependent interactions between Mac-1 and DC-SIGN.* Journal of Experimental Medicine, 2005. **201**(8): p. 1281-1292.

27. Scapini, P., F. Bazzoni, and M.A. Cassatella, *Regulation of B-cell-activating factor (BAFF)/B lymphocyte stimulator (BLyS) expression in human neutrophils.* Immunology letters, 2008. **116**(1): p. 1-6.

28. Huard, B., et al., *APRIL secreted by neutrophils binds to heparan sulfate proteoglycans to create plasma cell niches in human mucosa.* The Journal of clinical investigation, 2008. **118**(8): p. 2887-2895.

29. Blomgran, R. and J.D. Ernst, *Lung neutrophils facilitate activation of naive antigen-specific CD4+ T cells during Mycobacterium tuberculosis infection.* The Journal of Immunology, 2011. **186**(12): p. 7110-7119.

30. Gong, T., et al., *DAMP-sensing receptors in sterile inflammation and inflammatory diseases.* Nature Reviews Immunology, 2020. **20**(2): p. 95-112.

31. Hayashi, F., T.K. Means, and A.D. Luster, *Toll-like receptors stimulate human neutrophil function.* Blood, 2003. **102**(7): p. 2660-2669.

32. Manz, M.G. and S. Boettcher, *Emergency granulopoiesis.* Nature Reviews Immunology, 2014. **14**(5): p. 302-314.

33. Kato, T. and S. Kitagawa, *Regulation of neutrophil functions by proinflammatory cytokines.* International journal of hematology, 2006. **84**(3): p. 205-209.

34. Kitagawa, S., et al., *Recombinant human granulocyte colony-stimulating factor enhances superoxide release in human granulocytes stimulated by the chemotactic peptide.* Biochemical and Biophysical Research Communications, 1987. **144**(3): p. 1143-1146.

35. Yuo, A., et al., *Tumor necrosis factor as an activator of human granulocytes. Potentiation of the metabolisms triggered by the Ca2+-mobilizing agonists.* The Journal of Immunology, 1989. **142**(5): p. 1678-1684.

36. Suzuki, K., et al., *Selective activation of p38 mitogen-activated protein kinase cascade in human neutrophils stimulated by IL-1β.* The Journal of Immunology, 2001. **167**(10): p. 5940-5947.

37. Dahlgren, C. and A. Karlsson, *Respiratory burst in human neutrophils.* Journal of immunological methods, 1999. **232**(1-2): p. 3-14.

38. Lee, W.L., R.E. Harrison, and S. Grinstein, *Phagocytosis by neutrophils.* Microbes and infection, 2003. **5**(14): p. 1299-1306.

39. Shalaby, M., et al., *Activation of human polymorphonuclear neutrophil functions by interferon-gamma and tumor necrosis factors.* The Journal of Immunology, 1985. **135**(3): p. 2069-2073.

40. Brinkmann, V., et al., *Neutrophil Extracellular Traps Kill Bacteria.* Science, 2004. **303**(5663): p. 1532.

41. Papayannopoulos, V., *Neutrophil extracellular traps in immunity and disease.* Nature Reviews Immunology, 2018. **18**(2): p. 134-147.

42. Branzk, N., et al., *Neutrophils sense microbe size and selectively release neutrophil extracellular traps in response to large pathogens.* Nature immunology, 2014. **15**(11): p. 1017-1025.

43. Yipp, B.G., et al., *Infection-induced NETosis is a dynamic process involving neutrophil multitasking in vivo.* Nature medicine, 2012. **18**(9): p. 1386-1393.

44. Tillack, K., et al., *T lymphocyte priming by neutrophil extracellular traps links innate and adaptive immune responses.* The Journal of Immunology, 2012. **188**(7): p. 3150-3159.

45. Cassatella, M.A., *Neutrophil-derived proteins: selling cytokines by the pound.* Advances in immunology, 1999. **73**: p. 369-509.

46. Cassatella, M.A., et al., *Biological Roles of Neutrophil-Derived Granule Proteins and Cytokines.* Trends Immunol, 2019. **40**(7): p. 648-664.

47. Bazzoni, F., et al., *Phagocytosis of opsonized yeast induces TNF-tx mRNA accumulation and protein release by human polymorphonuclear leukocytes.* J. Leukocyte Biol, 1991.

48. Lord, P., et al., *Expression of interleukin-1 alpha and beta genes by human blood polymorphonuclear leukocytes.* The Journal of clinical investigation, 1991. **87**(4): p. 1312-1321.

49. Veglia, F., M. Perego, and D. Gabrilovich, *Myeloid-derived suppressor cells coming of age.* Nature Immunology, 2018. **19**(2): p. 108-119.

50. Fujishima, S., et al., *Regulation of neutrophil interleukin 8 gene expression and protein secretion by LPS, TNF-α, and IL-1β.* Journal of cellular physiology, 1993. **154**(3): p. 478-485.

51. Peveri, P., et al., *A novel neutrophil-activating factor produced by human mononuclear phagocytes.* The Journal of experimental medicine, 1988. **167**(5): p. 1547-1559.

52. Thelen, M., et al., *Mechanism of neutrophil activation by NAF, a novel monocyte-derived peptide agonist.* The FASEB journal, 1988. **2**(11): p. 2702-2706.

53. Teijeira, A., et al., *CXCR1 and CXCR2 chemokine receptor agonists produced by tumors induce neutrophil extracellular traps that interfere with immune cytotoxicity.* Immunity, 2020. **52**(5): p. 856-871. e8.

54. Kim, K., et al., *Eradication of metastatic mouse cancers resistant to immune checkpoint blockade by suppression of myeloid-derived cells.* Proceedings of the National Academy of Sciences, 2014. **111**(32): p. 11774-11779.

55. von Bruhl, M.L., et al., *Monocytes, neutrophils, and platelets cooperate to initiate and propagate venous thrombosis in mice in vivo.* J Exp Med, 2012. **209**(4): p. 819-35.

56. Kambas, K., I. Mitroulis, and K. Ritis, *The emerging role of neutrophils in thrombosis—the journey of TF through NETs.* Frontiers in immunology, 2012. **3**: p. 385.

57. de Boer, O.J., et al., *Neutrophils, neutrophil extracellular traps and interleukin-17 associate with the organisation of thrombi in acute myocardial infarction.* Thrombosis and haemostasis, 2013. **109**(02): p. 290-297.

58. Stakos, D.A., et al., *Expression of functional tissue factor by neutrophil extracellular traps in culprit artery of acute myocardial infarction.* European heart journal, 2015. **36**(22): p. 1405-1414.

59. Weckbach, L.T., et al., *Midkine drives cardiac inflammation by promoting neutrophil trafficking and NETosis in myocarditis.* Journal of Experimental Medicine, 2019. **216**(2): p. 350-368.

60. Demers, M., et al., *Cancers predispose neutrophils to release extracellular DNA traps that contribute to cancer-associated thrombosis.* Proc Natl Acad Sci U S A, 2012. **109**(32): p. 13076-81.

61. Demers, M. and D.D. Wagner, *NETosis: a new factor in tumor progression and cancer-associated thrombosis.* Semin Thromb Hemost, 2014. **40**(3): p. 277-83.

62. Rayes, R.F., et al., *Primary tumors induce neutrophil extracellular traps with targetable metastasis promoting effects.* JCI Insight, 2019. **5**.

63. Cools-Lartigue, J., et al., *Neutrophil extracellular traps sequester circulating tumor cells and promote metastasis.* The Journal of clinical investigation, 2013. **123**(8): p. 3446-3458.

64. Martinod, K. and D.D. Wagner, *Thrombosis: tangled up in NETs.* Blood, The Journal of the American Society of Hematology, 2014. **123**(18): p. 2768-2776.

65. Masucci, M.T., et al., *The emerging role of neutrophil extracellular traps (NETs) in tumor progression and metastasis.* Frontiers in Immunology, 2020. **11**.

66. Park, J., et al., *Cancer cells induce metastasis-supporting neutrophil extracellular DNA traps.* Science translational medicine, 2016. **8**(361): p. 361ra138-361ra138.

67. Ho-Tin-Noé, B., et al., *Innate immune cells induce hemorrhage in tumors during thrombocytopenia.* The American journal of pathology, 2009. **175**(4): p. 1699-1708.

68. Berger-Achituv, S., et al., *A proposed role for neutrophil extracellular traps in cancer immunoediting.* Frontiers in immunology, 2013. **4**: p. 48.

69. Cedervall, J., Y. Zhang, and A.K. Olsson, *Tumor-Induced NETosis as a Risk Factor for Metastasis and Organ Failure.* Cancer Res, 2016. **76**(15): p. 4311-5.

70. Sagiv, J.Y., et al., *Phenotypic diversity and plasticity in circulating neutrophil subpopulations in cancer.* Cell Rep, 2015. **10**(4): p. 562-73.

71. Casbon, A.J., et al., *Invasive breast cancer reprograms early myeloid differentiation in the bone marrow to generate immunosuppressive neutrophils.* Proc Natl Acad Sci U S A, 2015. **112**(6): p. E566-75.

72. Leliefeld, P.H.C., et al., *Differential antibacterial control by neutrophil subsets.* Blood Advances, 2018. **2**(11): p. 1344-1355.

73. Carlucci, P.M., et al., *Neutrophil subsets and their gene signature associate with vascular inflammation and coronary atherosclerosis in lupus.* JCI Insight, 2018. **3**(8).

74. Mistry, P., et al., *Transcriptomic, epigenetic, and functional analyses implicate neutrophil diversity in the pathogenesis of systemic lupus erythematosus.* Proc Natl Acad Sci U S A, 2019. **116**(50): p. 25222-25228.

75. Hacbarth, E. and A. Kajdacsy-Balla, *Low density neutrophils in patients with systemic lupus erythematosus, rheumatoid arthritis, and acute rheumatic fever.* Arthritis & Rheumatism, 1986. **29**(11): p. 1334-1342.

76. Evrard, M., et al., *Developmental Analysis of Bone Marrow Neutrophils Reveals Populations Specialized in Expansion, Trafficking, and Effector Functions.* Immunity, 2018. **48**(2): p. 364-379 e8.

77. Kwok, I., et al., *Combinatorial Single-Cell Analyses of Granulocyte-Monocyte Progenitor Heterogeneity Reveals an Early Uni-potent Neutrophil Progenitor.* Immunity, 2020. **53**(2): p. 303-318 e5.

78. Dinh, H.Q., et al., *Coexpression of CD71 and CD117 Identifies an Early Unipotent Neutrophil Progenitor Population in Human Bone Marrow.* Immunity, 2020. **53**(2): p. 319-334 e6.

79. Zhang, Y., et al., *Neutrophil subsets and their differential roles in viral respiratory diseases.* Journal of Leukocyte Biology, 2022.

80. Bowers, N.L., et al., *Immune suppression by neutrophils in HIV-1 infection: role of PD-L1/PD-1 pathway.* PLoS Pathog, 2014. **10**(3): p. e1003993.

81. Vlkova, M., et al., *Neutrophil and Granulocytic Myeloid-Derived Suppressor Cell-Mediated T Cell Suppression Significantly Contributes to Immune Dysregulation in Common Variable Immunodeficiency Disorders.* J Immunol, 2019. **202**(1): p. 93-104.

82. Corzo, C.A., et al., *Mechanism regulating reactive oxygen species in tumor-induced myeloid-derived suppressor cells.* The Journal of Immunology, 2009. **182**(9): p. 5693-5701.

83. Schmielau, J. and O.J. Finn, *Activated granulocytes and granulocyte-derived hydrogen peroxide are the underlying mechanism of suppression of t-cell function in advanced cancer patients.* Cancer research, 2001. **61**(12): p. 4756-4760.

84. Beury, D.W., et al., *Myeloid-derived suppressor cell survival and function are regulated by the transcription factor Nrf2.* The Journal of Immunology, 2016. **196**(8): p. 3470-3478.

85. Pillay, J., et al., *A subset of neutrophils in human systemic inflammation inhibits T cell responses through Mac-1.* J Clin Invest, 2012. **122**(1): p. 327-36.

86. Nagaraj, S., et al., *Altered recognition of antigen is a mechanism of CD8+ T cell tolerance in cancer.* Nature medicine, 2007. **13**(7): p. 828-835.

87. Elghetany, M.T., *Surface antigen changes during normal neutrophilic development: a critical review.* Blood Cells Mol Dis, 2002. **28**(2): p. 260-74.

88. Marini, O., et al., *Mature CD10(+) and immature CD10(-) neutrophils present in G-CSF-treated donors display opposite effects on T cells.* Blood, 2017. **129**(10): p. 1343-1356.

89. Hsu, B.E., et al., *Immature Low-Density Neutrophils Exhibit Metabolic Flexibility that Facilitates Breast Cancer Liver Metastasis.* Cell Rep, 2019. **27**(13): p. 3902-3915 e6.

90. Kawamura, S., et al., *Identification of a human clonogenic progenitor with strict monocyte differentiation potential: a counterpart of mouse cMoPs.* Immunity, 2017. **46**(5): p. 835-848. e4.

91. Guilliams, M., A. Mildner, and S. Yona, *Developmental and functional heterogeneity of monocytes.* Immunity, 2018. **49**(4): p. 595-613.

92. Jakubzick, C., et al., *Blood monocyte subsets differentially give rise to CD103+ and CD103− pulmonary dendritic cell populations.* The Journal of Immunology, 2008. **180**(5): p. 3019-3027.

93. Yona, S., et al., *Fate mapping reveals origins and dynamics of monocytes and tissue macrophages under homeostasis.* Immunity, 2013. **38**(1): p. 79-91.

94. Passlick, B., D. Flieger, and H.W. Ziegler-Heitbrock, *Identification and characterization of a novel monocyte subpopulation in human peripheral blood.* Blood, 1989. **74**(7): p. 2527-2534.

95. Ziegler-Heitbrock, L., *Reprint of: Monocyte subsets in man and other species.* Cellular immunology, 2014. **291**(1-2): p. 11-15.

96. Geissmann, F., S. Jung, and D.R. Littman, *Blood monocytes consist of two principal subsets with distinct migratory properties.* Immunity, 2003. **19**(1): p. 71-82.

97. Patel, A.A., et al., *The fate and lifespan of human monocyte subsets in steady state and systemic inflammation.* Journal of Experimental Medicine, 2017. **214**(7): p. 1913-1923.

98. Serbina, N.V. and E.G. Pamer, *Monocyte emigration from bone marrow during bacterial infection requires signals mediated by chemokine receptor CCR2.* Nature immunology, 2006. **7**(3): p. 311-317.

99. Jakubzick, C.V., G.J. Randolph, and P.M. Henson, *Monocyte differentiation and antigen-presenting functions.* Nature Reviews Immunology, 2017. **17**(6): p. 349-362.

100. Kim, T.S. and T.J. Braciale, *Respiratory dendritic cell subsets differ in their capacity to support the induction of virus-specific cytotoxic CD8+ T cell responses.* PloS one, 2009. **4**(1): p. e4204.

101. Nakano, H., et al., *Blood-derived inflammatory dendritic cells in lymph nodes stimulate acute T helper type 1 immune responses.* Nature immunology, 2009. **10**(4): p. 394-402.

102. Hamers, A.A., et al., *Human monocyte heterogeneity as revealed by high-dimensional mass cytometry.* Arteriosclerosis, thrombosis, and vascular biology, 2019. **39**(1): p. 25-36.

103. Auffray, C., et al., *Monitoring of blood vessels and tissues by a population of monocytes with patrolling behavior.* Science, 2007. **317**(5838): p. 666-670.

104. Carlin, L.M., et al., *Nr4a1-dependent Ly6Clow monocytes monitor endothelial cells and orchestrate their disposal.* Cell, 2013. **153**(2): p. 362-375.

105. Dutertre, C.-A., et al., *Pivotal role of M-DC8+ monocytes from viremic HIV-infected patients in TNFα overproduction in response to microbial products.* Blood, The Journal of the American Society of Hematology, 2012. **120**(11): p. 2259-2268.

106. Gabrilovich, D.I., S. Ostrand-Rosenberg, and V. Bronte, *Coordinated regulation of myeloid cells by tumours.* Nature Reviews Immunology, 2012. **12**(4): p. 253-268.

107. Bronte, V., et al., *Recommendations for myeloid-derived suppressor cell nomenclature and characterization standards.* Nat Commun, 2016. **7**: p. 12150.

108. Movahedi, K., et al., *Different tumor microenvironments contain functionally distinct subsets of macrophages derived from Ly6C (high) monocytes.* Cancer research, 2010. **70**(14): p. 5728-5739.

109. Gabrilovich, D.I., *Myeloid-Derived Suppressor Cells.* Cancer Immunol Res, 2017. **5**(1): p. 3-8.

110. Diaz-Montero, C.M., et al., *Increased circulating myeloid-derived suppressor cells correlate with clinical cancer stage, metastatic tumor burden, and doxorubicin–cyclophosphamide chemotherapy.* Cancer immunology, immunotherapy, 2009. **58**(1): p. 49-59.

111. Solito, S., et al., *A human promyelocytic-like population is responsible for the immune suppression mediated by myeloid-derived suppressor cells.* Blood, The Journal of the American Society of Hematology, 2011. **118**(8): p. 2254-2265.

112. Mandruzzato, S., et al., *Toward harmonized phenotyping of human myeloid-derived suppressor cells by flow cytometry: results from an interim study.* Cancer Immunology, Immunotherapy, 2016. **65**(2): p. 161-169.

113. Dumitru, C.A., et al., *Neutrophils and granulocytic myeloid-derived suppressor cells: immunophenotyping, cell biology and clinical relevance in human oncology.* Cancer immunology, immunotherapy, 2012. **61**(8): p. 1155-1167.

114. Condamine, T., et al., *Lectin-type oxidized LDL receptor-1 distinguishes population of human polymorphonuclear myeloid-derived suppressor cells in cancer patients.* Sci Immunol, 2016. **1**(2).

115. Movahedi, K., et al., *Identification of discrete tumor-induced myeloid-derived suppressor cell subpopulations with distinct T cell-suppressive activity.* Blood, 2008. **111**(8): p. 4233-44.

116. Molon, B., et al., *Chemokine nitration prevents intratumoral infiltration of antigen-specific T cells.* Journal of Experimental Medicine, 2011. **208**(10): p. 1949-1962.

117. Huang, B., et al., *Gr-1+ CD115+ immature myeloid suppressor cells mediate the development of tumor-induced T regulatory cells and T-cell anergy in tumor-bearing host.* Cancer research, 2006. **66**(2): p. 1123-1131.

118. Hoechst, B., et al., *Plasticity of human Th17 cells and iTregs is orchestrated by different subsets of myeloid cells.* Blood, The Journal of the American Society of Hematology, 2011. **117**(24): p. 6532-6541.

119. Rebmann, V., et al., *Soluble HLA-DR is a potent predictive indicator of disease progression in serum from early-stage melanoma patients*. International journal of cancer, 2002. **100**(5): p. 580-585.

120. Ugurel, S., et al., *Down-regulation of HLA class II and costimulatory CD86/B7-2 on circulating monocytes from melanoma patients.* Cancer Immunology, Immunotherapy, 2004. **53**(6): p. 551-559.

121. Łuczyński, W., et al., *Monocytes in children with leukemias and lymphomas--down-regulation of HLA and costimulatory molecules.* Acta Biochimica Polonica, 2004. **51**(4): p. 1067-1073.

122. Wang, L., et al., *Breast cancer induces systemic immune changes on cytokine signaling in peripheral blood monocytes and lymphocytes.* EBioMedicine, 2020. **52**: p. 102631.

123. Ramos, R.N., et al., *CD163+ tumor-associated macrophage accumulation in breast cancer patients reflects both local differentiation signals and systemic skewing of monocytes.* Clinical & translational immunology, 2020. **9**(2): p. e1108.

124. Hayashi, T., et al., *Peripheral blood monocyte count reflecting tumor-infiltrating macrophages is a predictive factor of adverse pathology in radical prostatectomy specimens.* The Prostate, 2017. **77**(14): p. 1383-1388.

125. Elliott, L.A., et al., *Human tumor-infiltrating myeloid cells: phenotypic and functional diversity.* Frontiers in immunology, 2017. **8**: p. 86.

126. Cassetta, L., et al., *Human tumor-associated macrophage and monocyte transcriptional landscapes reveal cancer-specific reprogramming, biomarkers, and therapeutic targets.* Cancer cell, 2019. **35**(4): p. 588-602. e10.

127. Venneri, M.A., et al., *Identification of proangiogenic TIE2-expressing monocytes (TEMs) in human peripheral blood and cancer.* Blood, The Journal of the American Society of Hematology, 2007. **109**(12): p. 5276-5285.

128. Coffelt, S.B., et al., *Angiopoietin-2 regulates gene expression in TIE2-expressing monocytes and augments their inherent proangiogenic functions.* Cancer research, 2010. **70**(13): p. 5270-5280.

129. Bolzoni, M., et al., *IL21R expressing CD14(+)CD16(+) monocytes expand in multiple myeloma patients leading to increased osteoclasts.* Haematologica, 2017. **102**(4): p. 773-784.

130. Olingy, C.E., H.Q. Dinh, and C.C. Hedrick, *Monocyte heterogeneity and functions in cancer.* J Leukoc Biol, 2019. **106**(2): p. 309-322.

131. Abe, M., et al., *Osteoclasts enhance myeloma cell growth and survival via cell-cell contact: a vicious cycle between bone destruction and myeloma expansion.* Blood, 2004. **104**(8): p. 2484-2491.

132. Feng, A.L., et al., *CD16+ monocytes in breast cancer patients: expanded by monocyte chemoattractant protein-1 and may be useful for early diagnosis.* Clinical & Experimental Immunology, 2011. **164**(1): p. 57-65.

133. Song, Y., et al., *Frequency of circulating CD14++ CD16+ intermediate monocytes as potential biomarker for the diagnosis of oral squamous cell carcinoma.* Journal of Oral Pathology & Medicine, 2018. **47**(10): p. 923-929.

134. Hu, R.-j., J.-y. Ma, and G. Hu, *Lymphocyte-to-monocyte ratio in pancreatic cancer: Prognostic significance and meta-analysis.* Clinica chimica acta, 2018. **481**: p. 142-146.

135. Tan, D., et al., *Prognostic significance of lymphocyte to monocyte ratio in colorectal cancer: A meta-analysis.* International journal of surgery, 2018. **55**: p. 128-138.

136. Lu, C., et al., *Prognostic value of lymphocyte-to-monocyte ratio in ovarian cancer: A meta-analysis.* Medicine, 2019. **98**(24).

137. Shen, M., et al., *Tumor-associated neutrophils as a new prognostic factor in cancer: a systematic review and meta-analysis.* PloS one, 2014. **9**(6): p. e98259.

138. Carus, A., et al., *Tumour-associated CD66b+ neutrophil count is an independent prognostic factor for recurrence in localised cervical cancer.* British journal of cancer, 2013. **108**(10): p. 2116-2122.

139. Walsh, S., et al., *Neutrophil-lymphocyte ratio as a prognostic factor in colorectal cancer.* Journal of surgical oncology, 2005. **91**(3): p. 181-184.

140. Koh, C., et al., *Utility of pre-treatment neutrophil–lymphocyte ratio and platelet–lymphocyte ratio as prognostic factors in breast cancer.* British journal of cancer, 2015. **113**(1): p. 150-158.

141. Masucci, M.T., M. Minopoli, and M.V. Carriero, *Tumor associated neutrophils. Their role in tumorigenesis, metastasis, prognosis and therapy.* Frontiers in oncology, 2019. **9**: p. 1146.

142. Liang, W. and N. Ferrara, *The complex role of neutrophils in tumor angiogenesis and metastasis.* Cancer immunology research, 2016. **4**(2): p. 83-91.

143. Houghton, A.M., et al., *Neutrophil elastase–mediated degradation of IRS-1 accelerates lung tumor growth.* Nature medicine, 2010. **16**(2): p. 219-223.

144. Queen, M.M., et al., *Breast cancer cells stimulate neutrophils to produce oncostatin M: potential implications for tumor progression.* Cancer research, 2005. **65**(19): p. 8896-8904.

145. Gaudry, M., et al., *Intracellular pool of vascular endothelial growth factor in human neutrophils.* Blood, The Journal of the American Society of Hematology, 1997. **90**(10): p. 4153-4161.

146. Coussens, L.M., et al., *MMP-9 supplied by bone marrow–derived cells contributes to skin carcinogenesis.* Cell, 2000. **103**(3): p. 481-490.

147. Pahler, J.C., et al., *Plasticity in tumor-promoting inflammation: impairment of macrophage recruitment evokes a compensatory neutrophil response.* Neoplasia, 2008. **10**(4): p. 329-IN2.

148. Koga, Y., et al., *Neutrophil-derived TNF-related apoptosis-inducing ligand (TRAIL): a novel mechanism of antitumor effect by neutrophils.* Cancer research, 2004. **64**(3): p. 1037-1043.

149. Colombo, M.P., et al., *Granulocyte colony-stimulating factor (G-CSF) gene transduction in murine adenocarcinoma drives neutrophil-mediated tumor inhibition in vivo. Neutrophils discriminate between G-CSF-producing and G-CSF-nonproducing tumor cells.* The Journal of Immunology, 1992. **149**(1): p. 113-119.

150. Fridlender, Z.G., et al., *Polarization of tumor-associated neutrophil phenotype by TGF-β:"N1" versus "N2" TAN.* Cancer cell, 2009. **16**(3): p. 183-194.

151. Fridlender, Z.G. and S.M. Albelda, *Tumor-associated neutrophils: friend or foe?* Carcinogenesis, 2012. **33**(5): p. 949-955.

152. Granot, Z., et al., *Tumor Entrained Neutrophils Inhibit Seeding in the Premetastatic Lung.* Cancer Cell, 2011. **20**(3): p. 300-314.

153. Yan, J., et al., *Human polymorphonuclear neutrophils specifically recognize and kill cancerous cells.* Oncoimmunology, 2014. **3**(7): p. e950163.

154. Riise, R.E., et al., *TLR-stimulated neutrophils instruct NK cells to trigger dendritic cell maturation and promote adaptive T cell responses.* The Journal of Immunology, 2015. **195**(3): p. 1121-1128.

155. Loukinova, E., et al., *Growth regulated oncogene-α expression by murine squamous cell carcinoma promotes tumor growth, metastasis, leukocyte infiltration and angiogenesis by a host CXC receptor-2 dependent mechanism.* Oncogene, 2000. **19**(31): p. 3477-3486.

156. Jablonska, J., et al., *Neutrophils responsive to endogenous IFN-β regulate tumor angiogenesis and growth in a mouse tumor model.* The Journal of clinical investigation, 2010. **120**(4): p. 1151-1164.

157. Mishalian, I., et al., *Tumor-associated neutrophils (TAN) develop pro-tumorigenic properties during tumor progression.* Cancer Immunology, Immunotherapy, 2013. **62**(11): p. 1745-1756.

158. Veglia, F., E. Sanseviero, and D.I. Gabrilovich, *Myeloid-derived suppressor cells in the era of increasing myeloid cell diversity.* Nat Rev Immunol, 2021.

159. Thomas, G.D., et al., *Human blood monocyte subsets: a new gating strategy defined using cell surface markers identified by mass cytometry*. Arteriosclerosis, thrombosis, and vascular biology, 2017. **37**(8): p. 1548-1558.

160. Ying, H.-Q., et al., *The prognostic value of preoperative NLR, d-NLR, PLR and LMR for predicting clinical outcome in surgical colorectal cancer patients.* Medical oncology, 2014. **31**(12): p. 1-8.

161. Dimopoulos, M., et al., *Consensus recommendations for standard investigative workup: report of the International Myeloma Workshop Consensus Panel 3*. Blood, 2011. **117**(18): p. 4701-5.

162. Rajkumar, S.V., et al., *International Myeloma Working Group updated criteria for the diagnosis of multiple myeloma.* The Lancet Oncology, 2014. **15**(12): p. e538-e548.

163. Weiss, B.M., et al., *A monoclonal gammopathy precedes multiple myeloma in most patients.* Blood, The Journal of the American Society of Hematology, 2009. **113**(22): p. 5418-5422.

164. Landgren, O., et al., *Monoclonal gammopathy of undetermined significance (MGUS) consistently precedes multiple myeloma: a prospective study.* Blood, The Journal of the American Society of Hematology, 2009. **113**(22): p. 5412-5417.

165. Kyle, R.A., et al., *Prevalence of monoclonal gammopathy of undetermined significance.* New England Journal of Medicine, 2006. **354**(13): p. 1362-1369.

166. Saleun, J., et al., *Monoclonal gammopathies in the adult population of Finistere, France.* Journal of clinical pathology, 1982. **35**(1): p. 63-68.

167. Kyle, R.A., et al., *A long-term study of prognosis in monoclonal gammopathy of undetermined significance.* New England Journal of Medicine, 2002. **346**(8): p. 564-569.

168. Kyle, R.A., et al., *Clinical course and prognosis of smoldering (asymptomatic) multiple myeloma.* New England Journal of Medicine, 2007. **356**(25): p. 2582-2590.

169. Siegel, R.L., et al., *Cancer statistics, 2021.* CA: a cancer journal for clinicians, 2021. **71**(1): p. 7-33.

170. Noone, A., et al., *SEER cancer statistics review, 1975–2015.* Bethesda, MD: National Cancer Institute, 2018. **4**.

171. Brown, L.M., et al., *Multiple myeloma and family history of cancer among blacks and whites in the US.* Cancer: Interdisciplinary International Journal of the American Cancer Society, 1999. **85**(11): p. 2385-2390.

172. Wallin, A. and S.C. Larsson, *Body mass index and risk of multiple myeloma: a meta-analysis of prospective studies.* European journal of cancer, 2011. **47**(11): p. 1606-1615.

173. Romano, A., et al., *The NLR and LMR ratio in newly diagnosed MM patients treated upfront with novel agents.* Blood cancer journal, 2017. **7**(12): p. 1-3.

174. Lee, G.-W., et al., *The derived neutrophil-to-lymphocyte ratio is an independent prognostic factor in transplantation ineligible patients with multiple myeloma.* Acta Haematologica, 2018. **140**(3): p. 146-156.

175. Solmaz Medeni, S., et al., *Can Neutrophil-to-Lymphocyte Ratio, Monocyte-to-Lymphocyte Ratio, and Platelet-to-Lymphocyte Ratio at Day+ 100 be used as a prognostic marker in Multiple Myeloma patients with autologous transplantation?* Clinical Transplantation, 2018. **32**(9): p. e13359.

176. Romano, A., et al., *PMN-MDSC and arginase are increased in myeloma and may contribute to resistance to therapy.* Expert Rev Mol Diagn, 2018. **18**(7): p. 675-683.

177. Karle, H., N.E. Hansen, and T. Plesner, *Neutrophil defect in multiple myeloma: studies on intraneutrophilic lysozyme in multiple myeloma and malignant lymphoma.* Scandinavian Journal of Haematology, 1976. **17**(1): p. 62-70.

178. Favaloro, J., et al., *Myeloid derived suppressor cells are numerically, functionally and phenotypically different in patients with multiple myeloma.* Leukemia & Lymphoma, 2014. **55**(12): p. 2893-2900.

179. Ramachandran, I.R., et al., *Myeloid-derived suppressor cells regulate growth of multiple myeloma by inhibiting T cells in bone marrow.* J Immunol, 2013. **190**(7): p. 3815-23.

180. Ramachandran, I.R., et al., *Bone marrow PMN-MDSCs and neutrophils are functionally similar in protection of multiple myeloma from chemotherapy.* Cancer Lett, 2016. **371**(1): p. 117-24.

181. Romano, A., et al., *High-density neutrophils in MGUS and multiple myeloma are dysfunctional and immune-suppressive due to increased STAT3 downstream signaling.* Sci Rep, 2020. **10**(1): p. 1983.

182. Puglisi, F., et al., *Plasticity of High-Density Neutrophils in Multiple Myeloma is Associated with Increased Autophagy Via STAT3.* Int J Mol Sci, 2019. **20**(14).

183. Giallongo, C., et al., *Granulocyte-like myeloid derived suppressor cells (G-MDSC) are increased in multiple myeloma and are driven by dysfunctional mesenchymal stem cells (MSC).* Oncotarget, 2016. **7**(52): p. 85764.

184. Görgün, G.T., et al., *Tumor-promoting immune-suppressive myeloid-derived suppressor cells in the multiple myeloma microenvironment in humans.* Blood, The Journal of the American Society of Hematology, 2013. **121**(15): p. 2975-2987.

185. Scavelli, C., et al., *Vasculogenic mimicry by bone marrow macrophages in patients with multiple myeloma.* Oncogene, 2008. **27**(5): p. 663-74.

186. Calcinotto, A., et al., *Microbiota-driven interleukin-17-producing cells and eosinophils synergize to accelerate multiple myeloma progression.* Nat Commun, 2018. **9**(1): p. 4832.

187. Feng, X., et al., *Targeting CD38 suppresses induction and function of T regulatory cells to mitigate immunosuppression in multiple myeloma.* Clinical cancer research, 2017. **23**(15): p. 4290-4300.

188. Nakamura, K., et al., *Dysregulated IL-18 Is a Key Driver of Immunosuppression and a Possible Therapeutic Target in the Multiple Myeloma Microenvironment.* Cancer Cell, 2018. **33**(4): p. 634-648 e5.

189. Hofbauer, D., et al., *β2-microglobulin triggers NLRP3 inflammasome activation in tumor-associated macrophages to promote multiple myeloma progression.* Immunity, 2021. **54**(8): p. 1772-1787. e9.

190. Thangaraj, J.L., et al., *Expansion of cytotoxic natural killer cells in multiple myeloma patients using K562 cells expressing OX40 ligand and membrane-bound IL-18 and IL-21.* Cancer Immunology, Immunotherapy, 2021: p. 1-13.

191. Binsky-Ehrenreich, I., et al., *CD84 is a survival receptor for CLL cells.* Oncogene, 2014. **33**(8): p. 1006-1016.

192. Lewinsky, H., et al., *CD84 is a regulator of the immunosuppressive microenvironment in multiple myeloma.* JCI insight, 2021. **6**(4).

193. Blockmans, D., H. Deckmyn, and J. Vermylen, *Platelet activation.* Blood reviews, 1995. **9**(3): p. 143-156.

194. Heemskerk, J.W., E.M. Bevers, and T. Lindhout, *Platelet activation and blood coagulation.* Thrombosis and haemostasis, 2002. **88**(08): p. 186-193.

195. Smyth, S.S., et al., *Platelet functions beyond hemostasis.* J Thromb Haemost, 2009. **7**(11): p. 1759-66.

196. Weyrich, A.S., et al., *Monocyte tethering by P-selectin regulates monocyte chemotactic protein-1 and tumor necrosis factor-alpha secretion. Signal integration and NF-kappa B translocation.* The Journal of clinical investigation, 1995. **95**(5): p. 2297-2303.

197. Kuijper, P., et al., *Platelet-dependent primary hemostasis promotes selectin-and integrin-mediated neutrophil adhesion to damaged endothelium under flow conditions.* 1996.

198. Martins, P.A.d.C., et al., *Platelet binding to monocytes increases the adhesive properties of monocytes by up-regulating the expression and functionality of β1 and β2 integrins.* Journal of leukocyte biology, 2006. **79**(3): p. 499-507.

199. Peters, M.J., et al., *Circulating platelet-neutrophil complexes represent a subpopulation of activated neutrophils primed for adhesion, phagocytosis and intracellular killing.* British Journal of Heamatology, 1999(106): p. 391-399.

200. McCabe, D.J., et al., *Platelet degranulation and monocyte–platelet complex formation are increased in the acute and convalescent phases after ischaemic stroke or transient ischaemic attack.* British journal of haematology, 2004. **125**(6): p. 777-787.

201. Gardiner, E.E., et al., *Regulation of P-selectin binding to the neutrophil P-selectin counter-receptor P-selectin glycoprotein ligand-1 by neutrophil elastase and cathepsin G.* Blood, The Journal of the American Society of Hematology, 2001. **98**(5): p. 1440-1447.

202. Evangelista, V., et al., *Platelet/polymorphonuclear leukocyte interaction: p-selectin triggers protein-tyrosine phosphorylation–dependent CD11b/CD18 adhesion: role of PSGL-1 as a signaling molecule.* Blood, The Journal of the American Society of Hematology, 1999. **93**(3): p. 876-885.

203. Yang, J., B.C. Furie, and B. Furie, *The biology of P-selectin glycoprotein ligand-1: its role as a selectin counterreceptor in leukocyte-endothelial and leukocyte-platelet interaction.* Thrombosis and haemostasis, 1999. **81**(01): p. 1-7.

204. Celi, A., et al. *Platelet-leukocyte-endothelial cell interaction on the blood vessel wall*. in *Seminars in hematology*. 1997.

205. Simon, D.I., et al., *Platelet glycoprotein Ibα is a counterreceptor for the leukocyte integrin Mac-1 (CD11b/CD18).* The Journal of experimental medicine, 2000. **192**(2): p. 193-204.

206. Setianto, B.Y., et al., *Circulating soluble CD40 ligand mediates the interaction between neutrophils and platelets in acute coronary syndrome.* Heart and Vessels, 2010. **25**(4): p. 282-287.

207. Jin, R., et al., *Soluble CD40 ligand stimulates CD40-dependent activation of the β2 integrin Mac-1 and protein kinase C zeda (PKCζ) in neutrophils: implications for neutrophil-platelet interactions and neutrophil oxidative burst.* PLoS One, 2013. **8**(6): p. e64631.

208. Johansson, D., O. Shannon, and M. Rasmussen, *Platelet and neutrophil responses to Gram positive pathogens in patients with bacteremic infection.* PloS one, 2011. **6**(11): p. e26928.

209. Gawaz, M., et al., *Platelet activation and interaction with leucocytes in patients with sepsis or multiple organ failure.* European journal of clinical investigation, 1995. **25**(11): p. 843-851.

210. Totani, L. and V. Evangelista, *Platelet-leukocyte interactions in cardiovascular disease and beyond.* Arterioscler Thromb Vasc Biol, 2010. **30**(12): p. 2357-61.

211. Arber, N., et al., *Heterotypic leukocyte aggregation in the peripheral blood of patients with leukemia, inflammation and stress.* Nouv Rev Fr Hematol, 1991. **33**(3): p. 251-255.

212. Hottz, E.D., et al., *Platelet activation and platelet-monocyte aggregate formation trigger tissue factor expression in patients with severe COVID-19.* Blood, 2020. **136**(11): p. 1330-1341.

213. Allen, N., et al., *Circulating monocyte-platelet aggregates are a robust marker of platelet activity in cardiovascular disease.* Atherosclerosis, 2019. **282**: p. 11-18.

214. Kasper, B., et al., *Platelet factor 4 (CXC chemokine ligand 4) differentially regulates respiratory burst, survival, and cytokine expression of human monocytes by using distinct signaling pathways.* The Journal of Immunology, 2007. **179**(4): p. 2584-2591.

215. Lee, S.J., et al., *Activated platelets convert CD14+ CD16-into CD14+ CD16+ monocytes with enhanced FcγR-mediated phagocytosis and skewed M2 polarization.* Frontiers in immunology, 2021. **11**: p. 3363.

216. Singhal, R., et al., *Engulfment of Hb-activated platelets differentiates monocytes into pro-inflammatory macrophages in PNH patients.* European journal of immunology, 2018. **48**(8): p. 1285-1294.

217. Carestia, A., et al., *Platelets promote macrophage polarization toward pro-inflammatory phenotype and increase survival of septic mice.* Cell reports, 2019. **28**(4): p. 896-908. e5.

218. Fuchs, T.A., et al., *Extracellular DNA traps promote thrombosis.* Proc Natl Acad Sci U S A, 2010. **107**(36): p. 15880-5.

219. Kornerup, K.N., et al., *Circulating platelet-neutrophil complexes are important for subsequent neutrophil activation and migration.* J Appl Physiol (1985), 2010. **109**(3): p. 758-67.

220. Caudrillier, A., et al., *Platelets induce neutrophil extracellular traps in transfusion-related acute lung injury.* Journal of Clinical Investigation, 2012. **122**(7): p. 2661-2671.

221. Zhang, Y., et al., *Neutrophil extracellular traps induced by activated platelets contribute to procoagulant activity in patients with colorectal cancer.* Thrombosis research, 2019. **180**: p. 87-97.

222. Teague, H.L., et al., *Neutrophil Subsets, Platelets, and Vascular Disease in Psoriasis.* JACC Basic Transl Sci, 2019. **4**(1): p. 1-14.

223. Lecot, P., et al., *Gene signature of circulating platelet-bound neutrophils is associated with poor prognosis in cancer patients.* 2021.

224. Manfredi, A.A., et al., *Platelet phagocytosis via PSGL1 and accumulation of microparticles in systemic sclerosis.* Arthritis Rheumatol, 2021.

225. Maugeri, N., et al., *Neutrophils phagocytose activated platelets in vivo: a phosphatidylserine, P-selectin, and {beta}2 integrin-dependent cell clearance program.* Blood, 2009. **113**(21): p. 5254-65.

226. Criswell, K.A., M.A. Breider, and M.R. Bleavins, *EDTA-dependent platelet phagocytosis: A cytochemical, ultrastructural, and functional characterization.* American journal of clinical pathology, 2001. **115**(3): p. 376-384.

227. Senzel, L. and C. Chang, *Platelet phagocytosis by neutrophils.* Blood, The Journal of the American Society of Hematology, 2013. **122**(9): p. 1543-1543.

228. Paul, P., et al., *Co-existent platelet phagocytosis, satellitism and clumping causing spurious thrombocytopenia.* Indian Journal of Hematology and Blood Transfusion, 2013. **29**(3): p. 158-160.

229. Wu, X., Y. Li, and X. Yang, *Platelet phagocytosis by leukocytes in a patient with cerebral hemorrhage and thrombocytopenia caused by gram-negative bacterial infection.* Journal of International Medical Research, 2022. **50**(2): p. 03000605221079102.

230. Bazarbachi, A.H., et al., *Relapsed refractory multiple myeloma: a comprehensive overview.* Leukemia, 2019. **33**(10): p. 2343-2357.

231. Naymagon, L. and M. Abdul-Hay, *Novel agents in the treatment of multiple myeloma: a review about the future.* Journal of hematology & oncology, 2016. **9**(1): p. 1-20.

232. Perez, C., et al., *Immunogenomic identification and characterization of granulocytic myeloid-derived suppressor cells in multiple myeloma.* Blood, 2020. **136**(2): p. 199-209.

233. Ohsaka, A., et al., *Increased Expression of the High-Affinity Receptor for IgG (FcRI, CD64) on Neutrophils in Multiple Myeloma.* Hematopathology and Molecular Hematology, 1996. **10**: p. 151-160.

234. Hirsh, M., et al., *Overexpression of the high-affinity Fcgamma receptor (CD64) is associated with leukocyte dysfunction in sepsis.* Shock (Augusta, Ga.), 2001. **16**(2): p. 102-108.

235. Groselj-Grenc, M., A. Ihan, and M. Derganc, *Neutrophil and monocyte CD64 and CD163 expression in critically ill neonates and children with sepsis: comparison of fluorescence intensities and calculated indexes.* Mediators of inflammation, 2008. **2008**.

236. Beyer, M., et al., *In vivo peripheral expansion of naive CD4+CD25high FoxP3+ regulatory T cells in patients with multiple myeloma.* Blood, 2006. **107**(10): p. 3940-9.

237. Zhu, Y.P., et al., *Identification of an Early Unipotent Neutrophil Progenitor with Pro-tumoral Activity in Mouse and Human Bone Marrow.* Cell Rep, 2018. **24**(9): p. 2329-2341 e8.

238. Hardisty, G.R., et al., *High purity isolation of low density neutrophils casts doubt on their exceptionality in health and disease.* Frontiers in Immunology, 2021. **12**: p. 2057.

239. Jan, M.-S., et al., *CC chemokines induce neutrophils to chemotaxis, degranulation, and α-defensin release.* JAIDS Journal of Acquired Immune Deficiency Syndromes, 2006. **41**(1): p. 6-16.

240. Sun, R., et al., *Dysfunction of low-density neutrophils in peripheral circulation in patients with sepsis.* Scientific Reports, 2022. **12**(1): p. 1-10.

241. Stoeckius, M., et al., *Simultaneous epitope and transcriptome measurement in single cells.* Nature methods, 2017. **14**(9): p. 865-868.

APPENDIX A

A. SUPPLEMENTAL METHODS (EXTENDED)

Supplemental Methods (Extended)

Morphological characterization of LDN subpopulations

Wright-Giemsa staining

Sorted cells were suspended into 200 μl RPMI Media (Corning, Corning, NY) of 5 x 10^5 aliquots. The Shandon Cytospin3™ cytocentrifuge and cytology funnels purchased from ThermoFisher were utilized for all cytospin experiments. The aliquots were then loaded into the cytospin chamber, spun at medium acceleration at 800 x g for 4 minutes, and left to air dry overnight. Slides were stored at 4°C until ready for staining. Slides were removed from 4°C and left at RT for 15 minutes. 200 μl of chilled methanol (ThermoFisher) was added for 5 minutes, and then aspirated. 200 μl of Wright-Giemsa stain (Electron Microscopy Sciences, Hatfield, PA) was added and slides were incubated for 4 minutes at RT. After 4 minutes 400 μl of DPBS was added on top of the Wright-Giemsa stain and slides were set to incubate for 8 minutes at RT. The stain and buffer were decanted from slides and slides were washed in running water for 3 minutes. Slides were left to air dry at minimum 1 hour. 110 μl of Fisher Chemical™ Permount™ Mounting Medium (ThermoFisher) and was added to slides and full coverslips were placed on top of slides. Slides were stored at 4°C until imaged for quantification.

Isolation of PMNs from PBMCs

Plasma and ficoll were removed from the 15ml conical tube and the remaining red blood cell and PMN pellet was gently mixed. The tube was filled with isotonic lysis buffer (as described previously) and inverted. The tube was set to rotate for 5-7 minutes until red blood cell lysis completed. The sample was centrifuged for 200 x g for 10 minutes. The supernatant was aspirated and the cell pellet was suspended in DPBS. This step was

repeated twice more. After, the cell pellet was suspended in 10% human serum in DPBS and counted as described previously. 2 x 10^6 cells at 1 x 10^6 aliquots were utilized for PMN imaging per sample.

Transmission electron microscopy (TEM)

Protocol was adapted from the High Resolution Imaging and Shared Facility at the University of Alabama at Birmingham (Birmingham, AL) for sorted imLDNs and mLDNs, and PMNs isolated from the PBMC layer as described previously.

Reagents. Millipore water (Burlington, MA) was utilized for this protocol. Phosphate buffer and glutaraldehyde were purchased from ThermoFisher, Fisher Chemicals™. Cacodylate (CaCo) buffer, paraformaldehyde, and the EPON812 resin embedding kit with the DMP-30 accelerator were from Electron Microscopy Sciences. 100 proof Ethanol (EM grade) was from Acros Organics (Geel, Belgium). Osmium tetroxide (OsO_4), uranyl acetate, low-melting point agarose, and Evans Blue were purchased from Sigma Aldrich. The Tecnai Spirit T12 Transmission Electron Microscope (Field Electron and Ion Company, Hillsboro, OR) was used for imaging at 3200x magnification.

Immersion fixation. 1 x 10^5 cell aliquots were suspended in 600 µl 0.1M Caco buffer, pH 7.4. Tubes were centrifuged for 10 minutes at 500 x g. The supernatant was aspirated and the pellets were suspended in 1 ml 3% glutaraldehyde buffered in 0.1M CaCo buffer and incubated for 2 hours at RT with mixing every 30 minutes. After, tubes were centrifuged for 10 minutes at 500 x g. After, the supernatant was aspirated and pellets were suspended in 600 µl of 0.1M CaCo buffer. The tubes set to rotate for 15 minutes at medium speed. This step was repeated once more. Cell suspensions were transferred to 0.5 ml microcentrifuge tubes. Tubes were then centrifuged for 10 minutes at 500 x g. After, the

supernatant was aspirated and the pellets were suspended in 75 µl of low-melting point 2% agarose in Millipore water (stored at 37°C). Tubes were left on ice for 20 minutes while the agarose solidified. 300 µl of 0.1M CaCo buffer was added and tubes incubated for 5 minutes at RT. 250 µl of the buffer was aspirated and the solidified agarose pellets were transferred into a new 1.5 ml Eppendorf tube that contained 500 µl 0.1M CaCo buffer. After, the buffer was removed and 1 ml of 1% OsO_4 in 0.1M CaCo buffer was added. Tubes were set to rotate in the dark for 1 hour at RT. The OsO_4 was removed, 1 ml of 0.1M CaCo buffer was added, and tubes were left to incubate in the dark at RT for five minutes. The buffer was removed, 1 ml of 0.1M CaCo buffer was added, and tubes were left to rotate in the dark at RT for 15 minutes. This step was repeated three times.

Dehydration. After the last 1 ml of 0.1M CaCo buffer was removed 1 ml of 50% EtOH was added. Tubes were left to rotate for 5 minutes in the dark at RT. The 1 ml 50% EtOH was removed and 1 mlof 50% EtOH with 2% uranyl acetate was added in a 1:1 dilution. Tubes were left to rotate for 1 hour in the dark at RT. The 1 ml of 50% EtOH with 2% uranyl acetate was removed and replaced with 1 ml of 50% EtOH. Tubes were left to rotate for 5 minutes in the dark at RT. After, the 1 ml 50% EtOH was removed and the above step was repeated using 1 ml 50% EtOH, 1 ml 80% EtOH, and finally 1 ml 95% EtOH. After the 1 ml 95% EtOH was removed 1 ml of 100% EtOH was added and tubes were left to rotate in the dark at RT for 10 minutes. This step was repeated four more times.

Pre-embedding and Embedding. After removing the last 1 ml of 100% EtOH, 1 ml of equal parts 100% EtOH with EPON812 resin mix with the DMP-30 accelerator was added to the sample and tubes were left to rotate in the dark overnight at RT. The 1 ml 100% EtOH resin mix was removed and replaced with 1 ml of equal parts 100% EtOH

with EPON812 resin mix with the accelerator. Tubes were left to rotate in the dark for 24 hours at RT. This step was repeated once more. The final 1 ml 100% EtOH resin mix was removed, 1 ml of 100% EPON812 resin mix was added, and tubes were left at 60°C for 24-48 hours. Samples were removed then left to cool for a minimum of 24 hours at RT. After cooling, samples were cut using ultramicrotomy with the assistance of the High Resolution Imaging and Shared Facility at the University of Alabama at Birmingham and imaged.

Quantification of nuclear lobes. Slides were imaged with a Keyence BZ-X700 microscope (Keyence, Ithaca, IL) at 40X magnification. Manual quantification of neutrophil nuclear lobes was performed where independent lobes were determined when the connection between two lobes was greater than 33% of the width of adjacent lobes.

Appendix A: Supplemental Table 1. **Antibodies used for staining whole blood and PBMCs**

Antibodies (Anti-human)	Source	Identifier
Base panel		
Anti-CD3-BV605TM, clone OKT3	Biolegend	Cat# 317322; RRID: AB_2561991
Anti-CD14-APC/FireTM750, clone 63D3	Biolegend	Cat# 367120; RRID: AB_2572099
Anti-CD15-eF450, clone HI98	eBioscience™	Cat# 48-0159-42; RRID: AB_2016661
Anti-CD16-APC, clone eBioCB16	eBioscience™	Cat# 17-0168-42; RRID: AB_2016663
Anti-CD19-BV605TM, clone HIB19	Biolegend	Cat# 302244; RRID: AB_2562015
Anti-CD62L-BV711, clone DREG-56	BD Biosciences	Cat# 740783; RRID: AB_2740446
Anti-CD193 (CCR3)-BV510, clone 5E8	BD Biosciences	Cat# 563071; RRID: AB_2737988
Antobodies used for Whole blood and PBMC staining		
Anti-CD10-Per CP/Cy5.5, clone HI10a	Biolegend	Cat# 312216; RRID: AB_10642819
Anti-CD11b-PerCP/Cy5.5, clone ICRF44	Biolegend	Cat# 301328; RRID: AB_10933428
Anti-CD31-FITC, clone WM59	Biolegend	Cat# 303104; RRID: AB_314330
Anti-CD36-FITC, clone 5-271	Biolegend	Cat# 336204; RRID: AB_1575025
Anti-CD54-FITC, clone HA58	Biolegend	Cat# 353108; RRID: AB_10900254
Anti-CD63-PerCP/Cy5.5, clone H5C6	Biolegend	Cat# 353020; RRID: AB_2561685
Anti-CD64-PE/Cy7, clone 10.1	Biolegend	Cat# 305022; RRID: AB_2561584
Anti-CD66b-FITC, clone G10F5	Biolegend	Cat# 305104; RRID: AB_314496
Anti-CD142-PE, clone NY2	Biolegend	Cat# 365204; RRID: AB_2564566

Anti-CD163-PE/Cy7, clone GHI/61	Biolegend	Cat# 333614; RRID: AB_2562641
Anti-CD169-PE, clone 7-239	Biolegend	Cat# 346004; RRID: AB_2189029
Anti-CD274 (PD-L1)-PE/Cy7, clone 29E.2A3	Biolegend	Cat# 329718; RRID: AB_2561687
Anti-CD284 (TLR-4)-PE/Cy7, clone HTA125	eBioscience™	Cat# 25-9917-42; RRID: AB_11219074
Anti-CD182 (CXCR2)-PerCP/Cy5.5, clone 5E8/CXCR2	Biolegend	Cat# 320718; RRID: AB_2564599
Anti-CD184 (CXCR4)-PE, clone 12G5	Biolegend	Cat# 306506; RRID: AB_314612
Anti-CX3CR1-PerCP/Cy5.5, clone 2A9-1	Biolegend	Cat# 341614; RRID: AB_11219203
Anti-HLA-DR-PE/Cy7, clone L243	Biolegend	Cat# 307616; RRID: AB_493588
Anti-LOX-1-PE, clone 15C4	Biolegend	Cat# 358604; RRID: AB_2562181
Anti-MPO-PE, clone 2C7	Novus	Cat# NB100-64803; RRID: AB_964678
Absolute count panel		
Anti-CD3-FITC, clone OKT3	Biolegend	Cat# 317306; RRID: AB_571907
Anti-CD4-PE, clone RPA-T4	Biolegend	Cat# 300508; RRID: AB_314076
Anti-CD8a-PerCP/Cy5.5, clone RPA-T8	Biolegend	Cat# 301032; RRID: AB_2288911
Anti-CD14-APC/FireTM750, clone 63D3	Biolegend	Cat# 367120; RRID: AB_2572099
Anti-CD15-eF450, clone HI98	eBioscience™	Cat# 48-0159-42; RRID: AB_2016661
Anti-CD16-APC, clone eBioCB16	eBioscience™	Cat# 17-0168-42; RRID: AB_2016663
Extracellular Ki67 panel		
Anti-CD3-BV605TM, clone OKT3	Biolegend	Cat# 317322; RRID: AB_2561991
Anti-CD14-APC/FireTM750, clone 63D3	Biolegend	Cat# 367120; RRID: AB_2572099
Anti-CD15-eF450, clone HI98	eBioscience™	Cat# 48-0159-42; RRID: AB_2016661
Anti-CD16-PE, clone eBioCB16	eBioscience™	Cat# 12-0168-42; RRID:AB_11043436
Anti-CD19-BV605TM, clone HIB19	Biolegend	Cat# 302244; RRID: AB_2562015
Anti-CD62L-BV711, clone DREG-56	BD Biosciences	Cat# 740783; RRID: AB_2740446
Anti-CD64-PE/Cy7, clone 10.1	Biolegend	Cat# 305022; RRID: AB_2561584
Anti-CD182 (CXCR2)-PerCP/Cy5.5, clone 5E8/CXCR2	Biolegend	Cat# 320718; RRID: AB_2564599
Anti-CD193 (CCR3)-BV510, clone 5E8	BD Biosciences	Cat# 563071; RRID: AB_2737988
Ki67 stain		
Anti-Ki67-APC, clone Ki-67	Biolegend	Cat# 350514; RRID:AB_10959327
DCFDA (ROS) panel		
Anti-CD14-APC/FireTM750, clone 63D3	Biolegend	Cat# 367120; RRID: AB_2572099
Anti-CD15-eF450, clone HI98	eBioscience™	Cat# 48-0159-42; RRID: AB_2016661
Anti-CD16-PE, clone eBioCB16	eBioscience™	Cat# 12-0168-42; RRID:AB_11043436
Anti-CD64-PE/Cy7, clone 10.1	Biolegend	Cat# 305022; RRID: AB_2561584
Anti-CD101-PE, clone BB27	Biolegend	Cat# 331012; RRID:AB_2716107
Anti-CD193 (CCR3)-BV510, clone 5E8	BD Biosciences	Cat# 563071; RRID: AB_2737988
MitoSOX, TMRE, MitoTracker Green panel		
Anti-CD14-APC/FireTM750, clone 63D3	Biolegend	Cat# 367120; RRID: AB_2572099
Anti-CD15-eF450, clone HI98	eBioscience™	Cat# 48-0159-42; RRID: AB_2016661

Anti-CD16-PE, clone eBioCB16	eBioscience™	Cat# 12-0168-42; RRID:AB_11043436
Anti-CD64-PE/Cy7, clone 10.1	Biolegend	Cat# 305022; RRID: AB_2561584
Anti-CD193 (CCR3)-BV510, clone 5E8	BD Biosciences	Cat# 563071; RRID: AB_2737988
pHrodo panel		
Anti-CD64-PE/Cy7, clone 10.1	Biolegend	Cat# 305022; RRID: AB_2561584
Anti-CD66b-FITC, clone G10F5	Biolegend	Cat# 305104; RRID: AB_314496
Anti-CD182 (CXCR2)-PerCP/Cy5.5, clone 5E8/CXCR2	Biolegend	Cat# 320718; RRID: AB_2564599
Sorting panel		
Anti-CD14-PE/Cy7, clone 63D3	Biolegend	Cat# 367112; RRID:AB_2566714
Anti-CD15-PE, clone HI98	Biolegend	Cat# 301905; RRID:AB_314197
Anti-CD16-APC, clone eBioCB16	eBioscience™	Cat# 17-0168-42; RRID: AB_2016663
Anti-CD193 (CCR3)-FITC, clone 5E8	Biolegend	Cat# 310720; RRID:AB_2571959

APPENDIX

B. INSTITUTIONAL REVIEW BOARD APPROVAL

THE UNIVERSITY OF ALABAMA AT BIRMINGHAM
Office of the Institutional Review Board for Human Use

470 Administration Building
701 20th Street South
Birmingham, AL 35294-0104
205.934.3789 | Fax 205.934.1301 |
irb@uab.edu

APPROVAL LETTER

TO: Hel, Zdenek

FROM: University of Alabama at Birmingham Institutional Review Board
Federalwide Assurance # FWA00005960
IORG Registration # IRB00000196 (IRB 01)
IORG Registration # IRB00000726 (IRB 02)

DATE: 21-Jan-2020

RE: IRB-151210008
The Guts of HIV: Inmate Immune Dysregulation as a Central Mechanism of Gastrointestinal and Liver Disease in HIV-1-Infected Individuals

---

The IRB reviewed and approved the Continuing Review submitted on 17-Jan-2020 for the above referenced project. The review was conducted in accordance with UAB's Assurance of Compliance approved by the Department of Health and Human Services.

Type of Review: Full (Institutional Review Board 01 (UAB))
Determination: Approved
Approval Date: 21-Jan-2020
Approval Period: One Year
Expiration Date: 14-Jan-2021

The following apply to this project related to informed consent and/or assent:

- Waiver (Partial) of HIPAA

Please note:

- The IRB reviewed the Problem Summary Sheet submitted with this renewal. The dates of the Problem Summary Sheet are 10/25/17 to 01/06/20. It lists 2 events in Table A and 0 events in Table B.

Documents Included in Review:

- ipr clean.200117
- problemsummary.200106
- consent main clean.200117
- consent substudy biopsy clean.200117
- consent substudy additional clean.200117